

University of Sao Paulo  
"Luiz de Queiroz" College of Agriculture

Effects of climate change on corn: numerical simulation of soil water dynamics  
in a corn crop in Illinois (USA)

Nicole Costa Resende Ferreira

Thesis presented to obtain the degree of Doctor in  
Science: Area: Agricultural Systems Engineering

Piracicaba  
2017

**Nicole Costa Resende Ferreira**  
**Bachelor of Agricultural Engineering**

**Effects of climate change on corn: numerical simulation of soil water dynamics in a corn crop  
in Illinois (USA)**

versão revisada de acordo com a resolução CoPGr 6018 de 2011

Advisor:

Prof. Dr. **JARBAS HONORIO MIRANDA**

Co-advisor:

Prof. Dr. **RICHARD ANDREW COOKE**

Thesis presented to obtain the degree of Doctor in  
Science: Area: Agricultural Systems Engineering

**Piracicaba**  
**2017**

**Dados Internacionais de Catalogação na Publicação**  
**DIVISÃO DE BIBLIOTECA – DIBD/ESALQ/USP**

Ferreira, Nicole Costa Resende

Effects of climate change on corn: numerical simulation of soil water dynamics in a corn crop in Illinois (USA) / Nicole Costa Resende Ferreira. - - versão revisada de acordo com a resolução CoPGr 6018 de 2011. - - Piracicaba, 2017.

118 p.

Tese (Doutorado) - - USP / Escola Superior de Agricultura "Luiz de Queiroz".

1. Mudanças climáticas 2. Milho 3. Dinâmica de água 4. Drenagem I. Título

## ACKNOWLEDGEMENTS

I would like to thank the faculty, staff and colleagues of the postgraduate program in Agricultural Systems Engineering at the University of Sao Paulo. Especially my advisor, Prof. Dr. Jarbas Honorio Miranda, for the teachings and the disposition to help. To our research group GPEAS, especially Carlos Faundez Urbina, Katarina Grecco and Luciano Alves for the friendship and for helping in the integration of Hydrus software. Thanks also to my co-advisor Dr. Richard Cooke for receiving me at the University of Illinois at Urbana Champaign (UIUC), and its staff for contributing to the realization of this work, especially Timothy Lecher, Timothy Rendall and Duane Ross Kimme. To the National Council for Research and Technological Development (CNPq) and the Science without Frontiers (CSF) program for funding.

## CONTENTS

RESUMO.....	6
ABSTRACT.....	7
LIST OF FIGURES .....	8
1. INTRODUCTION .....	15
2. LITERATURE REVIEW .....	19
2.1. CLIMATE MODELING AND ASSOCIATED ERRORS IN CLIMATE PROJECTIONS.....	19
2.2. CLIMATE CHANGE AND EXTREME EVENTS .....	20
2.3. EFFECT OF CLIMATE CHANGE IN AGRICULTURE AND WATER RESOURCES .....	27
2.4. IMPORTANCE AND CHALLENGES OF CORN CROP .....	30
2.5. DYNAMIC OF WATER IN SOIL .....	34
3. MATERIAL AND METHODS.....	37
3.1. CLIMATOLOGICAL ANALYSIS.....	37
3.1.1. Study Area and Climatological Data .....	37
3.1.2. CMIP5 Climate Projections Models and Associated Errors.....	38
3.1.3. Extreme Events Detection.....	42
3.2. EXPERIMENTAL FIELD DATA.....	43
3.2.1. Study Area .....	43
3.2.2. Experiment Configuration .....	44
3.3. SIMULATION OF SOIL WATER DYNAMICS IN HYDRUS: MODEL CONSTRUCTION, INPUT AND OUTPUT DATA .....	49
4. RESULTS AND DISCUSSION .....	57
4.1. CLIMATOLOGICAL ANALYSIS.....	57
4.1.1. Climatology Evaluation .....	57
4.1.2. Extreme Events Occurrence.....	60
4.1.3. Statistical Analysis Of Errors.....	62
4.1.4. Climate Projections Scenarios .....	66
4.2. HYDRUS MODEL SIMULATION .....	76
4.2.1. Meteorological Analysis And Sensitivity Of Drainage Parameters .....	76
4.2.2. Applications In Climate Projections .....	84
4.2.2.1. Past Analysis.....	84

4.2.2.2. Short, Medium and Long Time Variations .....	87
4.2.3. Correlation between hydrological variables and extreme climatic events.....	96
5. CONCLUSIONS .....	101
6. FINAL REMARKS .....	103
REFERENCES .....	105
APENDIX.....	109

## RESUMO

### Efeito das mudanças climáticas sobre o milho: simulações numéricas da dinâmica de água em solos na cultura do milho em Illinois (USA)

Dada a importância das condições climáticas no ambiente agrícola, mais especificamente no transporte de água, é necessário compreender o efeito da mudança climática dinâmica da água no solo. Muitos modelos teóricos foram desenvolvidos para caracterizar os processos físicos envolvidos no transporte da água. Os modelos de previsão climática, como o conjunto de modelos do CMIP5, permitem gerar dados climáticos que podem ser usados para caracterizar processos físicos e biológicos. Esta pesquisa foca em dois aspectos principais: 1) efeito das mudanças climáticas na ocorrência de eventos extremos que podem afetar os processos agrícolas na região e 2) efeitos das mudanças climáticas na dinâmica da água no solo sob uma cultura de milho (dois campos experimentais, ANW e ASW) em uma região de Illinois (EUA). Os resultados encontrados indicam que a variação da precipitação no futuro pode causar o aumento de RX1DAY, RX5DAY, CDD e CWD. Considerando os eventos extremos de temperatura, percebemos que o aumento da temperatura média, máxima e mínima será refletido no aumento dos índices TNn, TNx, TXn, TXx e SU; e na diminuição dos índices ID e FD. Este aumento de temperaturas representará um risco para a agricultura considerando a evapotranspiração, que aumentará a necessidade de água das plantas e poderá criar um estresse hídrico. Os resultados apresentam as simulações do modelo IPSL aplicado no modelo Hydrus para simular, fluxo superficial, fluxo superficial acumulado, escoamento superficial, escoamento superficial acumulado, armazenamento de água do solo e infiltração acumulada. Essas variáveis são importantes na produção de milho e são função das variáveis climáticas, condições do solo e também alguns parâmetros da região de estudo, como o sistema de drenagem, as características da cultura e outros. O campo ANW apresentou valores mais baixos de fluxo superficial em comparação ao campo ASW. Isso indica que o risco associado ao sistema de drenagem ASW é maior que o ANW, que está relacionado ao maior espaçamento entre os drenos e a dificuldade em drenar a quantidade necessária de água. A tendência do fluxo superficial e do fluxo cumulativo de superfície, em geral, é de aumento em cenários de mudanças climáticas (em valores máximos e médios). Também é notável que toda a simulação indica o aumento do escoamento superficial em termos de valores máximos. O percentil de mudanças nos valores médios de escoamento mostra que a projeção climática tende a aumentar o escoamento superficial em diferentes cenários de simulação. Esta faixa crescente é de 5,61 a 24,4% em curto prazo (2011-2040), 16,45 a 39,32% em médio prazo (2041-2070) e 3,32 a 19,98% em longo prazo (2071-2100) em relação à simulação histórica (1976-2005). Os valores máximos de infiltração tendem a ser maiores em todas as simulações quando comparados ao período de referência (em ambos os campos). Além disso, mudanças na infiltração acumulada indicam que a infiltração média tende a aumentar no futuro. Considerando a correlação entre o escoamento superficial e os eventos de extremos climáticos, todas as simulações indicaram que a correlação entre o escoamento e os eventos extremos de precipitação RX1DAY (varia entre 0,76 e 0,78) e RX5DAY (varia entre 0,5 e 0,66), sendo estas maiores do que a correlação entre o escoamento superficial e a precipitação (intervalos entre 0,31 e 0,43). Conclui-se, portanto, que a ocorrência de eventos de extremos climáticos está mais associada as variáveis estudadas do que a condição climática em si, tendo impactos diretos na agricultura. O estudo mostra diferentes indicações do impacto das mudanças climáticas no recurso hídrico usando diferentes projeções. Uma dificuldade da pesquisa é sobre a grande quantidade de dados e a necessidade de tempo de passagem diário para a integração de variáveis. Esta abordagem pode melhorar a compreensão dos impactos das mudanças climáticas na gestão sustentável das águas subterrâneas com base no gerenciamento adaptativo. As informações obtidas neste trabalho podem ser usadas para projetar sistemas de monitoramento para gerenciar águas subterrâneas de maneira sustentável em regimes climáticos futuros e criar medidas de mitigação para garantir a segurança alimentar.

Palavras-chave: Mudanças climáticas; Milho; Dinâmica de água; Drenagem

## ABSTRACT

### Effects of climate change on corn: numerical simulation of soil water dynamics in a corn crop in Illinois (USA)

Given the importance of climate conditions in the agricultural environment, more specifically in the transport of water in the soil, there is a need to understand the effects of climate change on the water dynamics in the soil. This influence of climate conditions in the agricultural environment seems to be important in evapotranspiration, water availability for plants and roots, and for other processes. Many theoretical models have been developed to characterize the physical processes involved in water and transport. Climate prediction models such as the suite of models in the Coupled Model Intercomparison Project Phase 5 (CMIP5) make it possible generate climate data that can be used to characterize physical and biological processes. This research focuses on two main aspects: 1) the effects of climate change on the occurrence of extreme events that may affect agricultural processes in the region of Urbana-Champaign, in Illinois (USA) and 2) the effects of climate change on the dynamic of soil water in a corn crop (two fields, ANW and ASW) in the studied area. To explore the impacts of climate change on the occurrence of extreme events, the errors of some climate models from CMIP5 were evaluated and the models were subsequently used to develop indices to represent the occurrence of extreme events. These indices were calculated from observed data, and historical and future simulations, considering pessimistic and optimistic scenarios of climate change. The model that best represents the climate in the region was used to provide input data for Hydrus simulation of the soil water dynamics in two fields with different drainage system layout. These simulations with the Hydrus model were made for current conditions and for near term, mid-century, and end of century time periods (2011-2040, 2041-2070, 2071-2100, respectively). The results indicate that the variation of precipitation in the future may result in increased in one (RX1DAY) and five days (RX5DAY) maximum precipitation, and in the number of consecutive dry days (CDD) and consecutive wet days (CWD). Changes in temperature will be reflected as an increase of the indices of maximum and minimum values of temperatures and summer days (TN<sub>n</sub>, TN<sub>x</sub>, TX<sub>n</sub>, TX<sub>x</sub> and SU); and decreasing of the index of icing and frost days (ID, FD). This increasing of temperatures will represent a risk for agriculture, due to increased evapotranspiration, which will increase crop water demand and can create a hydric stress. Results of Hydrus simulations of surface flux, cumulative surface flux, runoff, cumulative runoff, soil water storage and cumulative infiltration, with input data from the IPSL model, are presented. These variables are critical in a corn crop, and are dependent on climate variables, soil conditions, parameters of the study region, drainage system, crop characteristics, *inter alia*. The ANW field had lower values of surface flux and cumulative surface flux comparing to the ASW field. This results is indicative that the risk associated with the ASW drainage system layout is higher than that of the ANW drainage system layout, related to the wider spacing between drains and the difficulty in removing water at the required rate. In general, the maximum and average values of surface flux and cumulative surface flux, will increase over time. In addition, it is noticeable that all Hydrus simulation indicates increasing maximum surface runoff and cumulative surface runoff over time. Percentile changes in average runoff and cumulative runoff are dependent on the period simulated. Increases range from 5.61 to 24.4% in the short term (2011-2040), 16.45 to 39.32% in the medium term (2041-2070) and 3.32 to 19.98% in the long term (2071-2100) compared to historical simulation. The maximum values of infiltration tend to be higher in all simulations when compared to the reference period in both fields. Changes in cumulative infiltration are indicative that infiltration will increase in the future. With respect to the correlation between runoff and extreme events, all simulations showed that the correlation between runoff and extreme precipitation events (RX1DAY ranges between 0.76 and 0.78, and RX5DAY ranges between 0.5 and 0.66), are higher than the correlation between runoff and precipitation (ranges between 0.31 and 0.43). This approach can improve the understanding of climate changes impacts on sustainable groundwater management based on adaptive management. Information gained in this work can be used to design monitoring systems to manage a sustainable groundwater in future climate regimes and create mitigation measures to prevent any risk for food security. An implication of the study is that the impact of climate change on water resources is a function of the projection scenario. The study was limited by the use of daily time step, necessitated by the large data sets.

Keywords: Climate changes; Corn; Dynamic of water; Drainage

## LIST OF FIGURES

Figure 1. Earth surface temperature variation, between 1901 and 2012 (STOCKER et al., 2014). .....	21
Figure 2. Simulation of CMIP5 multi-model ensemble (top) and errors of simulation (CMIP5 – ERA Interim, bottom), considering the maximum and minimum temperature and annual of maximum precipitation in 20 years (1986-2006). Source: Kharin et al. (2013). .....	22
Figure 3. The multimodel median of temporally averaged changes in the minimum of TN (TN <sub>n</sub> , left) and the maximum of TX (TX <sub>x</sub> , right) over the time period 2081–2100 displayed as differences (in C) relative to the reference period (1981–2000) for RCP2.6 (top), RCP4.5 (middle), and RCP8.5 (bottom). All changes are significant at the 5% significance level. Source: Sillmann et al., (2013b). .....	24
Figure 4. The multimodel median of temporally averaged changes in the frost days (FD, left) and the consecutive dry days (CDD, right) over the time period 2081–2100 displayed as differences relative to the reference period (1981–2000) for RCP2.6 (top), RCP4.5 (middle), and RCP8.5 (bottom). Stippling indicates grid points with changes that are not significant at the 5% significance level. Source: Adapted from Sillmann et al., (2013b). .....	25
Figure 5. Projected change (°C) in the 20-yr return value of annual minimum (top) and maximum daily air temperature at the end of this century (2081–2100) relative to the recent past (1986–2005) for the lower (left) RCP2.6 and higher (right) RCP8.5 scenarios. ....	26
Figure 6. Projected change (%) in the 20-yr return value of annual maximum daily precipitation at the end of this century (2081–2100) relative to the recent past (1986–2005) for the lower (left) RCP2.6 and higher (right) RCP8.5 scenarios. ....	26
Figure 7. Change in average annual runoff by the 2050s. Source: Arnell et al (1999). .....	31
Figure 8. Percent change in mean maximum decadal yield for long-season (a) and medium-season (b) maize according to HadCM2. Source: Southworth et al. (2000). .....	34
Figure 9. Location of meteorological station in Champaign (Illinois, USA). .....	37
Figure 10. Maps of the multi model CMIP5 for RCP2.6 and RCP8.5 simulated scenarios, considering the difference between the future years (2081 to 2100) and the past years (1986 to 2005 - can also be expressed as "current climate"), where: (a) the average percentage of annual	

precipitation. The number of CMIP5 models used to calculate the mean multi-model is shown in the upper right corner of each panel. Source: (STOCKER et al., 2014).....	39
Figure 11. The global increase of average surface temperature as a function of the total emission of CO <sub>2</sub> accumulated until 2100. Source: (STOCKER et al., 2014).....	39
Figure 12. Corn field located in Champaign (Illinois, USA) in a) May, b) July and c) September, 2015.....	45
Figure 13. Data-loggers installed in the field and used to collect data in a frequency of 15 minutes. ....	46
Figure 14. Scheme of the drainage system and the variables that affect the dynamic of water in soil, where wt1 and wt2 are the water table depth in diferente positions. ....	47
Figure 15. Meteorological station installed in the field, collecting data from April to September, 2015.....	48
Figure 16. Comparison between data from meteorological station installed in the field and data from the city of Urbana from May to September.....	48
Figure 17. Representative layout of soil materials in field generated by Hydrus. ....	52
Figure 18. Variation if monthly accumulated precipitation (mm/month) (a), and average temperature (°C) (b) in the region of Urbana-Champaign (Illinois, USA) between 1901 to 2015.....	58
Figure 19. Variation of precipitation (a) and temperature (b) in the region of Urbana-Champaign (Illinois, USA), from 1901 to 2015.....	59
Figure 20. Anomalies of observed precipitation (a) accumulated per year and average temperature (b) per year (maximum, minimum and average) in Urbana-Champaign (IL, USA) between the period 1901 to 2015.....	59
Figure 21. Extreme events of precipitation, considering observed data from 1901 to 2015. The dashed line means the tendency of each index, the letter a) presents the index of maximum value of rainfall in one and five days (RX1DAY, RX5DAY) and b) the maximum number of consecutive dry and wet days (CDD, CWD).....	60
Figure 22. Extreme events of temperature, considering observed data from 1901 to 2015. The dashed line means the tendency of each index, the letter a) presents the index of maximum value of maximum and minimum temperature (TXx, TNx), b) minimum value of maximum and	

minimum temperature ( $TX_n$ ,  $TN_n$ ), c) daily temperature range (DTR) and d) number of summer, frost and icing days (SU, FD and ID).....61

Figure 23. Statistical analysis of errors of temperature (maximum, average and minimum, °C) and precipitation (mm) in the climate models, based on mean (absolute and bias) error (MAE, MBE) considering systematic and unsystematic errors.....62

Figure 24. Statistical analysis of errors of temperature (maximum, average and minimum, °C) and precipitation (mm) in the climate models, based on root mean square error (RMSE) considering systematic and unsystematic errors.....63

Figure 25. Statistical analysis of errors of temperature (maximum, average and minimum) and precipitation in the climate models, based on correlation and coefficient of determination  $R^2$ . ...63

Figure 26. Occurrence of extreme events of precipitation according to observed data (blue box) and climate models (grey box), between 1901 and 2015. The indices are a) Maximum value of rainfall in one day (RX1DAY), b) Maximum value of rainfall in five days (RX5DAY), c) consecutive dry days (CDD), d) consecutive wet days (CWD).....64

Figure 27. Occurrence of extreme events of temperature according to observed data (blue box) and climate models (grey box), between 1901 and 2015. The indices are maximum value of a) maximum ( $TX_x$ ) and b) minimum temperature ( $TN_x$ ), minimum value of c) maximum ( $TX_n$ ) and d) minimum temperature ( $TN_n$ ). .....65

Figure 28. Occurrence of extreme events of temperature according to observed data (blue box) and climate models (grey box), between 1901 and 2015. The indices are maximum value of a) summer days (SU), b) icing days (ID), c) frozing days (FD) and d) daily temperature range (DTR). .....66

Figure 29. Observed and simulated data of precipitation and maximum, average, and minimum temperature (projected by IPSL(CM5MR)) for 1901 to 2100. The simulated data includes historical simulation (grey) and RCP2.6 (blue), RCP4.5 (green) and RCP8.5 (red).....68

Figure 30. Changes on precipitation, maximum, average and minimum temperature, considering the percentile of difference between climate projections (divided into periods: 2011-2040, 2041-2070, 2071-2100) and the reference period of 1976 to 2005. These changes were calculated for the scenarios RCP2.6, RCP4.5 and RCP8.5.....69

Figure 31. Indices of extreme events of precipitation calculated based on observed and simulated data (projected by IPSL(CM5MR)) for 1901 to 2100. The indices calculated are maximum value

of rainfall in one (RX1DAY) and five days (RX5DAY) and consecutive dry (CDD) and wet days (CWD). The simulated data includes historical simulation (grey) and RCP2.6 (blue), RCP4.5 (green) and RCP8.5 (red). ..... 70

Figure 32. Changes on index of extreme precipitation, as RX1DAY, RX5DAY, CDD and CWD, considering the percentile of difference between climate projections (divided into periods: 2011-2040, 2041-2070, 2071-2100) and the reference period of 1976 to 2005. These changes were calculated for the scenarios RCP2.6, RCP4.5 and RCP8.5..... 71

Figure 33. Indices of extreme events of temperature calculated based on observed and simulated data (projected by IPSL(CM5MR)) for 1901 to 2100. The index are maximum value of maximum ( $TX_x$ ) and minimum temperature ( $TN_x$ ), minimum value of maximum ( $TX_n$ ) and minimum temperature ( $TN_n$ ). The simulated data includes historical simulation (grey) and RCP2.6 (blue), RCP4.5 (green) and RCP8.5 (red). ..... 72

Figure 34. Changes on extreme indices, as  $TX_x$ ,  $Tn_x$ ,  $Tx_n$  and  $TN_n$  considering the percentile of difference between climate projections (divided into periods: 2011-2040, 2041-2070, 2071-2100) and the reference period of 1976 to 2005. These changes were calculated for the scenarios RCP2.6, RCP4.5 and RCP8.5..... 73

Figure 35. Indices of extreme events of temperature calculated based on observed and simulated data (projected by IPSL(CM5MR)) for 1901 to 2100. The index are maximum value of maximum ( $TX_x$ ) and minimum temperature ( $TN_x$ ), minimum value of maximum ( $TX_n$ ) and minimum temperature ( $TN_n$ ), summer days (SU), icing days (ID), daily temperature range (DTR) and freezing days (FD). The simulated data includes historical simulation (grey) and RCP2.6 (blue), RCP4.5 (green) and RCP8.5 (red). ..... 74

Figure 36. Changes on extreme indices, as SU, ID, DTR and FD, considering the percentile of difference between climate projections (divided into periods: 2011-2040, 2041-2070, 2071-2100) and the reference period of 1976 to 2005. These changes were calculated for the scenarios RCP2.6, RCP4.5 and RCP8.5..... 75

Figure 37. Meteorological fluxes, between April to September, 2015. The fluxes are divided into a) rainfall (blue) and relative humidity (black), b) maximum (blue) and minimum temperature (red), c) wind speed (black), d) evaporation (blue), transpiration (red) and evapotranspiration (black), e) radiative term (red) and aerodynamic term (blue), f) net short wave radiation ( $Rns$ , blue) and net out-going long wave radiation ( $Rnl$ , red). ..... 77

Figure 38. Potential root water uptake, considering the corn crop in the experimental field, from April to September (2015). .....	78
Figure 39. Meteorological fluxes, between April to September (2015). The data was collect in ANW (red) and ASW (blue) field. ....	79
Figure 40. Profile information of: a) surface flux ( $v_{Top}$ , cm.day-1) and b) cumulative surface flux ( $Sumv_{Top}$ , cm.day-1) in the fields ANW (red) and ASW (blue) in Illinois (USA), between April to September, 2015. ....	80
Figure 41. Profile information of: a) soil water storage (volume, cm) and c) cumulative infiltration ( $Sum\ Inf$ , cm.day-1) in the fields ANW (red) and ASW (blue) in Illinois (USA), between April to September, 2015. ....	80
Figure 42. Profile information of surface runoff (flux, cm/day) and cumulative surface runoff ( $Sum\ Inf$ , cm) in the fields ANW (red) and ASW (blue) in Illinois (USA), between April to September, 2015. ....	82
Figure 43. Profile information of a) water flux, b) hydraulic conductivity, c) hydraulic capacity, d) pressure head and e) water content, in a soil in Illinois (USA), between April to September, 2015. The variables were simulated for three fields (ANW and ASW) showed with different line types and were simulated in five different times showed with different colors. ....	83
Figure 44. Profile information of: a) surface flux ( $v_{Top}$ , cm.day-1) and b) cumulative surface flux ( $Sumv_{Top}$ , cm.day-1) in the fields ANW (red) and ASW (blue) in Illinois (USA), considering the periof of 1976 to 2005 in the historical simulation of IPSL model. ....	84
Figure 45. Profile information of: a) soil water storage (Volume, cm) and b) cumulative infiltration ( $Sum\ Inf$ , cm.day-1) in the fields ANW (red) and ASW (blue) in Illinois (USA), considering the periof of 1976 to 2005 in the historical simulation of IPSL model. ....	85
Figure 46. Profile information of: a) surface runoff (flux, cm/day) and c) cumulative surface runoff ( $Sum\ Inf$ , cm) in the fields ANW (red) and ASW (blue) in Illinois (USA), considering the period of 1976 to 2005 in the historical simulation of IPSL model. ....	86
Figure 47. Climate scenarios applied to simulations of surface flux (top) and cumulative surface flux (bottom), considering the fields ANW (shades of red) and ASW (shades of blue). Scenarios were divided into historical (1976-2005, circle symbol) and short (2011-2040, triangle symbol), medium (2041-2070, cross symbol) and long time variation (2071-2100, x symbol).....	88

- Figure 48. Percentile of changes in surface flux and cumulative surface flux, considering ANW (red) and ASW (blue) field. The percentile was calculated for the climate projections RCP2.6, RCP4.5 and RCP8.5, considering the periods of 2011-4040; 2041-2070 and 2071-2100, compared to the reference period (1976-2005).....89
- Figure 49. Climate scenarios applied to simulations of surface runoff (top) and cumulative surface runoff (bottom), considering the fields ANW (shades of red) and ASW (shades of blue). Scenarios were divided into historical (1976-2005, circle symbol) and short (2011-2040, triangle symbol), medium (2041-2070, cross symbol) and long time variation (2071-2100, x symbol). .....90
- Figure 50. Percentile of changes in surface runoff and cumulative surface runoff, considering ANW (red) and ASW (blue) field. The percentile was calculated for the climate projections RCP2.6, RCP4.5 and RCP8.5, considering the periods of 2011-4040; 2041-2070 and 2071-2100, compared to the reference period (1976-2005).....91
- Figure 51. Climate scenarios applied to simulations of soil water storage (top) and cumulative infiltration (bottom), considering the fields ANW (shades of red) and ASW (shades of blue). Scenarios were divided into historical (1976-2005, circle symbol) and short (2011-2040, triangle symbol), medium (2041-2070, cross symbol) and long time variation (2071-2100, x symbol). .....92
- Figure 52. Percentile of changes in soil water storage and cumulative infiltration, considering ANW (red) and ASW (blue) field. The percentile was calculated for the climate projections RCP2.6, RCP4.5 and RCP8.5, considering the periods of 2011-4040; 2041-2070 and 2071-2100, compared to the reference period (1976-2005).....94
- Figure 53. Surface flux, surface runoff and precipitation, considering the fields ANW (red) and ASW (blue), in the RCP2.6 (a, b), RCP4.5 (c, d) and RCP8.5 (e, f). The analyzed period was from 2011 to 2100. ....95
- Figure 54. Summary of percentile fo changes (considering climate scenarios and historical simulations) of extreme events and hydrological variables. Variables with hatch is considered statistically different, considering a significant level of 5%. .....96
- Figure 56. Correlation between climate indices and maximum values of surface runoff in ANW (top) and ASW (bottom) fields, considering the climate scenarios of RCP2.6, RCP4.5 and RCP8.5.....99



## 1. INTRODUCTION

Observed data from different parts of the world showed that many natural systems are being affected by climate change. In 1988, the Intergovernmental Panel on Climate Change (IPCC) was created to study the issue of global climate change. IPCC is the primary scientific organization that evaluates variations in climate, and provides clear scientific views of the current state of knowledge of climate change. Also, the aim of this organization is to describe the potential social, economic and environmental impact of climate change. To achieve this goal, it produces reports that are based on studies by several different researchers and research groups.

Models have been used as a tool in studies to evaluate the impacts of climate change in different sectors, such as agriculture, health, industry, and others. Projections of changes the climate system are made using climate models which range from simple climate models to more comprehensive climate models. Climate prediction models such as the suite of models in the Coupled Model Inter-comparison Project Phase 5 (CMIP5) make it possible generate climate data that can be used to characterize physical and biological processes. A huge set of data is available to help in climate change studies, which can make choosing an adequate model for one particular region difficult. Climate models can be classified as General Circulation Models (GCM's) and Regional Climate Models (RCM's). Each type of model has advantages and disadvantages. For example, RCM's can represent better complex topography, but their use requires more computational time and effort. On the other hand, GCM's are simpler and more available, although in some cases there is a need to evaluate their accuracy before application. Studies using GCM's, even with the need to evaluate their performance, remain relevant, considering the fact that RCM's needs data from GCM as input for their simulations.

Although the use of atmospheric models has proven to be a useful tool in various sectors, there are still some limitations to be overcome before they can be used for climate predictions. Climate models may have some errors which makes it necessary to evaluate them before they can be applied. These limitations occur mainly due to uncertainties in current forecasts, related to simplifications and parametrization in forecasting models. Uncertainties in climate models, sometimes, is considered a limiting factor, especially when the intent is to apply this data on a local scale. When performing a numerical forecast, it is possible to find errors propagated from those uncertainties, resulting in a model with a tendency to underestimate or overestimate a particular variable for a given region. This issue makes it essential to conduct research to identify the areas where these errors are prominent. This errors occurs due to the parametrization necessary in these models and also due to the streamlined equations used to describe chaotic systems.

Different sectors already notice the effects of climate change. The expectation is that in the future, these effects will be compounded. Some climate models can approach the average values of the variable but have difficulty in forecasting extreme events. This problem happens mostly when a long-term integration is made. This is an issue considering that in general, the extreme events can have a bigger impact than average values. An important task is the analysis and evaluation of climate models performance in representing extreme events, in addition to mean climate.

Climate change can influence many aspects of, and processes in, the hydrological cycle, such as temperature, evapotranspiration, and other variables. An example of this effect can be found at corn crop, which depends on climate conditions. Corn productivity it has been at risk due to the increase in temperature, and changes in the pattern of precipitation. This occurs because the climate conditions might be reflected as moisture stress and

extreme heat during flowering, pollination, and grain filling (Southworth et al., 2000; Rosenzweig and Hillel, 1993; Jones & Thornton, 2003).

Researchers have studied the effects of climate change in various fields of study, including the consequences of climate change on the dynamics of water in the soil. These studies depend on specific characteristics of the study region (soil, crop, drainage system, management, etc.), and sometimes they are not accurate when simulations are done on a global scale. The association between climate change and soil water dynamics can be made using mathematical models which try to describe this dynamic, using climate and soil data. An understanding of water movement is necessary to control nutrient losses and movement of pollutants through the soil, and to supply the crop necessity, and to infer about risks of drought and floods. Changes in temperature, hydrological processes, and frequency of extreme events can lead to changes in soil water dynamics. Such changes could compromise water resources in the future, as chemical transport in the soil can result in groundwater contamination. Also, nutrients released as a byproduct of agricultural activities could be more concentrated due to the reduced flows in summer. It is possible to assess the impacts of climate change on water storage and groundwater recharge, modeling climate conditions and dynamic of water in the soil. The best likelihood of accurately predicting these impacts is through the combination of field monitoring and mathematical modeling, which helps in the understanding of these complex processes and may help to find sustainable solutions in the field.

Hydrus is a mathematical model with practical applications for the technological development of production. It can be used to investigate relationships among the hydraulic and physical parameters and soil wetting patterns as affected by drainage design and management practices. Planning and managing the use of water resources in the soil-plant-atmosphere system, require an understanding of the physical processes of flow, and water storage in the soil. Physical and mathematical models are important for numerical simulations of infiltration and drainage processes, evaporation, and setting the water balance. Mathematical modeling allows for fast and accurate characterization of soil water dynamics, making it possible to quickly address environmental impacts. Modeling is important in hydrological studies and helps the analysis of the risk in the management of surface and subsurface waters. By theoretically describing the physical processes occurring in the soil, combined with numerical techniques to solve the resulting equations, and adequate computational resources, it is possible to predict the risk and impacts that climate change can cause in the soil, water and plants.

The aim of the first part of this research is to evaluate generated data for climate scenarios, given by CMIP5 models, by characterizing the errors associated with these models. The best models to represent the local climate of the region of Urbana – Champaign (Illinois), were selected based on minimum values of specific errors. This region is part of a zone that has a significant place in the corn production. The region of Illinois is known as one of the areas that contribute to the eutrophication of the Gulf of Mexico, due to the extensive application of herbicides and fertilizers in the Midwestern USA. This research can help other studies to choose an adequate model to use to simulate the climate in this region, giving more accurate results to the research. The climatology, and the possible changes of climate and extreme events in the area which may affect the local agriculture, based on several projection scenarios, will be described.

The second part of this research is a study of the soil water dynamics in two fields in the region, based in the incorporation of climate model data for different scenarios, in the Hydrus model. The aim of this analysis is to estimate how climate changes can affect the soil water dynamics under corn grown in fields with different drainage systems. The study also describes the possible effects of climate change on various drainage systems parameters. This

research can also help other researchers to develop techniques to manage the water, to maintain the sustainable production.



## 2. LITERATURE REVIEW

### 2.1. Climate Modeling and Associated Errors in Climate Projections

Estimates the impacts of climate changes is important because it may affect society in different ways. The Intergovernmental Panel on Climate Change (IPCC) is a scientific organization which evaluates the variation in climate conditions and provide clear scientific views of the current state of knowledge of climate change. To describe the potential social, economic and environmental impact of climate change, the IPCC produce reports that are based on different studies of several researchers.

According to one of the IPCC's report (SOLOMON et al., 2007), in the 20<sup>th</sup> century, observed data indicates that the earth experimented increase of average temperature of approximately 0.65°C, and this mostly happened in the 1990s. Climate models based on registered data of ocean, biosphere, and atmosphere, indicate an increase of 1.4°C and 5.8°C in the global average temperature until the end of the 20<sup>th</sup> century (SOLOMON et al., 2007). The causes of this variations are still unknown and can be due to natural or anthropogenic activities, or the combination of both. Many studies have been looking for the cause of this climate change, but there is still no full agreement on the causes.

The impacts of climate changes rely on projections from climate models, and for this reason, the scientific community organizes regular international projects to inter-compare this models. An example of this network is the Coupled Model Intercomparison Project (CMIP), which have been increasing the studies in the area through the available model outputs, leading to an extensive set of publications and providing valuable inputs to IPCC reports. Climate prediction models such as the suite of models in the Coupled Model Inter-comparison Project Phase 5 (CMIP5) make it possible to generate climate data that can be used to characterize physical and biological processes. This data set was created from the meeting of 20 climate modeling groups from around the world, the World Climate Research Programme's (WCRP), Working Group on Coupled Modeling (WGCM), with the input from the International Geosphere-Biosphere Programme's (IGBP) and Analysis, Integration and Modeling of the Earth System (AIMES) project.

Taylor et al. (2012) presented an overview of CMIP5 models. According to this work, the project intends to perform a suite of climate simulations that focus on major gaps in understanding of past and future climate changes. A study of Knutti & Sedlacek (2013) indicated that the spatial patterns of temperature and precipitation change are very consistent with the projections simulated in Phase 4 of CMIP5. Also, Knutti et al. (2013) concluded that the models in the new ensemble agreed better with the observations than those in older ones and eliminated the poorest models.

The CMIP5 experiments include two types of climate changes experiments, which is long-term (century time scale) and near-term (decadal) experiments (MEEHL et al., 2009). Within the long-term experiments, there is the historical run, which is forced by observed atmospheric composition changes and includes a time-evolving land cover. There is also future projection simulated forced with specified concentrations (also called representative concentration pathways (RCP's), which creates different ranges of emission, as described in Moss et al., 2010). As an example: high emission range (RCP8.5, i.e. a radiative forcing setting of 8.5 W.m<sup>-2</sup>), moderate emission (RCP4.5) and low emission (RCP2.6). Those RCP's is commonly called climate scenarios, which according to (PARRY et al., 2007) can be defined as a description of the future climate based on a range of climatological relationships and assumptions of radioactive forcing. More information about the CMIP5 dataset is available in the methodology section.

According to Hawkins and Sutton (2009), the primary source of uncertainty in long-term climate projections is a lack of understanding and observations of physical feedbacks reflected in a model. Friedlingstein et al. (2014) infer that the best estimate projections and uncertainty ranges for emission scenarios is related to physical processes and carbon cycle processes and their feedbacks, respectively.

As reported by Cuculeanu et al. (2002), since each climate model has its uncertainty, the use of more than one climate model will be better for dealing with the accurate projection problem. There is a lot of information regarding simulation scenarios, such as different models and emission scenarios, which creates a vast large range of possibilities. At times, different assumptions yield divergent results, presenting a source of uncertainty in research. Because of this factor, it is necessary to determine the most accurate information to apply to further studies.

Scientific papers often use some goodness-of-fit to evaluate this errors. Some of this indices are: Root Mean Square Error (RMSE), Mean Bias Error (MBE), Mean Absolute Error (MAE), Correlation (C) and Coefficient of Determination ( $R^2$ ). Some information about this indices can be found in studies by Stone (1993), Saghafian & Bondarabadi (2008), Daly et al. (2002), Basistha et al. (2008), Wei et al. (2005).

It is important to notice here that a model could be classified as better than another in two different ways: It can be 1) better in terms of the agreement with observations or, 2) better in the representation and description of processes. When statistical analysis is used, the analysis can measure the performance of the model when compared to observations, without direct evaluation of the representation of physical processes. In addition, models sometimes have the capability to represent average values but do not accurately represent extreme events. More information about those events is presented in next section.

## 2.2. Climate Change and Extreme Events

The effects of climate change are already noticed in different sectors. The expectation is that in the future these effects will be compounded. Due to the global warming in the near future is suppose to have more extreme climate scenarios with droughts, floods, and heat waves occurring more often (SALATI et al., 2004). In a research conducted by Kalnay & Cai (2003) the authors concluded that the temperature might rise to 0.008°C per decade. This value is near to the optimistic scenario presented in the IPCC report. The magnitude of this forecast is still uncertain because there are some uncertainties about the exchange process of heat, carbon, and radiation between the various sectors of the Earth system.

According to Thomas et al. (2004), with the elevation of temperature in the most optimistic scenario, 18 species are threatened by extinction by the year of 2050. Impacts such as the elevation of the ocean level and more often and extremes hurricanes, can also influence the melting glaciers (SALATI et al., 2004). Some researches have been done about climate change in hydrological studies (GREEN et al., 2011) and changes in extreme events and precipitation patterns (NEW et al., 2001; KAZMIERCZAK et al., 2014, SCOCCIMARRO et al., 2013; KUNKEL et al., 2003). According to the report of IPCC (STOCKER et al., 2014), data series from 1901 to 2012 indicates that almost the entire globe has experienced surface warming (Figure 1).

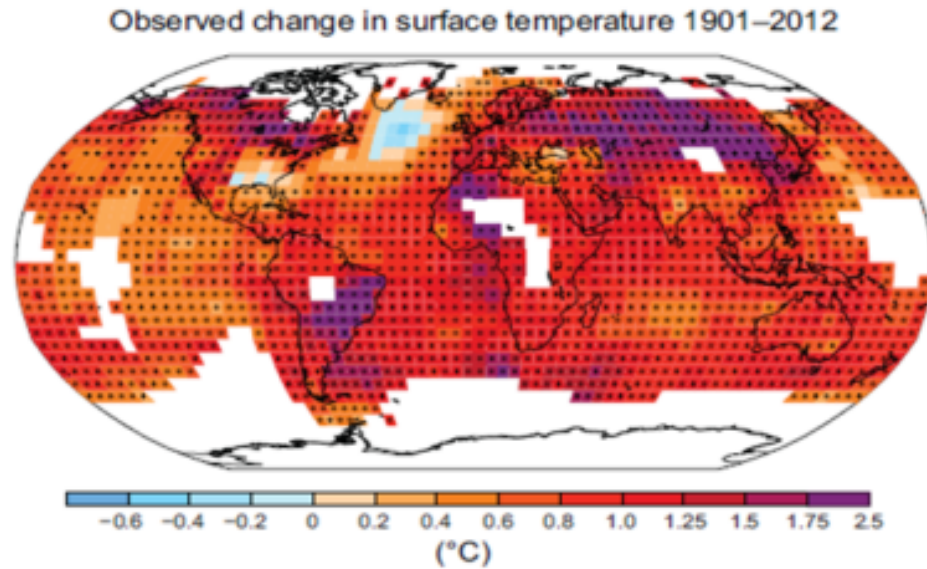


**Figure 1.** Earth surface temperature variation, between 1901 and 2012 (STOCKER et al., 2014).

Some climate models can approach the average values of the variable but have difficulty in forecasting extreme events. This happens mostly when a long-term integration is made. This is an issue considering that in general, the extreme events can have a bigger impact than average values. An important task is the analysis and evaluation of CMIP5 model performance in representing those extreme events, and not considering only the mean climate. The Special Report on Extreme Events (SREX) of the Intergovernmental Panel on Climate Change (STOCKER et al., 2014) emphasized this impact. The indices to measure extremes events were proposed by the World Meteorological Organization (WMO) and the Climate Research Program Variability and Predictability (CLIVAR) to enable the comprehensive analysis of extremes. Studies about the occurrence of these events are important because the increase in frequency or severity of extreme weather events are directly associated with human and monetary losses.

The IPCC report (STOCKER et al., 2014) also indicate the occurrence of extreme events, concluding that it is possible that the number of warm days and also the number of cold nights has increased on a global scale. Also, it is probable that the frequency of warm waves had an increase in the most part of Europe, Asia, and Australia. There is also an indication of increasing frequency and intensity of events of intense precipitation in North America and Europe.

A research of Kharin et al. (2013) used the ensemble of CMIP5 models to study twenty-year temperature and precipitation extremes and their projected future changes. The authors used three radiative forcing scenarios to simulate late 20<sup>th</sup> century extremes. Figure 2 shows the results founded by Kharin et al. (2013). They conclude that the warm extremes were represented reasonably well, compared to estimates from reanalyses. Also, the model discrepancies in simulating cold extremes are generally larger than those for warm extremes. Considering the precipitation extremes simulation they achieve to be plausible in the extra-tropics, but uncertainty in extreme precipitation in the tropics and subtropics remains large, both in the models and the observationally-constrained data sets.

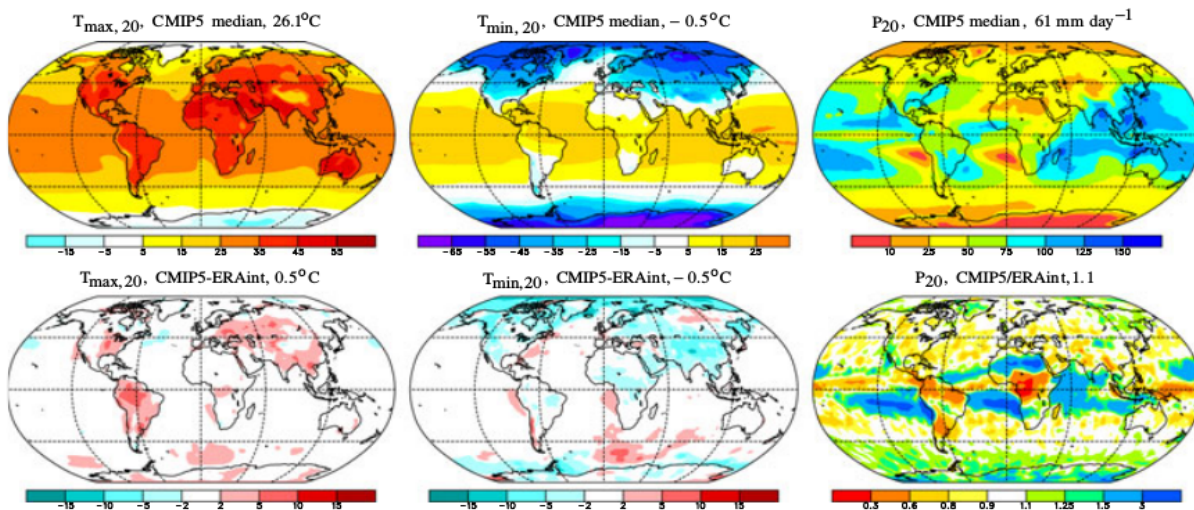


**Figure 2.** Simulation of CMIP5 multi-model ensemble (top) and errors of simulation (CMIP5 – ERA Interim, bottom), considering the maximum and minimum temperature and annual of maximum precipitation in 20 years (1986-2006). Source: Kharin et al. (2013).

Other researchers evaluated the extreme indices in a global scale. However, it is important to notice some uncertainties in this research as inferred by Sillman et al. (2013), that can be related to 1) the formulation of globally valid definitions of extremes, 2) the identification of datasets with sufficient spatial and temporal coverage that is appropriate for comparison with models and 3) performing analysis of the available model and observational datasets in a consistent manner.

Frich et al. (2002), using observed data, showed an increasing trend in the frequency of intense precipitation events in some regions of the world, accompanied by changes in the frequency of dry days in some areas. The results of this analysis indicated that the world has become warmer and wetter. Wet periods tends to produce significantly higher rainfall totals, and events of heavy rain have become more frequent during the second half of the 20<sup>th</sup> century. However, the data used were mainly stations in the northern hemisphere, which highlights the need for more studies over South America. Haylock et al. (2006) studied 54 weather stations to examine possible changes in total precipitation and extreme precipitation over the period 1960 to 2000. This study showed significant reductions in precipitation indicators in southern Peru and southern Chile. As a result, it showed a trend of decrease of consecutive dry days (CDD) and increased rates of consecutive wet days (CWD), maximum rainfall in one and five days (RX1DAY and RX5DAY) and heavy rains (R95P).

Groisman et al. (2005) and Marengo & Valverde (2007) identified in the subtropical part of Brazil a large systematic increase in rainfall since the 1950s and, in southeastern of Brazil, they found an increase in the frequency of extreme rainfall events. Carvalho et al. (2004) found that extreme rainfall events exhibit inter-annual variability linked to El Niño and La Niña and intra-seasonal variations associated with the activity of South Atlantic Convergence Zone (SACZ) and South America Low-Level Jet, in the state of Sao Paulo. A study from the Institute of Astronomy and Geophysics Station of the University of Sao Paulo (NOBRE et al., 2010) showed that heavy rains have become more frequent in Sao Paulo, Brazil. Also, daily rainfall totals exceeding 50 millimeters, which occurred with an average frequency of 9 times every ten years in the 1930s, began to occur with a frequency of 40 times in the 2000s.

Zhou et al. (2014) projected the indices of events extremes of temperature and precipitation in China using CMIP5 ensemble. They realize that compared to the reference period of 1986 to 2005, substantial changes are

projected in temperature and precipitation extremes under different emission scenarios, or representative concentration pathways (RCP4.5 and RCP8.5). These changes include a decrease in cold extremes, an increase in warm extremes, and an intensification of precipitation extremes. Also, they notice that the difference in the projected changes under the two RCP's begins to emerge in the 2040's. Chou et al. (2009) concluded that model projections indicate intensification of extreme precipitation in a warming climate, leading to wet areas getting wetter and dry areas getting drier on future.

Sillmann et al. (2013a) simulated extreme events between 1981 to 2000. Their research shows that the CMIP5 models are generally able to simulate climate extremes and their trend patterns as represented by indices derived from comparison to observed data. Sillmann et al. (2013b) show that changes in indices calculated using CMIP5, based on daily minimum temperatures (as a minimum of minimum temperature,  $TN_n$ , and frost days, FD) are found to be more pronounced than indices based on daily maximum temperatures (as a maximum of maximum temperature,  $TX_x$ ). Frost days mainly decrease in western North America, along with other regions, and this decrease is stronger in RCP8.5 with reductions of 80 frost days and more in western North America by the end of the 21st century. The study also shows that in regions, such as Australia, Central America, South Africa, and the Mediterranean, the indices indicates a future intensification of dry conditions (CDD). Figure 3 summarizes the changes in indices of  $TN_n$  and  $TN_x$ , and Figure 4, in FD and CDD. The period 2081-2100 is displayed as differences relative to the reference period (1981-2000) calculated by CMIP5 multi-model in RCP2.6, RCP4.5, and RCP8.5 scenarios.

As state in Houghton et al. (2001), the IPCC considers that it is highly likely that increases in heavy precipitation extremes will occur during the 21st Century. Regarding the North America, Groisman et al. (2001) reported a 50% increase during the 20th Century in the frequency of days with precipitation exceeding 101.6 mm in the upper Midwest U.S. Also, Wuebbles et al. (2014) show some evidence that indicates the occurrence of extreme events over the USA. They infer that in U.S., cold spell temperature increases range from around 3°C in Florida to more than 8°C in the north-central U.S., considering the period of 2071–99 compared to 1971–2000. Figures 5 and 6, showed in Wuebbles et al. (2014) related to the research of Kharin et al. (2013) indicates the projected changes in the 20-year return value of annual minimum and maximum daily temperature and precipitation.

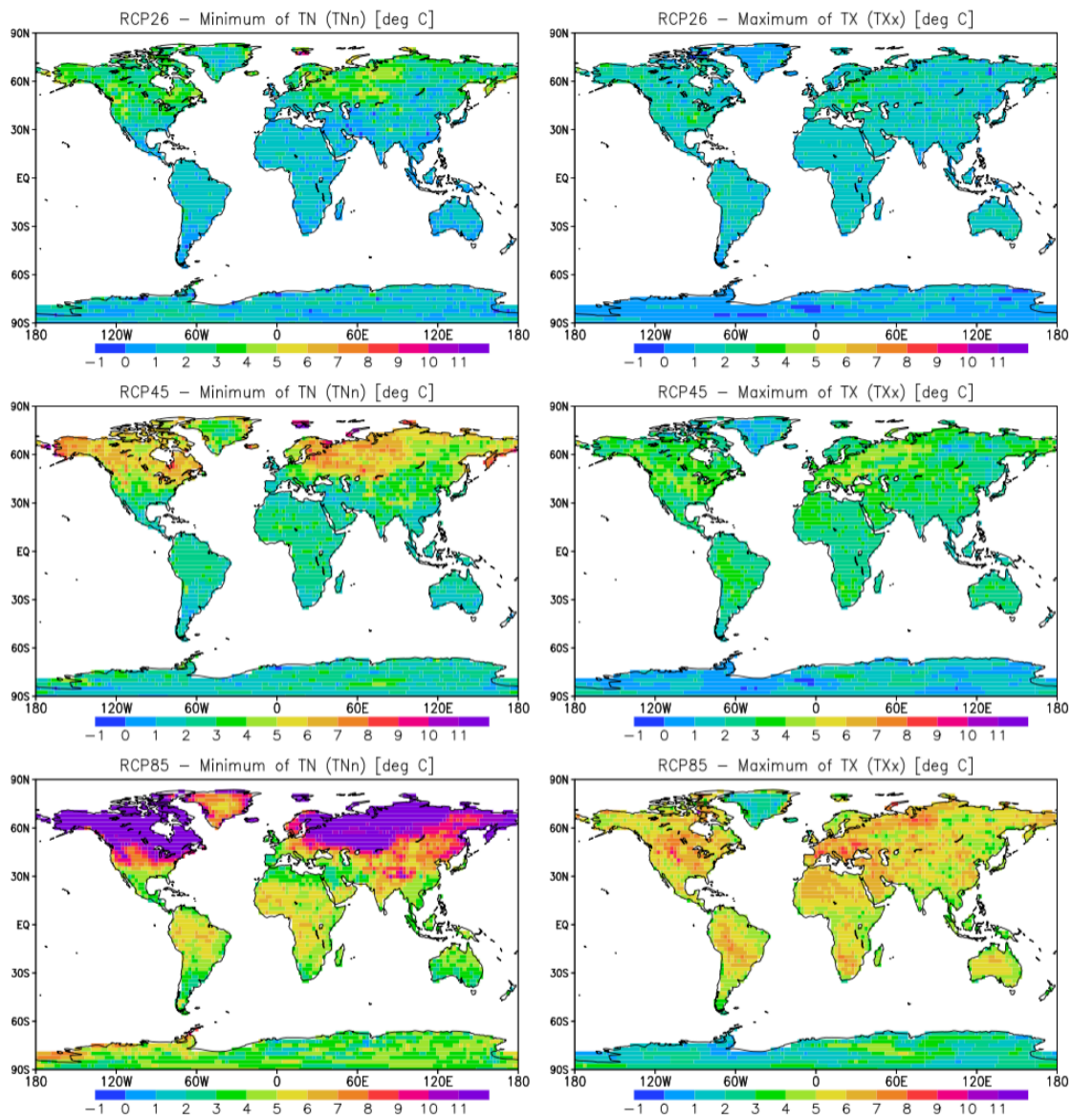


**Figure 3.** The multimodel median of temporally averaged changes in the minimum of TN (TNn, left) and the maximum of TX (TXx, right) over the time period 2081–2100 displayed as differences (in C) relative to the reference period (1981–2000) for RCP2.6 (top), RCP4.5 (middle), and RCP8.5 (bottom). All changes are significant at the 5% significance level. Source: Sillmann et al., (2013b).

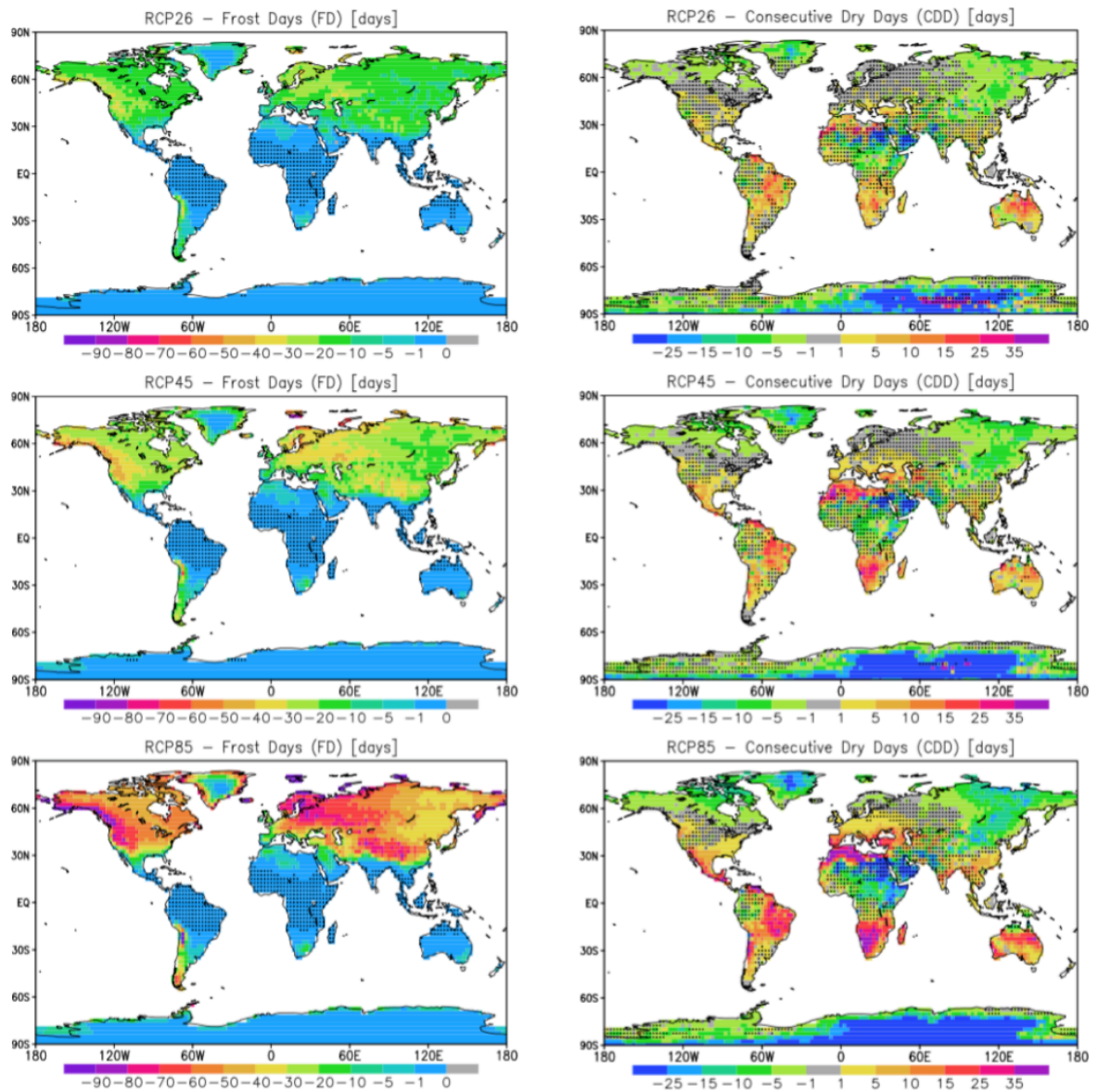


**Figure 4.** The multimodel median of temporally averaged changes in the frost days (FD, left) and the consecutive dry days (CDD, right) over the time period 2081–2100 displayed as differences relative to the reference period (1981–2000) for RCP2.6 (top), RCP4.5 (middle), and RCP8.5 (bottom). Stippling indicates grid points with changes that are not significant at the 5% significance level. Source: Adapted from Sillmann et al., (2013b).

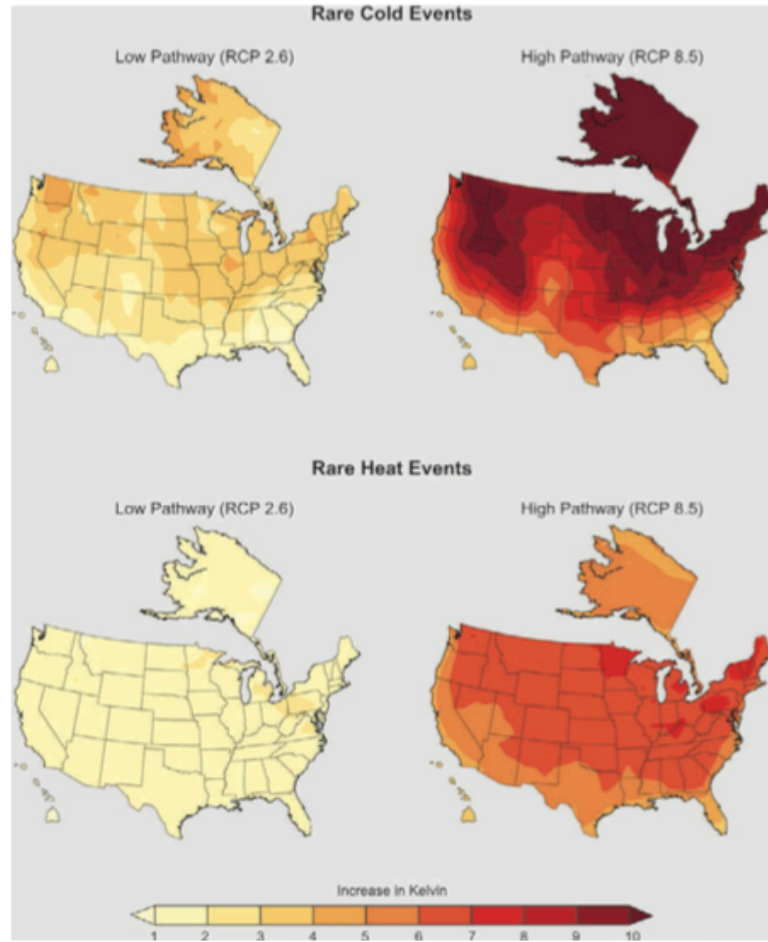


**Figure 5.** Projected change ( $^{\circ}\text{C}$ ) in the 20-yr return value of annual minimum (top) and maximum daily air temperature at the end of this century (2081–2100) relative to the recent past (1986–2005) for the lower (left) RCP2.6 and higher (right) RCP8.5 scenarios.

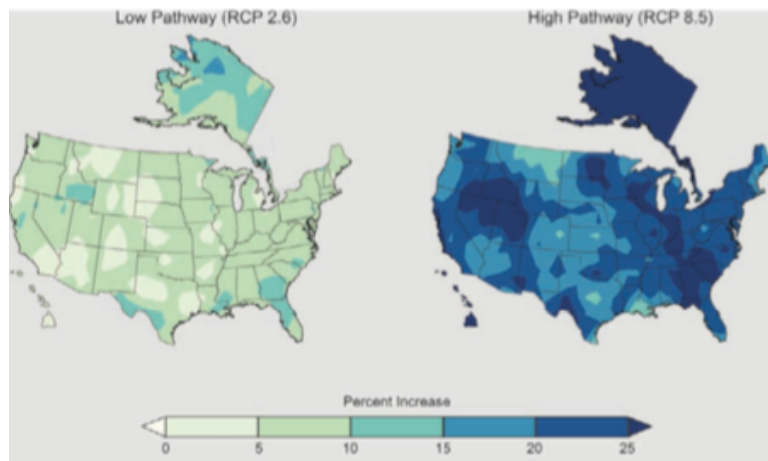


**Figure 6.** Projected change (%) in the 20-yr return value of annual maximum daily precipitation at the end of this century (2081–2100) relative to the recent past (1986–2005) for the lower (left) RCP2.6 and higher (right) RCP8.5 scenarios.

### 2.3. Effect of Climate Change in Agriculture And Water Resources

Climate affects agriculture in many different ways. As stated in Kane et al. (1992), the study of economic effects of climate change on agriculture is of particular importance because agriculture is one of the more climate sensitive sectors. Some examples of this effect are seen in the time of harvest, duration of the phenological stage, irrigation demand and in other areas.

An understanding of the interactions between the different processes in the soil-atmosphere system is essential to evaluate the long-term hydrological response of a crop production system. The study of the impact of climate changes in different aspects of agriculture is important to maintain water, energy and food security. Climate change is expected to result in long-term water and other resource shortages. Also, there may be worsening soil conditions, drought and desertification, disease and pest outbreaks on crops, and others (KOZDROJ & VAN ELSAS, 2000; ASHRAF, 1999). All these scenarios represent a risk for agriculture, water resources, and food security.

According to Adams et al. (1999), agricultural yield is related to physiological changes in crops due to climate change and also to changes in agricultural management practices, crop prices, costs and availability of inputs, and government policies. Also, climate change can decrease the crop rotation period, and for this reason and to maintain a reasonable yield, farmers need to consider crop varieties, sowing dates, crop densities, and fertilization levels when planting crops (CUCULEANU et al., 2002).

Each place of the world has their issues relating to climate change, since the effect of this change is location specific. Because of these differences, some impacts are expected to be favorable and others adverse. In some cases, it is difficult to measure and infer if the impact of climate change will be favorable or not. Individual crop growth processes are affected differently by climate change. Some researchers show the influence of climate change in corn productivity during the growth season (FANCELLI et al., 2005; DOURADO NETO, 1999; DUARTE & CRUZ, 2001).

The rise in temperature can increase the capacity of air to retain water vapor, and can cause higher crop water demand. In response to these changes, plant ecosystems may increase the biodiversity or suffer negative influences. According to Fuhrer et al. (2006), the effect of climate change on the potential productivity of agricultural systems range from extremely negative (in areas that were already water-limited) to positive (in areas that were temperature-limited). Easterling et al. (2007) infer that associated effects of higher temperatures and altered patterns of precipitation will probably combine to reduce yields.

Changes in climate can affect agriculture by solar radiation, temperature, wind, precipitation, among others meteorological variables. Besides the importance of the climate elements, it is also necessary to understand the best way to manage the soil, drainage system implanted and others components. Although crop biomass is predicted to increase in response to elevated CO<sub>2</sub> concentrations under many circumstances, it is also predicted that crops and soils may subsequently become nutrient limited, especially regarding nitrogen availability (DIAZ ET AL., 1993).

The variation of the patterns of climate conditions is important to agriculture and will affect the rainfall, evaporation, runoff and soil water storage. For example, a seasonal rise in temperature may increase the developmental rate of the crop, resulting in an earlier harvest. In the other hand, if the precipitation rate increase in dry regions this could allow the crop to increase.

Some researchers evaluate that the increase in the occurrence of extreme events, as total annual precipitation changes, often results in massive crop losses and other flood-related damages (CHAGNON et al., 1997; PIELKE & DOWNTOWN, 2002).

According to Rosenzweig & Hillel (1998) in middle and high latitudes, climate change could lead to the extension of the length of the potential growing season, allowing earlier planting of crops in the spring, earlier maturation and harvesting. As a result, there is a possibility of two or more cropping cycles during the same season. Regarding this research, also the authors indicated that moisture stress and extreme heat during flowering, pollination, and grain filling is harmful to most crops, such as corn, one of the most important commodity crops in the Midwestern United States. They concluded that the precipitation reduction could intensify further aquifer exploration for agriculture and place additional burdens on other surface and groundwater resources from nonagricultural use. On the other hand, the increase of potential evapotranspiration can intensify drought stress.

Chiotti and Johnston (1995) infer that future climate change could have significant impacts on agriculture, especially the combined effects of elevated temperatures, increased probability of droughts, and a reduced crop water availability, compromising productivity. Some researchers have been studied the effect of climate change on the frequency of floods and droughts all over the world. Some examples of this effect are reported by Mirza (2007), who infers that climate change will increase the frequency of floods and droughts in South Africa. Palmer and Raisanen (2002) conclude that currently observed trends toward increased precipitation and more extreme events are projected to intensify under future climate change, leading to higher flooding probability (according to McCarthy et al., 2001; Reilly et al., 2001) and increased damage to agricultural production compared to present.

According to Hallema et al. (2014), soil water dynamics depends on the local weather (precipitation, solar irradiance, temperature, and the wind), vegetation (distribution of the root system, growth stage), soil characteristics (texture, soil type, porosity) and upstream drainage area. Water availability, the frequency of runoff and surface flux will be an important factor for crop production and food security, so it is important to determine the impacts of climate change on crop production and water resources to develop possible adaptation strategies. A review of Kang et al., (2009) shows that the frequency of droughts and floods will increase under future climate conditions. According to Saarikko and Carter (1996) important direct effects will be through changes in temperature, precipitation, the length of growing season, and timing of extreme or critical threshold events about crop development. This can lead to a reduction of food quality and security. Also, the relationship between the behavior of vegetation under enhanced CO<sub>2</sub>, the effect of nutrient limitation and processes impacting infiltration, seen to be an effective way to study the impact of climate changes over agriculture.

Many studies only consider mean temperatures under climate scenarios. Although both changes in temperature and precipitation affect agriculture, hydrological models show that runoff and streamflow are more sensitive to rainfall than to evapotranspiration. Katz and Brown (1992) showed that for a given climate variable, a change in the variance has a larger effect on agricultural cropping systems than does a change in the mean. Guo et al. (2002) studied the climate change impacts on the runoff and water resources. They used GIS and GCMs and pointed out that runoff is more sensitive to precipitation variation than to temperature increase in China.

Soil water balance is important for the water management and water use strategy. Is expected that climate change will turn into fluctuations of temperature and rainfall, which can compromise soil evaporation and plant transpiration. De Silva et al. (2007) stated that the water balance would change with precipitation and evapotranspiration, and the resultant fluctuations in soil moisture status. Also, climate change impacts on water

balance may present changes in soil water storage, groundwater level, soil moisture status and can provide some information about irrigation quantity.

Some studies found changes in groundwater recharge in future scenarios. Study this impact is important because this is an international concern, considering that groundwater supplies a large part of a demand for drinking water. Increases in groundwater temperatures have been observed due to the rapid climate warming experienced in the past century. This increases in groundwater temperature could also affect bio-geochemical processes and consequently, groundwater quality. Increases in groundwater and soil temperatures could impact groundwater quality, harm groundwater-sourced ecosystems and contribute to the geotechnical failure of critical infrastructure (KURYLYCK et al., 2014). Groundwater temperatures tend to be cooler than surface water temperature in the summer and warmer in the winter (HAYASHI & ROSENBERRY, 2002).

Research of Crosbie et al. (2013) simulated the future recharge over the Australia continent from 16 GCM's, three emission scenarios and using the WAVES hydrological model and conclude that the range of projected change is large and spatially variable which makes difficult this studies. The authors concluded that in the southern Australia, climate variants projected a decrease in recharge. Serrat Capdevila et al. (2007) also used GCM's to estimate recharge and found that some simulations indicate that the recharge could cease entirely in San Pedro basin (Arizona, USA).

Kay et al. (2009) infer that the majority of uncertainty in the projected climate change appears to stem from the selection of the GCM, although other researchers (CROSBIE et al., 2011; HOLMAN et al., 2009; ROWELL, 2006) indicates that other factors, such as emission scenarios, downscaling methods can also contribute to this uncertainty. Doll (2009) simulated the vulnerability of groundwater to climatic change at the global scale and concluded that the uncertainty in the recharge estimated by two GCM's and two emission scenarios is due to the spatial heterogeneity of projected precipitation. However, uncertainty makes it difficult to characterize the direction of changes in groundwater recharge; it varies according to the GCM model chosen in the research. This makes clear the necessity of evaluating the accuracy of a model before applying it in further simulations.

According to Holman et al. (2012), the best practice for using climate model projections to assess the impact on groundwater was to analyze multiple GCMs and multiple emission scenarios. Teng et al. (2012) simulated the impact of climate change on runoff and also found that the selection of the GCM contributed more than the selection of hydrological models in the hydrological simulations results.

Kurylyk et al. (2013) simulated the annual recharge using GCM's, downscaling techniques and a hydrological model. They studied a region in Canada and found that the most pronounced increase of 58% and a most pronounced decrease of -6% in the annual average recharge, over the period of 2046-2065. Fujihara et al. (2008) pointed out that more important than the demand for water, it is important to evaluate the irrigated area. They concluded that if the irrigated area is expanded under present irrigation efficiency rates, water scarcity will occur.

Excess soil moisture, in addition to direct flood damage, is a major component of crop losses due to extreme precipitation events. Changes in climate will be amplified as a larger change in runoff (BOUGHTON and CHIEW, 2007; SANKARASUBRAMANIAN et al., 2001; WIGLEY and JONES, 1985). Alcamo et al. (2007) studied the changing frequency of extreme climate events to evaluate climate scenarios impacts on food security and water availability in 2020 and 2070s. They concluded that the food production in Russia might be affected by the increase of average water availability, and an increase in the frequency of high runoff events.

Some studies (SCHAAKE 1990; FOWLER et al. 2007; NYENJE and BATELAAN, 2009) have evaluated the interaction between climate changes and dynamic of water in the soil. A way to study this interaction is used observed streamflow data to calibrate hydrological models to do simulations, and then, future and historical runoff are compared to estimate the climate change impact on runoff. Other authors (KAY et al., 2009; WILBY and HARRIS, 2006) examined the sources of uncertainty and suggested that hydrological models have a minor impact on the results of hydrological simulations driven by climate projections. This highlight the importance of study the uncertainty of the climate model to know the limitations of each model and apply an adequate one for the study region.

Jiang et al. (2007) evaluated some models and concluded that hydrological models have similar capabilities in reproducing historical runoff. Also, studies as presented in Chiew (2006) and Jones et al. (2006) showed that some hydrological models estimate that a 1% change in mean annual rainfall resulted in a 2%–3% change in mean annual streamflow, in a region in Australia.

Arnell (1999) studied the effect of climate change on hydrological regimes at the global scale, using two versions of the HadCM model (HadCM2 GGax and HadCM3 GGal). These showed discrepancies in the projection for the middle east of USA. For example, when changes in runoff were analyzed, considering the difference between the projections of 1961 to 1990 (200 to 400 average annual runoff for middle east, according to the authors and using CRU data) and 2050's, one model showed an increase between 50 and 150 mm/year and other the decrease of -150 to -250 mm/year. Figure 7 presented these results. The results presented in this section shows the necessity of an analysis of the accuracy of the model and simulations to the study region.

## 2.4. Importance and Challenges of Corn Crop

The production of corn (*Zea mays* L.) has a large social and economic importance all over the world. Many factors are considered in the production of this cereal, including technological, economic and environmental factors. According to the Ministry of Agriculture, Livestock and Supply in Brazil (Ministério da Agricultura, Pecuária e Abastecimento / (PINAZZA et al., 2007)), in the last 15 years the world consumption of corn increased from 75.83 million tons in 1990 to 680,24 million tons 2005. This represented an average annual growth of 2.4%. Over this period the highest growth in the consumption of corn was in the United States, with an increase of 96.57 millions of tons (Table 1). Therefore, it appears that corn production in the United States has a significant influence on the international scene.

Corn production requires a lot of fertilizer, especially nitrogen fertilizer. According to Fernandes et al. (2006), the inadequate nitrogen supply is considered one of the main limiting factors to grain yield. França & Bahia Filho (1985) studied data from 170 corn-based experiments in Brazil. They concluded that in 90% of the cases, corn had a positive reply from the nitrogen fertilization. However, there is a great concern about the environmental aspects. Therefore, there is a need to minimize environmental impact by reducing losses as immobilization, volatilization, denitrification, and leaching. These processes are widely responsible for the low efficiency of nitrogen fertilizer use (IVANKO, 1972). The increase of lixiviation, associated with the risks and impacts of nitrate as a pollutant in soil and water, shows the necessity of more studies about the behavior of this pollutant in soil and how climate change can affect this behavior. Such studies are very important due to the large social, economic and environmental implication.

## Average annual runoff, 1961–1990 and 2050s

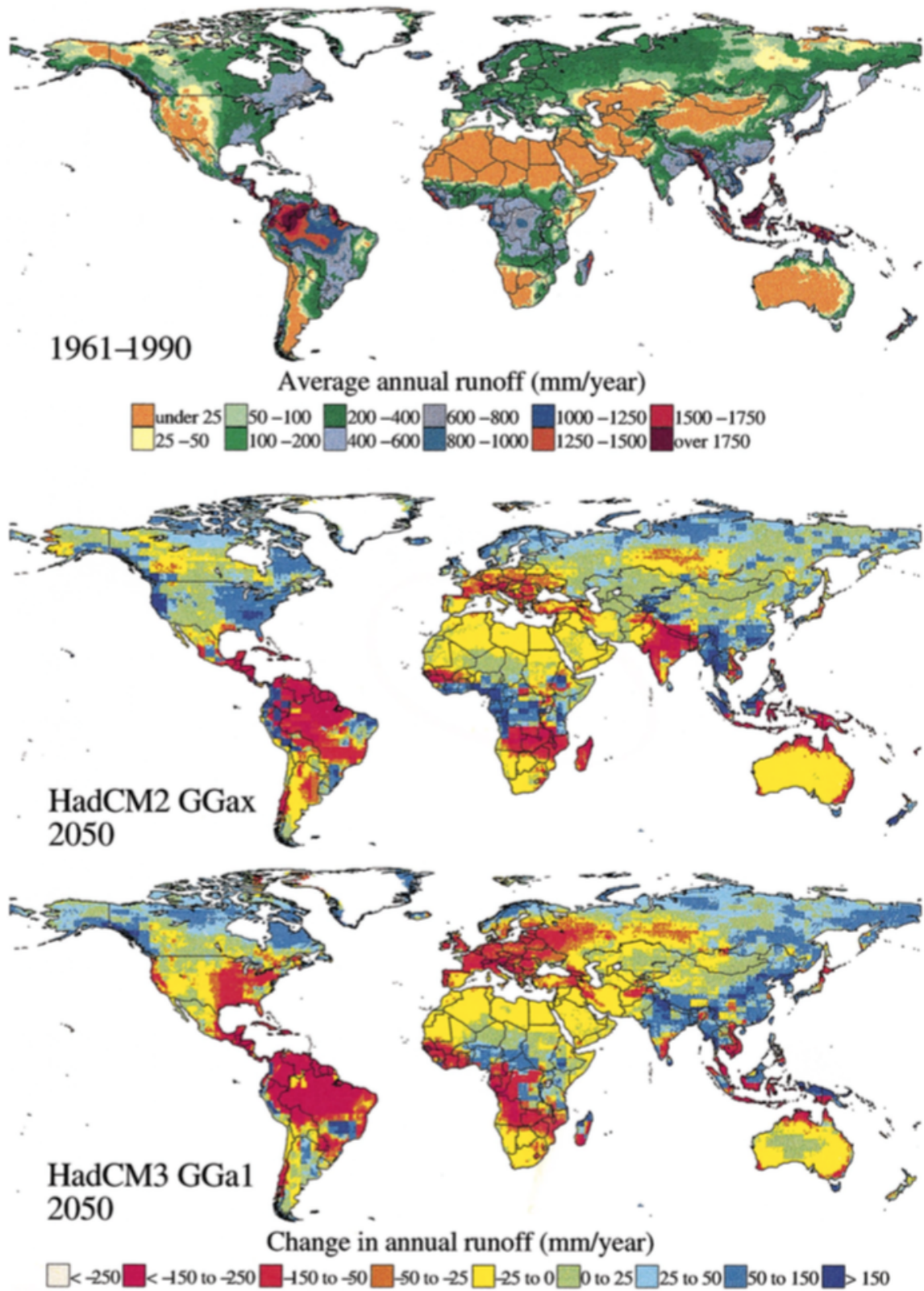


Figure 7. Change in average annual runoff by the 2050s. Source: Arnell et al (1999).

**Table 1.** Variation in corn consumption (millions of tons) by region, between 1989/1990 and 2004/2005.

Ranking	Region	Value*
1	North America	96.566
2	East Asia	58.679
3	South America	20.917
4	European Union	12.204
5	Africa Sub Saara	9.522
6	Southeast Asia	7.156
7	North Africa	6.753
8	Middle East	5.078
9	South Asia	3.854
10	Central America	1.831

\*Value in millions of tons. Source: U. S. Department of Agriculture (USDA)

As stated in the last section, climate change affects agriculture in different ways. According to Borah et al. (2003), it is important to understand the influence of farming practices and the relation between climatic, soil and land use conditions and water quality. One example of this importance is related to the timing of fertilizer and herbicide applications. There is a need to be cognizant of the storm occurrences since this is related to a storm water quality. Nelson et al. (2009) analyzed detailed modeling of crop growth under climate change and concluded that agriculture and human well-being would be negatively affected by climate change. The results show that crop yields will decline, production will be affected, crop and meat prices will increase, and consumption of cereals will fall.

Some studies indicate that the likely impacts of climate change on crop yield can be determined either by experimental data or by crop growth simulation models. Climate changes can also affect payments of crop insurances cooperation. An increase in extreme precipitation events under climate change will likely increase payments from government programs. Changes in the yield of USA can affect the price in the international market, and consequently, have an impact on general consumption.

Mati (2000) studied the influence of climate change on corn production in some areas in Kenya using GCM's. They concluded that to counter the adverse effects of climate change on maize production, it may be necessary to modify some aspects of production as 1) to use early maturing cultivars, 2) practice early planting, 3) or, in some cases, shift to growing maize during the short-rains season.

Southworth et al. (2000) evaluate the future climate change and changing climate variability on maize yields in the Midwestern United States, and found decreases in long-season and medium-season maize yields (Figure 8). Using IPCC models to simulate future climate scenarios in Illinois, they found that the frequency of maize killing freeze events will decrease although under doubled variance scenarios the intensity of the freeze event will increase. This may imply that the increased frost tolerance is not an important issue for future climate change and maize growth as initially expected. They also predicted that Western Illinois would have yield decreases of 10 to 50 % (long-season maize) and 10 to 40 % (medium-season maize). In Eastern Illinois, the yield would decrease by 10 to 40 % (long and medium-season maize), and 30 to 50 % decreases for short-season maize; and by 0 to 40 % for long-season maize, 10 to 40 % for medium-season maize, and 30 to 40 % for short-season maize in Southern Illinois. The results indicate that potential future adaptations to climate change for maize yields would require either increased tolerance of maximum summer temperatures in existing maize varieties or a change in the maize varieties grown. The

authors suggest the development of a more heat tolerant hybrid of long-season maize and changes in planting dates as mitigation measures.

Cuculeanu et al. (2002) studied rainfed maize yield using CERES-Maize, along with the CCCM and GISS climate models, and concluded that the dry matter would increase with the CCCM model but and even more so with the GISS model. Rosenzweig and Hillel (1993) stated that moisture stress and extreme heat during flowering, pollination, and grain filling is harmful to most crops, such as maize, one of the most important commodity crops in the Midwestern United States. Also, warmer climate scenarios showing 2 to 5° C temperature increases in North America, have yielded estimates of adverse impacts in the eastern, southeastern, and Maize Belt regions.

According to some researches, under scenarios of climate change and considering the increase in temperature over the season it is possible that the duration of the crop will change, resulting in yield reduction (ROBERTS and SUMMERFIELD, 1987, PARRY et al., 2007; TAO et al., 2008). Changes in maximum and minimum temperature are determinants in estimating evaporative and transpirative demand (PRIESTLEY and TAYLOR, 1972; RODERICK and FARQUHAR, 2002). As an example, some short episodes of high temperature at critical stages of crop development can cause sterility, and consequently, yield reduction, independently of any substantial changes in mean temperature (WHEELER et al., 2000; MCKEOWN et al., 2005).

Tao et al. (2003a, b) indicate that changes in the temporal and spatial pattern of precipitation directly impact crop water cycle and consequently water stress on crop development. Tao and Zhang (2010) highlighted the importance of addressing the impacts and adaptation options in the 'climate risk hot spot' over seeking effective adaptation strategies for other regions. They concluded, based on a large number of simulation outputs from projections, that for high-temperature sensitive varieties, early planting would be an effective adaptation option to reduce maize yield loss from climate change in North China. Jones & Thornton (2003) generate daily weather data for driving a detailed simulation model of the maize crop and showed the potential impacts of climate changes on maize production in Africa and Latin America. The results indicated an overall reduction of 10% in maize production by 2055.

The US Environmental Protection Agency (EPA) found a decrease in maize yields of 4–42% under conditions of future climate change, due to temperatures rising above the range of tolerance for the maize crop (CARSEL et al., 1998). Rosenzweig et al. (2002) simulate the effect of heavy precipitation on crop growth, plant damage from excess soil moisture and found that the US corn production losses due to this factor may double during the next 30 years, causing an estimated damage of \$3 billion per year.

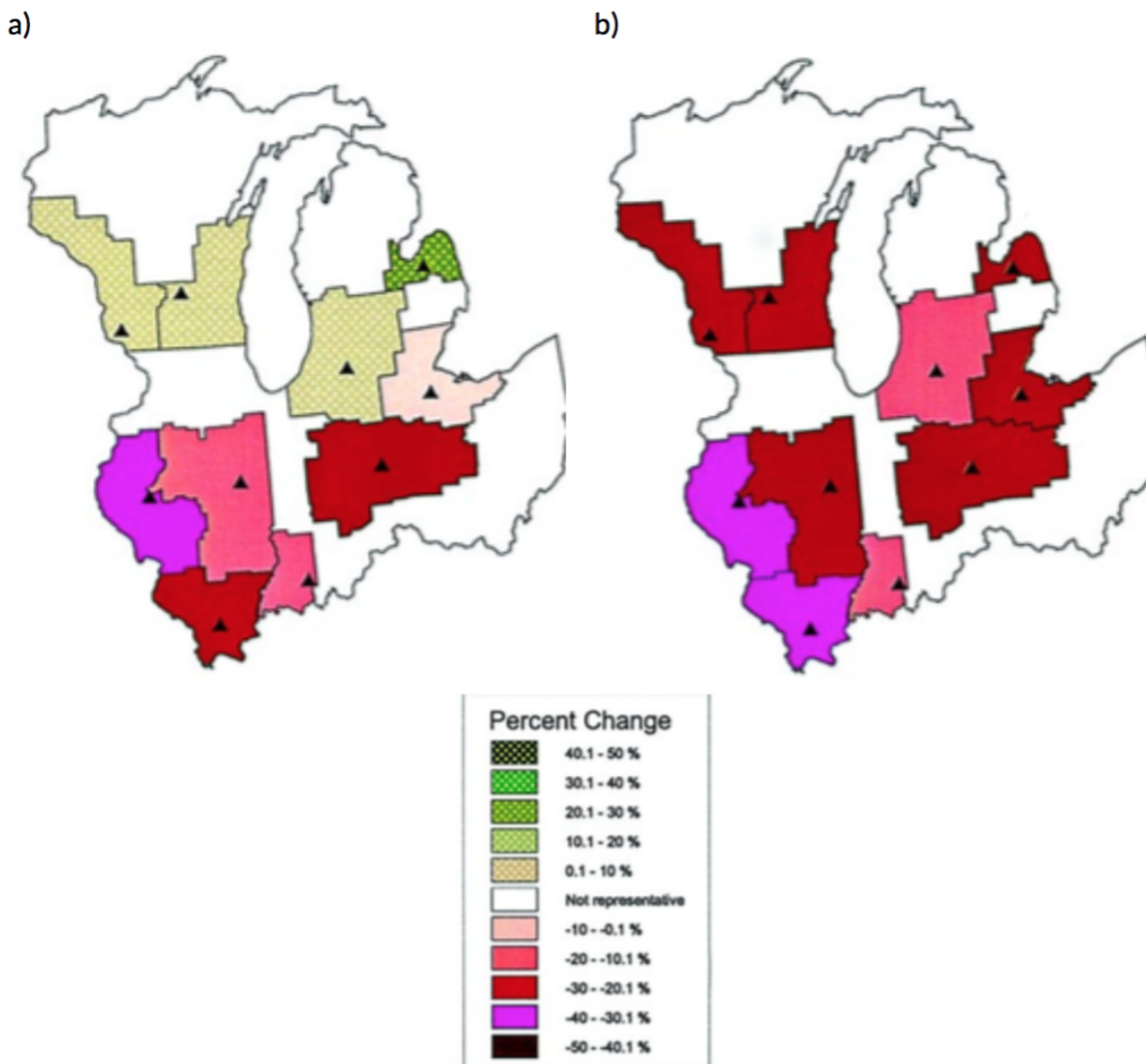


**Figure 8.** Percent change in mean maximum decadal yield for long-season (a) and medium-season (b) maize according to HadCM2. Source: Southworth et al. (2000).

## 2.5. Dynamic Of Water In Soil

Management of water resources in agriculture and tackling the issue of optimal water use, are needed to balance water supply and demand (TUONG and BHUIYAN, 1999; INES et al., 2002). Information on water quality and quantity is important for agricultural water management practices, such as designing irrigation and drainage systems.

The study of the unsaturated zone and the hydrological cycle is necessary, since they are at the interface between atmosphere and groundwater circulation. According to Rienznet et al. (2013), water fluxes in the unsaturated zone affect water status, development and production of crops. From an environmental point of view, these fluxes determine mobilization and transport of solutes and pollutants from the soil surface to the aquifer system.

Water movements can be described in the unsaturated zone using mathematical models based on different approaches to implementing the numerical solution of the Richards' differential equation (GANDOLFI et al., 2006; KROES and VAN DAM, 2003; ŠIMUNEK et al., 2005). Rienznet et al. (2013) inferred that a modelling

approach is particularly interesting at sites where there is a strong interaction between the processes occurring at the soil surface and the groundwater, as in areas characterized by shallow groundwater tables. They describe that in such situations, a water flow towards the roots zone is triggered by the strong potential gradient that occurs when the soil water content nearby the roots becomes very negative. In this case, model simulations can be very useful in the estimation of this upward flux, since a reliable direct measurement is a complex task.

While important for plant water demand, the investigation of groundwater, dynamic of water, and its redistribution within the soil and rootzone is complex because it involves processes that depend on the soil type and plant characteristics (HOWELL, 2001; GARRIGUES et al. 2006; Shah et al. 2007). Soil hydraulic properties, depth to the water table, soil moisture content, infiltration, root morphology, and plant physiological status strongly control water uptake at the root zone scale and consequently the productivity.

The planning and management of the use of water resources in the soil-plant-atmosphere system, require an understanding of physical processes of flow, and water storage in the soil. Due to the precision, facility, and speed to achieve results, computational models become an important tool for the prevention of environmental impacts (MIRANDA et al., 2005).

Mathematical modeling in the soil allows the monitoring of water in a fast and accurate way, preventing environmental impacts due to infiltration and drainage processes, evaporation, and water balance. Modeling is important in hydrological studies and helps the analysis of the risk in the management of surface and subsurface waters. By theoretically describing the physical processes occurring in the soil, combined with numerical techniques to solve the resulting equations, and adequate computational resources, it is possible to predict the risk and impacts that climate change can cause in soil, water and plants.

Is important to investigate relationships among the hydraulic and physical parameters and soil wetting patterns as affected by drainage design and management practices. In this context models are used to perform predictions of variables of hydrological cycle, and those models are expected to be useful in decision-making processes focused on hydrological issues (BEVEN, 2001).

Melo & Louzada (2012) used two models to evaluate the dynamics of water in soil (Hydrus and SWAP). Those models are extensively used to quantify water balance and soil water dynamics in agricultural scenarios. From their research they concluded that both models presented good performance to represent hydrological variables. Study the dynamic of water is necessary due to the importance of potable water for life and due to the vulnerability in terms of sensitivity to climate conditions.

In order to study the impacts of climate change on soil water dynamics, the Hydrus model is often used to simulate hydrological variables, such as surface flow, soil water storage, runoff, infiltration, among others. The Hydrus software is a mathematical model with practical application for the technological development of production.

Cordeiro et al. (2005) found that simulations using Hydrus-1D could satisfactorily predict soil water content and upward fluxes during short periods of time. Leterme & Mallants (2011) studied the impact of climate on groundwater recharge, also using Hydrus-1D and weather time series. Results showed that transition to a warmer climate is expected to yield a decrease in groundwater recharge.

The Hydrus model, based on the use of finite elements, is used to simulate the movement of water, solutes, and heat in the soil. The use of this model also requires a knowledge of the soil properties and atmospheric and boundary conditions. In the program water flow is described by solving the Richard's equation numerically. This flux equation can include a parameter to account for root water uptake. The equation for heat transport incorporates both conduction and convection of water. This program can also be use to analyze the water and solute movement

in unsaturated, saturated or partially saturated soil. More information about Hydrus model can be found at <http://www.pc-progress.com/en/Default.aspx?hydrus-2d#k1> .

All information regarding equations and parametrizations of Hydrus model are given in the Methodology section.

### 3. MATERIAL AND METHODS

#### 3.1. Climatological Analysis

##### 3.1.1. Study Area and Climatological Data

The study area is the region of Urbana-Champaign, in Champaign County, Illinois (United States of America). This region has a humid continental climate. This area is located in an important region of maize production.

The observed meteorological data in the region was given from a meteorological station located by the coordinates 40.0839°N and 88.2403°W, as shown in Figure 9. The altitude of the area is 219 meters. The data set includes meteorological variables provided by the Water and Atmospheric Resources Monitoring Program. The daily and monthly data set is available from 1901 to 2015 and includes the variables: rainfall and maximum, minimum and average temperature.

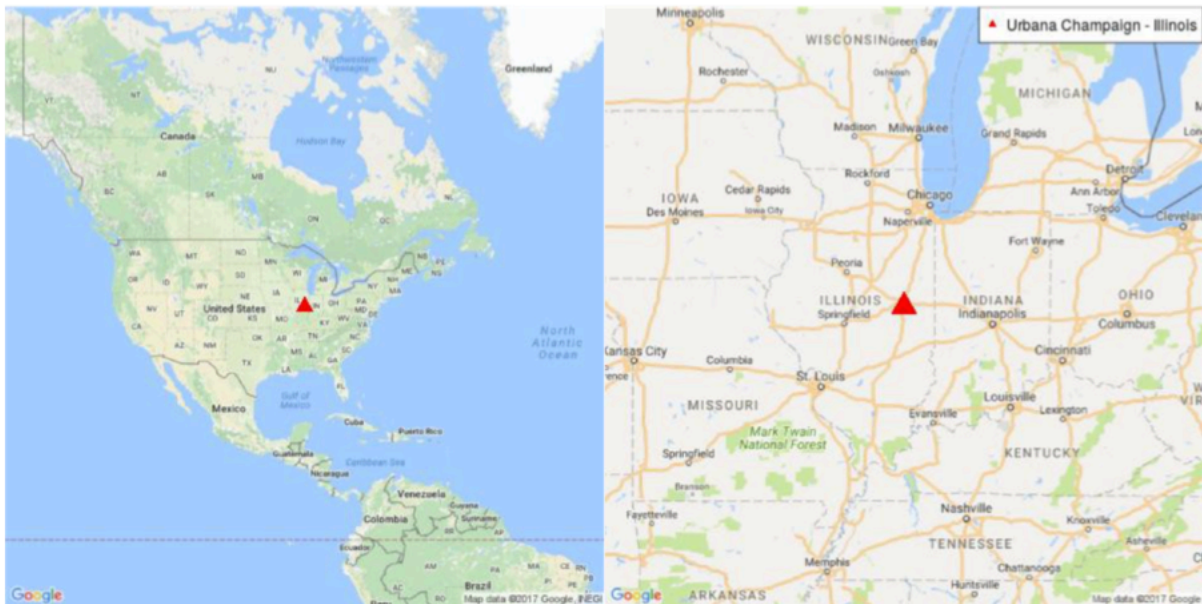


**Figure 9.** Location of meteorological station in Champaign (Illinois, USA).

The monthly data from the weather station were analyzed to describe the climate in the area. Building this climatology is important because it is possible to infer if there is any evidence of climate changes during the studied period and if there is, try to find the hypotheses that fit better the found pattern. It also sought to identify possible patterns of climate change from the analysis of the anomalies of the climatological variables, considering the period of 1901 to 2016. These anomalies were calculated from the deviation of the observation regarding the local climate (average period).

In addition to the analysis of climatology and anomalies, observed data also allowed the evaluation of climate projections models. Historical simulations of studied models were compared with observed data obtained

from the weather station, so it was possible to evaluate the accuracy of the projections of those models. More information about this methodology and the climate models projections are described in the next section.

The daily data is also used to describe the occurrence of extreme events in the region. Some climate models can approach the average values of the variable but have difficulty in forecasting extreme events, mainly with long-term simulations. This limitation is an issue considering that, in general, the extreme events can have a bigger impact on agriculture. In Section 3.1.3. the calculation of the indices to describe extreme events occurrence are outlined.

### 3.1.2. CMIP5 Climate Projections Models and Associated Errors

According to the fifth IPCC report (STOCKER et al., 2014), climate projection models simulate changes based on a set of scenarios. A new set of scenarios, the Representative Concentration Pathways (RCP's) were created from long-term integrations with possible greenhouse gas emission scenarios in the atmosphere and their impacts on climate variables. These scenarios are used as an input to weather and chemical modeling of the numerical experiments CMIP5 and were created for different ranges: high emission range (RCP8.5, i.e. a radiative forcing setting of  $8.5 \text{ W.m}^{-2}$ ), moderate emission (RCP4.5) and low emission (RCP2.6) as described by Moss et al. (2010).

Figure 10 indicates the surface temperature and precipitation changes according to different emission scenarios. More information about the various scenarios of emission in the CMIP5 models, including projections of  $\text{CO}_2$  accumulation and average temperature indicated by each scenario, are shown in Figure 11.

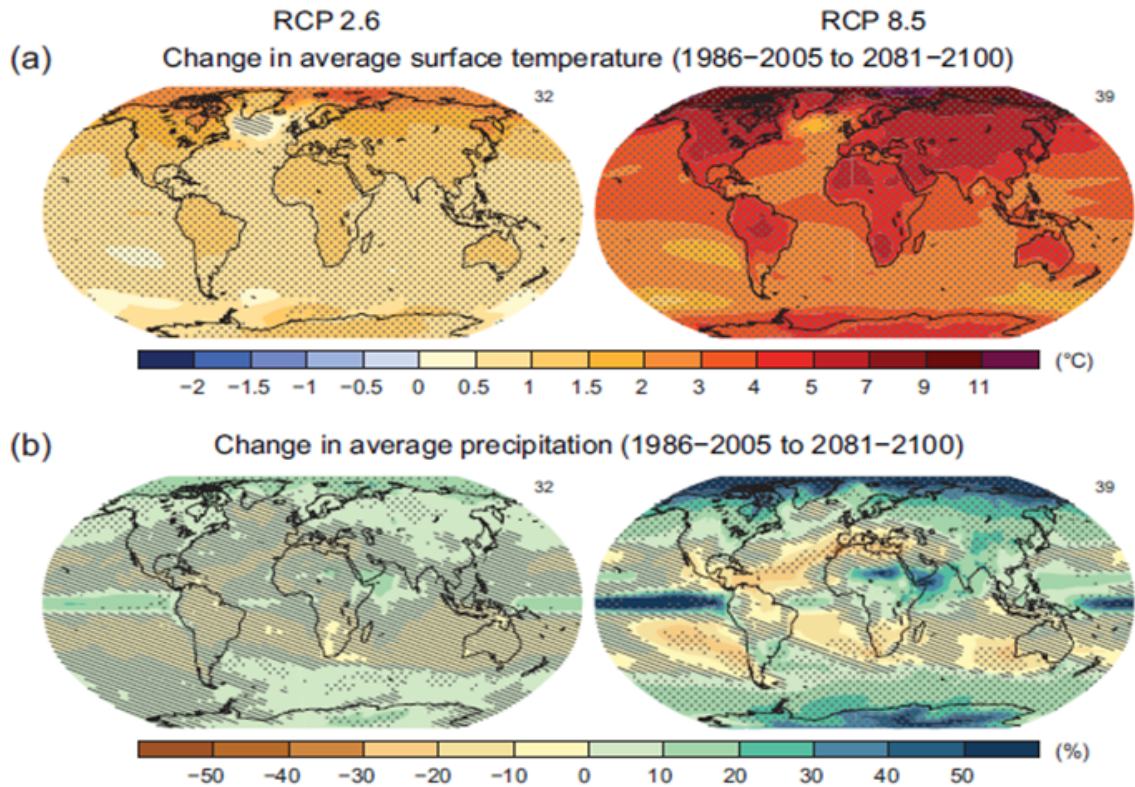


**Figure 10.** Maps of the multi model CMIP5 for RCP2.6 and RCP8.5 simulated scenarios, considering the difference between the future years (2081 to 2100) and the past years (1986 to 2005 - can also be expressed as "current climate"), where: (a) the average percentage of annual precipitation. The number of CMIP5 models used to calculate the mean multi-model is shown in the upper right corner of each panel. Source: (STOCKER et al., 2014).

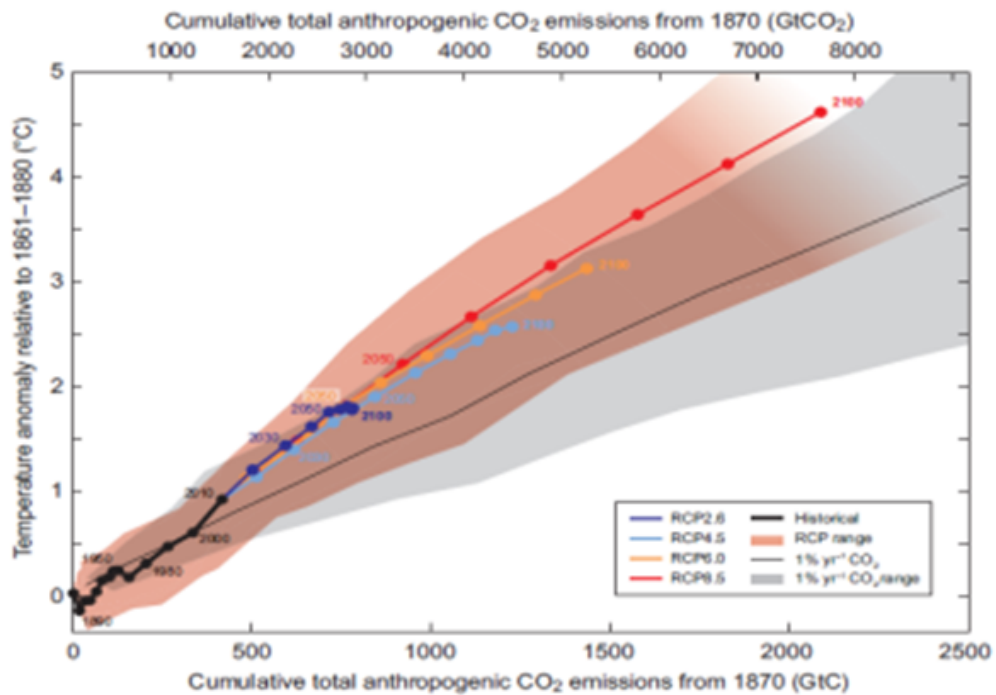


**Figure 11.** The global increase of average surface temperature as a function of the total emission of CO<sub>2</sub> accumulated until 2100. Source: (STOCKER et al., 2014).

Research based on data developed by CMIP are widely used by the academic community. More information about the CMIP5 data can be obtained from the website: <http://cmip-pcmdi.llnl.gov/cmip5>.

Daily CMIP5 data, from 1901 to 2100, for 14 models were selected covering historical periods and predictions for three different emission scenarios (RCP2.6, RCP4.5, and RCP8.5). The historical experiment included simulations for 1901-2012, that used to evaluate the errors of future projections (RCP's from 2006 to 2100). These RCP's are a set of projections of concentration of greenhouse gases and their emission pathways in order to support research on the impact and possible policy responses to climate change.

The chosen models, their respective research centers, home countries and horizontal resolution of each model, are listed in Table 2. Using historical data is possible to compare the observed data from meteorological stations with the model projections. The climatic variables precipitation and temperature (mean surface, maximum and minimum) were analyzed. This method allows for the identification of errors in the projections.

The analyzed indices were Mean Bias Error (MBE), Mean Absolute Error (MAE), Root Mean Square (RMSE), systematic part of the RMSE ( $RMSE_s$ ), unsystematic part of the error RMSE ( $RMSE_{us}$ ), correlation (C) and R-square ( $R^2$ ).

The Mean Bias Error (MBE) was used in order to show information about the performance of the model in the long term simulation. A positive values indicate overestimation and negative values indicates underestimation. However, caution is necessary when using this index, as positive values can be canceled by negative values, resulting in erroneously low bias values. For this reason, a good approach is to analyze MBE together with the Mean Absolute Error (MAE). The MAE accumulate the errors, independently of the sign. According to Carvalheiro et al. (2008), MAE indicate the distance from the predicted values to the observed values.

**Table 2.** Models from CMIP5 with simulations of RCP4.5, RCP6 and RCP8.5 scenarios of climate changes.

Model	Country	Center	Resolution
BCC-CSM	China	Beijing Climate Center	2.8° x 2.8°
CanESM2	Canada	Canadian Centre for Climate Modeling and Analysis	2.8° x 2.8°
CNRM-CM5	France	Centre Europeen de Recherche et For- mation Avancees em Calcul Scienti que	1.4° x 1.4°
FGOALS-G2	China	Institute of Atmospheric Physics	3.1° x 2.8°
GFDL-CM3	USA	Geophysical Fluid Dinamics Laboratory	2° x 2.5°
GFDL-ESM2G	USA	Geophysical Fluid Dinamics Laboratory	2° x 2.5°
GFDL-ESM2M	USA	Geophysical Fluid Dinamics Laboratory	2° x 2.5°
IPSL-CM5-LR	France	Institut Pierre-Simon Laplace	1.9° x 3.8°
IPSL-CM5-MR	France	Institut Pierre-Simon Laplace	1.3° x 2.5°
MIROC5	Japan	Atmosphere and Ocean Research In- stitute, National Institute for Environmental Studies, and Japan Agency for Marine-Earth Science and Technology	1.4° x 1.4°
MPI-ESM-LR	Germany	Max-Planck-Institut für Meteorologie	1.9° x 1.9°
MPI-ESM-MR	Germany	Max-Planck-Institut für Meteorologie	1.9° x 1.9°
MRI-CGCM3	Japan	Meteorological Research Institute	1.1° x 1.1°
NORESM1M	Norway	Norwegian Climate Centre	1.9° x 2.5°

Root Mean Square (RMSE) provides information about the performance of the model in the short term. In this case, the lower the value, the lower the dispersion of data around the model. The handicap is that a few outliers can generate a significant increase in its magnitude. The RMSE can be divided into systematic and unsystematic errors. The systematic errors show the tendency of the model in sub estimate or over estimate a variable. The unsystematic error is the intrinsic error of the model.

Correlation indicates the meaning statistical relationships between two or more random variables or observed data values. R square ( $R^2$ ) is a number that indicates the proportion of the variance in the dependent variable that is predictable from the independent variable and varies from 0 to 1. Higher values of  $R^2$  means that the model has a good adjustment to the observation.

These indices were calculated from the equations below.

$$MBE = N^{-1} \sum_{i=0}^n (P_i - O_i) \quad (3.1)$$

$$MAE = N^{-1} \sum_{i=0}^n |P_i - O_i| \quad (3.2)$$

$$RMSE = N^{-1} \sum_{i=0}^n \sqrt{(P_i - O_i)^2} \quad (3.3)$$

$$RMSE_s = N^{-1} \sum_{i=0}^n \sqrt{(P_i' - O_i)^2} \quad (3.4)$$

$$RMSE_{us} = N^{-1} \sum_{i=0}^n \sqrt{(P_i^* - O_i)^2} \quad (3.5)$$

$$COR_{OP} = N^{-1} \sum_{i=0}^n \frac{(O_i - \mu_o)(P_i - \mu_p)}{\sqrt{(P_i - P_i')(P_i - \mu_p)}} \quad (3.6)$$

$$R^2 = 1 - \frac{SS_{res}}{SS_{tot}} \quad (3.7)$$

$N$  is the number of observations,  $P_i$  means the predicted values and  $O_i$  are the observed data.  $P_i'$  is the result of the linear regression between  $P_i$  and  $O_i$ .  $SS_{res}$  and  $SS_{tot}$  are the sum of squares of residuals and the total sum of squares, respectively.

Although climate models are good tools, they also have some limitations and therefore should be used with caution. These limitations occur largely due to the uncertainties of the current forecasts, related to simplifications and parametrization required for models. Study this issue is essential to conduct research in order to verify the regions where these systematic errors are more prominent. The errors were calculated from the historical experiment (1900 to 2012) and observed data collected in meteorological stations in the region for the same period. The variables analyzed were rainfall, and maximum, minimum and average temperature. The model with lower errors was chosen after the statistical analysis of the performance of the models in the simulation of climatic conditions in the study area.

### 3.1.3. Extreme Events Detection

The study of extreme climate events and their changes are very important due to their strong impacts in society. Indices that estimate the occurrence of extreme events are used as good tools to indicate changes in climate. The indices were established by the World Meteorological Organization (WMO), the Research Program Climate Variability and Predictability (CLIVAR) and the Expert Team Climate Change Detection Monitoring and Indices (ETCCDMI). The Special Report on Extreme Events (SREX) of the Intergovernmental Panel on Climate Change (STOCKER et al., 2014) emphasized this impact. The indices can be used in different fields and applied to different researches, due to their straightforward calculation and interpretation. In this research, the indices were used to define the model with more accurate simulations to the study region and to infer about the difference of these extremes under different emission scenarios that represent climate changes.

The literature review showed the effects of the occurrence of extreme events over different sectors and scale. Due to this issue, the selected indices (Table 3) was calculated in order to quantify the occurrence of these extremes on observed and projected data and evaluate how accurate the models can simulate extreme events.

Indices were selected due to their extensive use in academic research, which makes it easy to compare the results with other studies and have a more accurate dataset. The indices are calculated daily for the historical simulation and projected scenarios RCP2.6, RCP4.5 and RCP 8.5.

Is important to highlight some differences between this indices. The indices can be divided into: 1) absolute, 2) threshold, 3) percentile and 4) duration indices.

**Table 3.** Indices to quantify the occurrence of extreme events in Champaign (IL).

Index	Description	Unit
RX1DAY	Maximum rainfall (RR) occurred in one day over the period.	mm
RX5DAY	Maximum RR occurred in interval of five days over the period.	mm
CDD	Consecutive Dry Days. Maximum number of consecutive days with $RR < 1\text{mm}$ .	days
CWD	Consecutive wet days. Maximum number of consecutive days with $RR \geq 1\text{mm}$	days
SU	Number of summer days: Annual count of days when $TX > 25^\circ\text{C}$ .	days
FD	Number of frost days: Annual count of days when $TN < 0^\circ\text{C}$	days
ID	Number of icing days: Annual count of days when $TX < 0^\circ\text{C}$	days
TXx	Maximum value of daily maximum temperature	$^\circ\text{C}$
TXn	Minimum value of daily maximum temperature	$^\circ\text{C}$
TNx	Maximum value of daily minimum temperature	$^\circ\text{C}$
TNn	Minimum value of daily minimum temperature	$^\circ\text{C}$
DTR	Daily temperature range: Mean difference between TX and TN	$^\circ\text{C}$

The absolute indices are based on absolute values of temperature and precipitation. In this research, the absolute indices of temperature are minimum and maximum of TN (TN<sub>n</sub> and TN<sub>x</sub>), maximum and minimum of TX (TX<sub>x</sub> and TX<sub>n</sub>), and daily temperature range (DTR). TN<sub>n</sub> and TN<sub>x</sub> represents the coldest or hottest day of a year, respectively. Absolute indices used to measure extreme events of precipitation were RX1DAY and RX5DAY which represents the maximum accumulated amount of precipitation in one (or five) day precipitation. According to Frich et al. (2002) this index is often used to describe changes in potential flood risks as heavy rain conditions over several consecutive days can contribute to flooding conditions.

The threshold indices used were, frost days (FD) which count the days when TN is below 0°C, icing days (ID) when TX is below 0°C, and summer days (SU) when TX is above 25°C. Those indices are particularly important for agriculture. Terando et al., (2012) states that changes in frost days can be relevant for agricultural practice and engineering applications.

The duration indices used were the indices CDD and CWD which are related to the consecutive days necessary to consider some event as an extreme event. CDD represents the length of the longest period of consecutive dry and is the only ETCCDI index that describes the lower tail of the precipitation distribution and is often referred to as a drought indicator. CWD represents the length of the longest period of consecutive wet.

Also, the indices can be associated with other studies and give a background regarding the climate changes impacts and relate those with other variables related to agriculture (flow, infiltration, runoff, and others). Box plots were used to analyze this data. This chart gives the variability of the indices between the studied years facilitating the comparison between the projections of the models in historical simulation (1901 to 2012). Besides, the chart can also show the median values and the range that represents 50% of the data.

## 3.2. Experimental Field Data

### 3.2.1. Study Area

In order to analyze the dynamic of water in the soil, the research was conducted in a Research Farm at University of Illinois at Urbana-Champaign (UIUC). The region is in the Illinois state, middlewest of USA with coordinates 40°04'18.68"N and 88°12'45.08"W. This area belongs to the Department of Agricultural and Biological Engineering (ABE) of UIUC. The drainage system associated with each field is presented in Table 4.

This is a region with groundwater near to the surface. This area has been monitored and has available information about the level of groundwater and flow. The region is located in the central part of the state of Illinois and is part of the region with the higher concentration of drainage systems in USA (COOKE & VERMA, 2012).

The area has continental climate, with an annual average temperature around 11.05°C and 968.8 millimeters of accumulated annual rainfall. The maximum and minimum annual temperature are around 16.46°C and 5.66°C, respectively. The climatological analysis of the region will be made in order to study the occurrence of extreme events and how climate changes may affect this occurrence.

**Table 4.** Drainage system configuration in the experimental field in Champaign (IL).

Field	Spacing between drains	Depth of the drains
ANW	18.3	0.76
ASW	24.4	1.07

### 3.2.2. Experiment Configuration

The field was planted to corn over the period of study. Each field is approximately one hectare in size. The cultivation period is between April and September. This experiment was accomplished in the year of 2015. Figure 12 presents the corn field in different stages, in months: a) May, b) July and c) September 2015.



**Figure 12.** Corn field located in Champaign (Illinois, USA) in a) May, b) July and c) September, 2015.

Table 5 shows information about the fertilizer and pesticides applied in the field during the experiment. These products were applied before planting, in 04/29/2015, and post emergence, in 06/28/15.

**Table 5.** Fertilizers applied in the fields, before planting and post emergence, in 2015.

Date	Product	Quantity
04/29/2015	SOLUTION UAN28	70 Gal/Acre
04/29/2015	86.700 LB AGROTAIN PLUS (EZ-FLO)	3.00 LB/Acre
04/29/2015	21.675 GL LUMAX EZ	3 QT/Acre
04/29/2015	7.225 GL INFANTRY 4L	1 QT/Acre
06/28/2015	LIBERTY 280 SL	29 GL/Acre
06/28/2015	FS AMS MAX DR BULK	24 OZ/Acre

UAN28 is a solution of urea and ammonium nitrate in water used as a fertilizer. This solution has 40% ammonium nitrate, 30% urea and 30% of water. According to the manufacturers, AGROTAIN PLUS nitrogen stabilizer is a product which contains the premier urease enzyme inhibitor technology and a proven nitrification inhibitor that protects nitrogen from ammonia volatilization, denitrification, and nitrate leaching. The product information sheet describes Lumax EZ herbicide as a combination of three highly effective active ingredients used for control of annual grasses and broadleaf weeds in the corn field. Infantry 4L is a restricted-use herbicide due to ground and surface water concerns, used for season-long weed control in corn crops. LIBERTY 280 SL HERBICIDE is a non-selective herbicide that provides control of a broad spectrum of broadleaf and grassy weeds. FS AMS MAX is a convenient-to-use liquid adjuvant premix of nonionic surfactant and ammonium sulfate. FS AMS MAX is designed to enhance the performance of crop protection products that benefit from the inclusion of a non ionic surfactants, ammonium ions and the water conditioning features of ammonium sulfate. All these information can be found in the respective product label.

The data was collected at 15 minutes intervals, from April to September (2015), a total of 183 days. Figure 13 shows the data-loggers used in the field. Flow was derived from measured depths over V-Notch weirs. These weirs were field calibrated to ensure that the values from the Weir equation matched the observed values.

**Figure 13.** Data-loggers installed in the field and used to collect data in a frequency of 15 minutes.

The data was collected in the corn fields (ANW and ASW), as presented before. The following scheme in Figure 14 represents the drainage system of the region and the meteorological variables that may have influence over the dynamics of water in the soil.

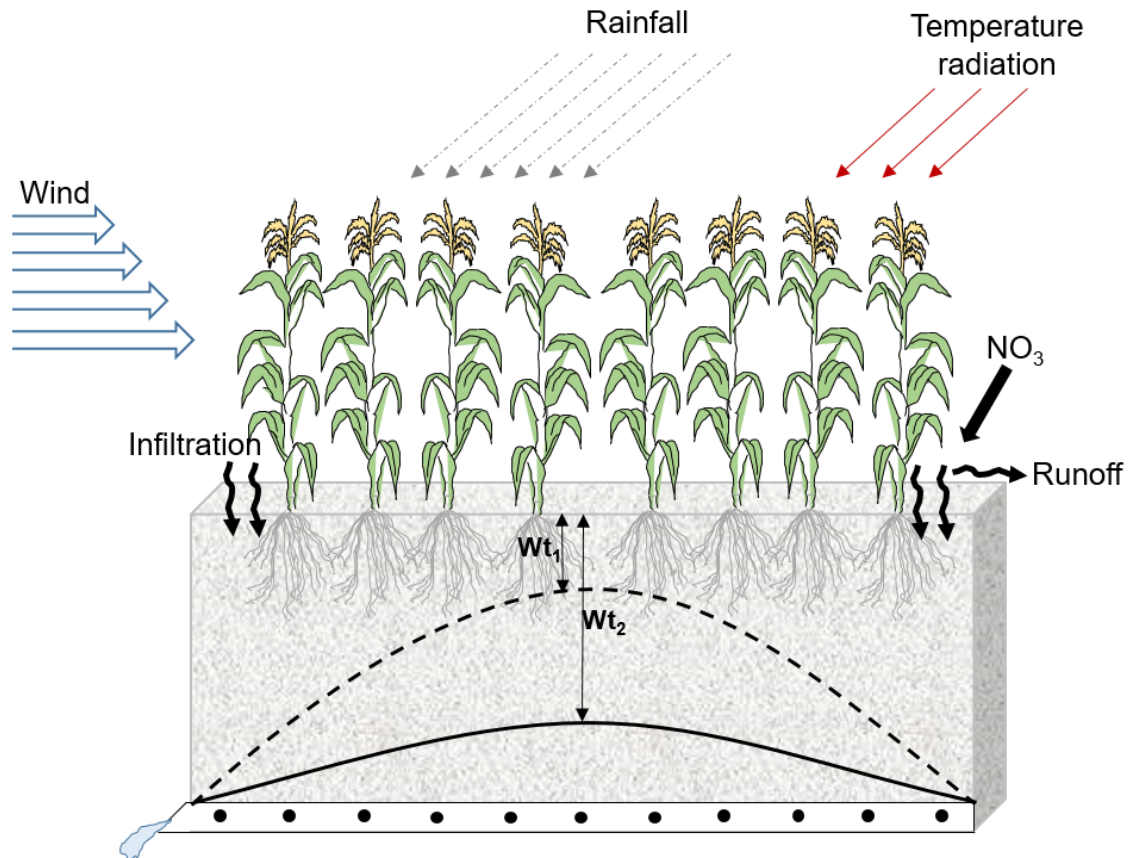


**Figure 14.** Scheme of the drainage system and the variables that affect the dynamic of water in soil, where  $w_{t1}$  and  $w_{t2}$  are the water table depth in different positions.

The data from the meteorological station (Figure 15) was also collected at 15 minutes intervals from April to September 2015. The meteorological station was installed in the field during the experimental site. In order to check if the values were consistent, it was compared the data from the meteorological station in the city of Urbana (Illinois, USA), near to the experiment. However, in comparing both stations, it was noticed that the one installed in the field underestimated wind speed. This was probably due to the height of the corn crop as it grows. For this reason, in the middle of the experiment, the position of the station was changed. Data from both stations were combined and used as an input to the mathematical model. Missing data from the meteorological station in the field was covered with data from the other station, in Urbana. The comparison between both stations is shown in Figure 16.



Figure 15. Meteorological station installed in the field, collecting data from April to September, 2015.

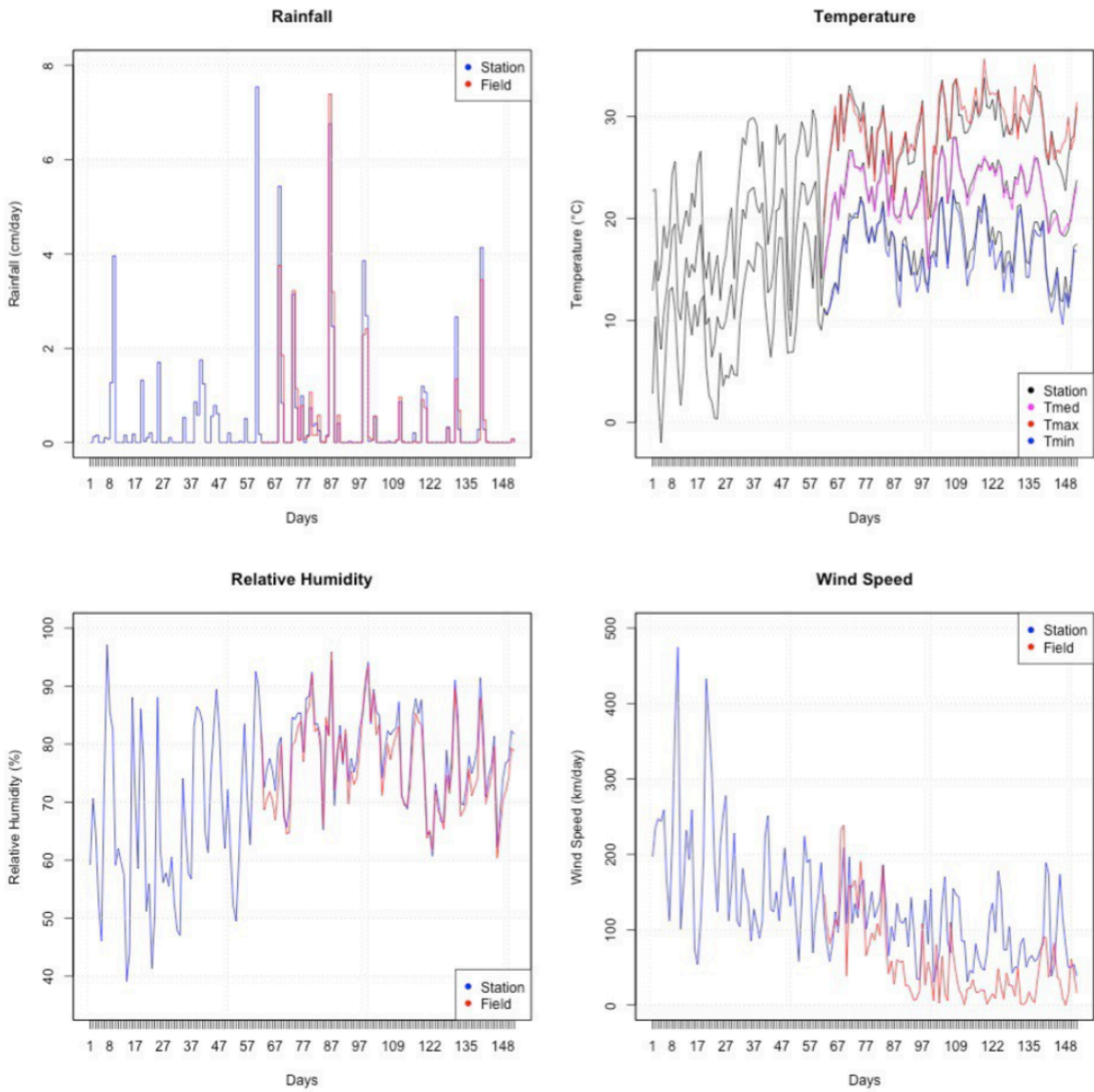


Figure 16. Comparison between data from meteorological station installed in the field and data from the city of Urbana from May to September.

### 3.3. Simulation of Soil Water Dynamics in Hydrus: Model Construction, Input and Output Data

As mentioned above, it is important to study the dynamics of water, because of the importance of potable water for life, and due to the vulnerability of water supplies to changes in climate conditions. As part of this study on the impacts of climate change on soil water dynamics, the Hydrus model was used to simulate some hydrological variables, such as surface flow, soil water storage, runoff, infiltration, among others. First, model simulations with observed weather data (Figure 15) were compared to the simulations with data from climate models. Simulations of soil water dynamics with observed weather data from April to September, 2015, labeled "present", were used to calibrate Hydrus, which was used for simulations from 2011 to 2100 (future projections), and to characterize the influence of the drainage layout. Those simulations with projected data were used to describe how climate change could affect soil water dynamics, and to evaluate the risks that this changes might have on corn production.

From meteorological station or climate models, it is necessary to obtain specific meteorological data that will be used as an input for the mathematical model used to describe soil water dynamics. For Hydrus, information is needed on: 1) solar radiation ( $\text{MJ}\cdot\text{m}^{-2}\cdot\text{day}^{-1}$ ), 2) relative humidity (%), 3) average, maximum and minimum temperature ( $^{\circ}\text{C}$  and  $\text{K}$ ), 4) rainfall (cm), and 5) wind speed ( $\text{km}\cdot\text{day}^{-1}$ ). The climate model used with Hydrus model was chosen after a detailed study of errors of the forecast from climate projections. Within this study, the model with the best ability to represent the climate in the study region was used. This data made it possible to simulate soil water dynamics in projected scenarios, and to make inference about effects of climate change. The simulations using different scenarios were made with daily data for the past; *historical* (30 years, since 1976 until 2005), *short term* (30 years, 2011 to 2040), *medium term* (30 years, 2041 to 2070) and *long term* (30 years, 2071 to 2100). The climate data used as an input in Hydrus model and space and time discretization used in Hydrus model can be found in Table 6 and Table 7.

All the simulations were made for the ANW and ASW fields, which have with different depth and spacing of drain tile. Table 8 summarizes this set of simulations. All information regarding Hydrus model can be found at <https://www.pc-progress.com/en/Default.aspx?HYDRUS-3D>.

**Table 6.** Climate data used as input in Hydrus model.

Type of simulation	Variation	Field	Time
Scenarios from climate model	RCP2.6	ANW	Historical (1976-2005)
	RCP4.5	ASW	Short term (2011-2040)
	RCP8.5		Medium term (2041-2070)
			Long term (2071-2100)
Observed data	Meteorological Station	ANW, ASW	Present (May to September - 2015)

Regarding to the geometry information the length units were given in centimeters. The number of soil materials and layers for mass balances were 4. The depth of the soil profile were 107 cm in ASW and 76 cm in ANW.

**Table 7.** Space and time discretization used in Hydrus model to produce scenarios of simulations.

Time information	Time units	Days
	Initial time	90 <sup>1</sup> , 0 <sup>2,3,4,5</sup>
	Final time	273 <sup>1</sup> , 10950 <sup>2,3,4,5</sup>
	Initial time step	0.001 <sup>1</sup> , 2.73973e-006 <sup>2,3,4,5</sup>
	Minimum step time	1e-005 <sup>1</sup> , 2.73973e-008 <sup>2,3,4,5</sup>
	Maximum step time	5 <sup>1</sup> , 0.0136986 <sup>2,3,4,5</sup>
Time-variable boundary conditions	Number of time variable boundary records	183 <sup>1</sup> , 10950 <sup>2,3,4,5</sup>
	Daily variations of transpiration during day generated by HYDRUS	yes
	Sinusoidal variation of precipitation generated by HYDRUS	yes
Meteorological data	Number of meteorological records	183 <sup>1</sup> , 10950 <sup>2,3,4,5</sup>
	Penman-Monteith Equation	yes
Print times	Number of print times	183 <sup>1</sup> , 10950 <sup>2,3,4,5</sup>
Iteration criteria	Maximum number of iterations	10
	Water content tolerance	0.001
	Pressure head tolerance (cm)	1
Time step control	Lower optimal iteration range	3
	Upper optimal Iteration range	7
	Lower time step multiplication factor	1.3
	Upper Time step Multiplication factor	0.7
Internal Interpolation Tables	Lower Limit of the Tension Interval (cm)	1e-006
	Upper Limit of the tension Interval (cm)	10000
Soil Hydraulic model	Single porosity models	van Genuchten-Mualem
	Hysteresis	No hysteresis

<sup>1</sup>Present<sup>1</sup> historical<sup>2</sup>, short<sup>3</sup>, medium<sup>4</sup> and long<sup>5</sup> term simulation.

Hydrus was used to determine daily variations in transpiration, corresponding to variations in the potential transpiration rate during the day. The model uses the assumption that hourly values of the potential transpiration between 0-6 a.m. and 18-24 p.m. represent 10% of the total daily value and that it has a sinusoidal shape during the rest of the day. This method is described in the followers equations 3.8 and 3.9, where the daily value of potential transpiration is  $\overline{T_p}$ .

$$T_p(t) = 0.24\overline{T_p} \quad (3.8)$$

If  $t < 0.264$  d and  $t > 0.736$  d

$$T_p(t) = 2.75 \overline{T_p} \sin\left(\frac{2\pi t}{1 \text{ day}} \cdot \frac{\pi}{2}\right) \quad (3.9)$$

when  $t \in (0.264 \text{ d}, 0.736)$

Sinusoidal simulations of precipitation were used in all simulations. In this case, variations of the precipitation rate can be approximated using a cosine function 3.10.

$$P(t) = \overline{P} \left(1 + \cos\left(\frac{2\pi t}{\Delta t} - \pi\right)\right) \quad (3.10)$$

Where  $\overline{P}$  is the average precipitation rate at duration  $\Delta t$ .

The potential evapotranspiration (ET) was calculated using the FAO recommended Penman-Monteith combination equation (MONTEITH, 1981; ALLEN et al., 1998), as showed in 3.11. The Penman-Monteith approach defines reference evapotranspiration (ET<sub>0</sub>) as the rate of evapotranspiration from a hypothetical crop height of 12 cm, a fixed canopy resistance of 70 sm<sup>-1</sup> and an albedo of 0.23.

$$ET_0 = \frac{0.408 \cdot \Delta(R_n - G) + \gamma \frac{900}{T+273} U_2 (e_a - e_d)}{\Delta + \gamma(1+0.34 U_2)} \quad (3.11)$$

ET<sub>0</sub> is the reference crop evapotranspiration [mm.d<sup>-1</sup>], R<sub>n</sub> is net radiation at the crop surface [MJ.m<sup>-2</sup>.d<sup>-1</sup>], G is the soil heat flux [MJ.m<sup>-2</sup>.d<sup>-1</sup>], T is the average air temperature [°C], U<sub>2</sub> is the windspeed measured at 2 m height [m.s<sup>-1</sup>]. (e<sub>a</sub> - e<sub>d</sub>) is the vapor deficit [KPa], where e<sub>a</sub> is the saturation vapor pressure at temperature T [Kpa], e<sub>d</sub> is the vapor pressure at dew point [KPa], and 900 is a conversion factor. Δ is the slope of the vapor pressure curve [KPa°C<sup>-1</sup>] (TETENS, 1930; MURRAY, 1966) and γ is the psychrometric constant [KPa°C<sup>-1</sup>] (BRUNT, 2011), as described in 3.12 and 3.13.

$$\Delta = \frac{4098 \cdot e_a}{(T+273.3)^2} \quad (3.12)$$

$$\gamma = \frac{C_p \cdot P}{\gamma \cdot \varepsilon} \cdot 10^{-3} = 0.00163 \cdot \frac{P}{\gamma} \quad (3.13)$$

Where C<sub>p</sub> is the specific heat of moist air (i.e., 1.013 kJ.Kg<sup>-1</sup>.°C<sup>-1</sup>), P is the atmospheric pressure [KPa], ε is the ratio of the molecular weights of water vapor and dry air (i.e. 0.622), and γ is the latent heat [MJ.kg<sup>-1</sup>]. Regarding to the hydraulic model, the single porosity model of van Genuchten-Mualem 3.14, 3.15 and 3.16 was used.

$$\theta(h) = \theta_r + \frac{\theta_s - \theta_r}{(1+(\alpha \cdot h)^n)^m} \quad (3.14)$$

when  $h < 0$  or

$$\theta(h) = \theta_s \quad (3.15)$$

when  $h \geq 0$

$$K(h) = k_s \cdot S_e^1 \cdot (1 - (1 - S_e^{1/m})^m)^2 \quad (3.16)$$

where  $h$  is the air entry value [L],  $\theta_s$  is the saturated water content [-],  $\theta_r$  is the residual water content [-].  $\alpha$ ,  $m$  and  $n$  are empirical parameters [1/L], [-], [-].  $S_e$  is the effective water content [-],  $K_s$  is the saturated hydraulic conductivity [L/T],  $K_r$  is the relative hydraulic conductivity [-],  $K_k(h_k)$  is the unsaturated hydraulic conductivity at pressure head  $h_k$  [L/T].

The soil type at the site is predominantly Drummer silty clay loam. Soil parameters measured and calibrated by Badiger (2001) for Hydrus simulation in this soil, shown in Table 8 were used. The arrangement of the soil layers in the ANW and ASW fields, used in Hydrus are shown in Figure 17.

**Table 8.** Field-calibrated soil hydraulic parameters.

Material	Layer	$\theta_r$ (cm <sup>3</sup> /cm <sup>3</sup> )	$\theta_s$ (cm <sup>3</sup> /cm <sup>3</sup> )	$\alpha$ (1/m)	$n$	$K_s$ (m/day)
1	0-39	0.1	0.4253	4.410	1.1853	0.160
2	39-48	0.1	0.3240	3.171	1.2227	0.204
3	48-80	0.0	0.3520	2.821	1.1859	0.420
4	80-100	0.1	0.3425	2.365	1.1481	0.410

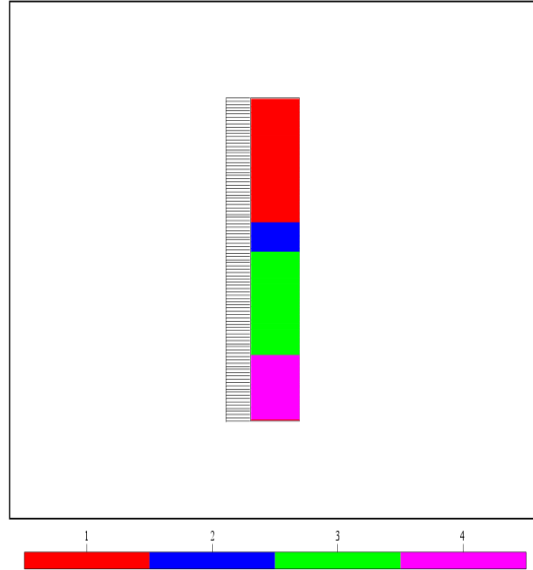


**Figure 17.** Representative layout of soil materials in field generated by Hydrus.

In Table 8,  $\theta_r$  represents the residual soil water content,  $\theta_s$  is the saturated soil water content,  $\alpha$  and  $n$  are parameters in the soil water retention function [L<sup>-1</sup>], [-].  $K_s$  is the saturated hydraulic conductivity [LT<sup>-1</sup>] and  $l$  is the tortuosity parameter in the conductivity function [-].

With respect to water flow boundary conditions, the soil surface, the upper boundary was assumed to be atmospheric. This assumption allows for water build up on the surface. The height of the surface water layer increases due to precipitation and reduces because of infiltration and evaporation. The subsurface drains were used as the lower boundary. When this option is selected, analytical solutions derived by Houghoudt et al. (1940) and

Emst (1963) are used to calculate water flow to horizontal drains (Equação 3.17). The initial condition used was in water contents.

$$q_{drain} = \frac{8.K_{hBot}.D_{eq}.h_{dr}+4.K_{hTop}.h_{dr}^2}{L_{dr}^2} + \frac{h_{dr}}{\gamma_{entr}} \quad (3.17)$$

The variable  $q_{drain}$  is the drain discharge rate [ $LT^{-1}$ ],  $K_{hTop}$  and  $K_{hBot}$  are respectively the horizontal saturated hydraulic conductivities above and below the drain system [ $LT^{-1}$ ]. The watertable height above the drain at the midpoint between the drains is  $h_{dr}$  [L],  $L_{dr}$  is the drain spacing [L],  $\gamma_{entr}$  is the entrance resistance into the drains [T] and  $D_{eq}$  is the equivalent depth [L].

According to the Hydrus guide, the equivalent depth as introduced by Hooghoudt is a function of  $L_{dr}$ , the depth to an impervious layer and the drain radius. Also, Hydrus adopts a numerical scheme as used in SWAT model (NEITSCH et al., 2011). Drained system is designed with homogeneous profile with drain on top of impervious layer. The drainage parameters were used according to the field of simulation (ANW and ASW), as showed in Table 4.

The water uptake model introduced by Feddes (FEDDES et al., 1974) was used. Typical values of crop water needs of corn were taken from Simunek et al. (1996) based in Wesseling (1991) and is presented in the Table 9.

**Table 9.** Root water uptake parameters for corn.

Parameter	Description of the variable	Value	Units
P0	Value of pressure head below which roots start to extract water from the soil	-0.15	m
P2H	Value of the limiting pressure head below which the roots cannot extract water at the minimum rate, considering the potential rate of r2H	-3.25	m
P2L	Similar as P2H, but consider a potential transpiration rate of r2L	-6	m
P3	Value of pressure head below which root water uptake ceases	-80	m
r2H	Average rate of potential transpiration	0.001	m/d
R2L	Average rate of potential evaporation	0.001	m/d

According to Hydrus manual guide (SIMUNEK et al., 2005),  $h_{Crita}$  is the minimum allowed pressure head at the soil surface and this value can be activated only by evaporation. As long as the pressure head at the soil surface is higher then  $h_{Crita}$ , the actual evapotranspiration rate is equal to the potential evapotranspiration rate. Once  $h_{Crita}$  value is reached, the actual evaporation rate is decreased from the potential value since the soil is then too dry to deliver the potential rate. This value is obtained with Equation 3.18.

$$H_r = \exp\left(\frac{hMg}{RT}\right) \quad (3.18)$$

$H_r$  is the relative humidity,  $g$  is the gravitational acceleration [ $LT^{-2}$ ],  $M$  is the molecular weight of water [ $M \text{ mol}^{-1}$ ],  $R$  is the universal gas constant [ $J \text{ mol}^{-1} \text{ K}^{-1}$ ],  $T$  is the absolute temperature [K] and  $h$  is the pressure head [L].

After giving information about time, precipitation and  $h_{Crita}$ , users need to specify the Latitude ( $^{\circ}$ ) and altitude (m), and also provide information on the Angstrom values  $a_s$  (the recommended value is 0.25) and  $b_s$  (0.5),  $a_1$

(0.9) and  $b_1$  (0.1) for calculating the effect of cloudiness on long wave radiation. Cloudiness factors from solar radiation  $a_c$  and  $b_c$  are also used (1.35, -0.35). Values  $a_1$  (0.34) and  $b_1$  (-0.139) were used for calculating the effect of emissivity on long wave radiation. Heights of wind speed, temperature, and humidity is usually 200 cm. The crop data also needs to be specified. This data includes crop height (used as 150 cm), albedo (0.2), LAI (2.5) and root depth (120 cm). Radiation extinction is 0.49. A summary of Hydrus model output data is described in Table 10.

**Table 10.** Information, parameter, description and units of output variables in Hydrus.

Information	Parameter	Description	Units
Profile	h	Pressure head	cm
	$\theta$	Water content	
	k	Hydraulic conductivity	cm.day <sup>-1</sup>
	C	Hydraulic capacity	1.cm <sup>-1</sup>
Water flow, boundary fluxes and heads	c	Water flux	cm.day <sup>-1</sup>
	rTop	Potential surface flux	cm.day <sup>-1</sup>
	rRoot	Potential root water uptake	cm.day <sup>-1</sup>
	vTop	Actual surface flux	cm.day <sup>-1</sup>
	vBot	Bottom flux	cm.day <sup>-1</sup>
	crTop	Cumulative potential surface flux	cm
	crRoot	Cumulative potential root water uptake	cm
	cvTop	Cumulative actual surface flux	cm
	cvBot	Cumulative bottom flux	cm
	hTop	Surface pressure head	cm
	hBot	Bottom pressure head	cm
	RunOff	Surface run-off	cm
	cumRunOff	Cumulative surface run-off	cm
	Volume	Soil water storage	cm
	cumInf	Cumulative infiltration	cm
	cumEvap	Cumulative evaporation	cm
Meteorological	ET	Potential evapotranspiration	mm.day <sup>-1</sup>
	Evap	Potential evaporation	mm.day <sup>-1</sup>
	Transp	Potential transpiration	mm.day <sup>-1</sup>
	Rns	Net short wave radiation	MJ.m <sup>-2</sup> .day <sup>-1</sup>
	Rnl	Net long wave radiation	MJ.m <sup>-2</sup> .day <sup>-1</sup>
	Rad	Radiation term	mm.day <sup>-1</sup>
	Aero	Aerodynamic term	mm.day <sup>-1</sup>
	Prec	Precipitation	mm.day <sup>-1</sup>

In the Hydrus program the Richard's equation for water flow is solved numerically. In Hydrus, this flux equation includes a term for root water uptake. The equation of heat transport incorporates both water conduction

and convection. This program can also be use to analyze the water and solute movement in unsaturated, saturated or partially saturated soil.



## 4. RESULTS AND DISCUSSION

### 4.1. Climatological Analysis

#### 4.1.1. Climatology Evaluation

The climatological analysis of the region it was made in order to identify patterns in the historical data. The heatmaps shown in Figure 18 indicate the seasonality of observed data of precipitation (mm/month) and average temperature ( $^{\circ}\text{C}$ ). This data was obtained from a meteorological station in Urbana, Illinois. In total, 115 years of monthly data are displayed. The region does not have a well-defined rainy season. Despite the summer (June to September) having the highest rainfall, there are also frequent storms in other seasons. The wettest month in the record was of July of 1992 with approximately 352 mm of rainfall. Before 1970, there were only two months with accumulation greater than 25 centimeters (1902 and 1943). However, after 1970, there were five such months (1971, 1977, 1985, 1992, 1993, 1995). Seasons are well defined, with an average temperature of  $23^{\circ}\text{C}$  in summer (June to September) and  $-2^{\circ}\text{C}$  in winter (December to March).

Precipitation and temperature (average, maximum and minimum) between 1901 and 2015 are shown in Figure 19. Annual rainfall is highly variable. The average annual rainfall of 968.8 and is represented on the chart (left) by a straight line. The dotted line shows an increasing precipitation trend over the years. The chart also shows the average temperatures, maximum and minimum observed. The average values of these variables are  $11.06^{\circ}\text{C}$ ,  $16.46^{\circ}\text{C}$ ,  $5.65^{\circ}\text{C}$ , respectively. The temperature variables are highly correlated. Temperature increases slightly over the years. This trend is represented by the dotted line. From the annual average, it is difficult to identify patterns in the variables that may be taken as evidence of changes in climate region. One way to try to identify patterns is to evaluate anomalies of the variables (Figure 20).

The study of precipitation anomalies indicates a small upward trend in the positive anomaly of precipitation in recent years, mainly from the year 1965. Regarding to the temperature, notably at the beginning of the 20<sup>th</sup> century tended to be negative, then began to increase until the middle of 1950. Between the late 1950s and early 1980s, it is possible identify a reduction in the anomalies (highly positive for highly negative) and a reduction in the mean temperature during this period. Some hypotheses may explain this change in temperature patterns. These might be related to the presence of aerosols in the atmosphere. Some aerosol particles (such as sulfate) alter the Earth's energy balance reflecting and scattering solar radiation back into space. These particles reduce the amount of radiation reaching the Earth's surface and thus cools the surface. The most likely hypothesis is based on a working model (TEGEN, 1990) which infers that since 1950 there was significant growth of aerosol emissions in the US, mainly sulfate. Since 1980 however, there was a reduction of the emission of this component, based on campaigns as "Clean Air Act." There are other hypothesis such as that shown in Handler (1985) which relates volcanic activities throughout the world, with the amount of aerosol in the atmosphere. Another explanation for variations in temperature anomaly can be based on fluctuations in the ocean heat transport, which can contribute to multidecadal climate variations.

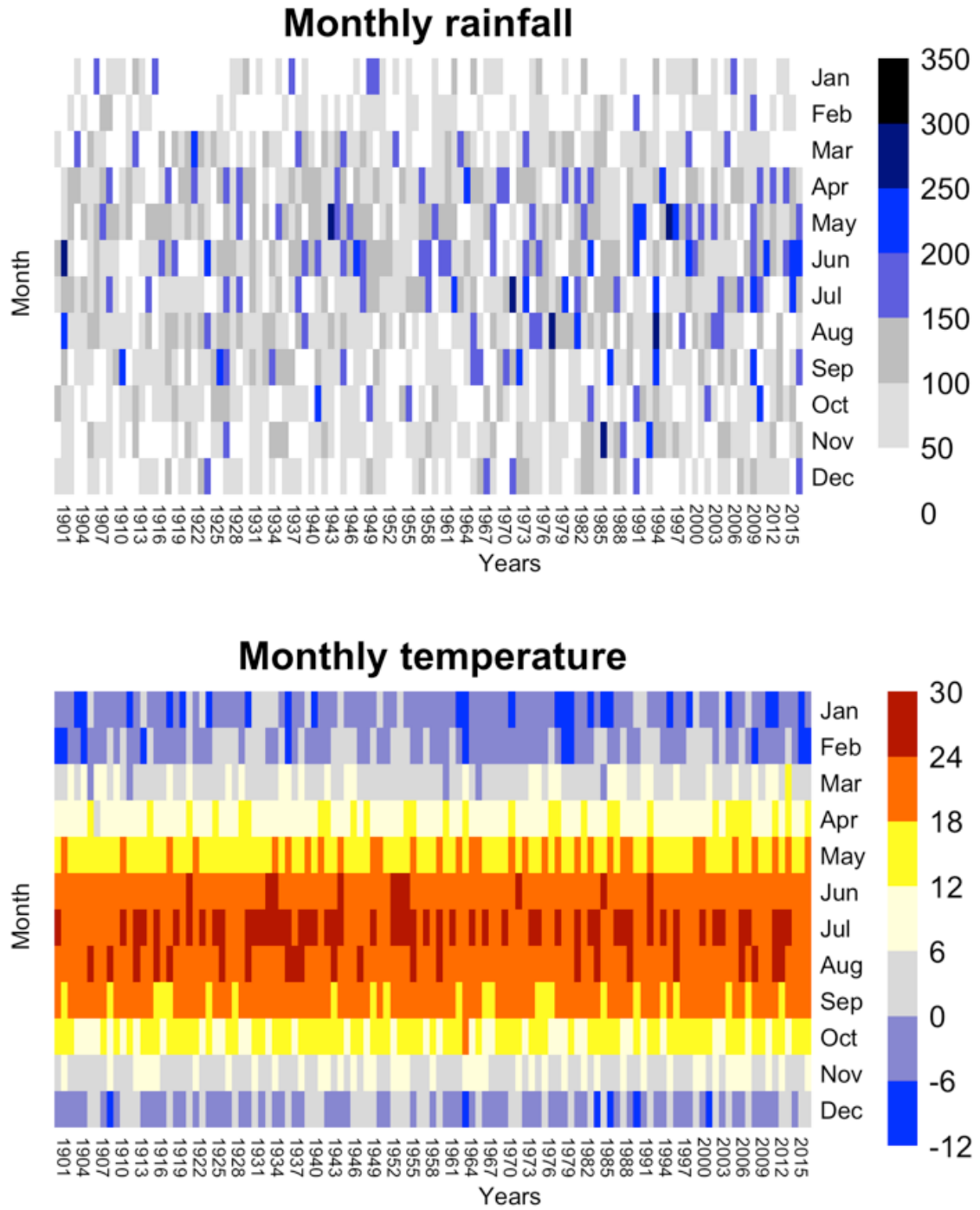


**Figure 18.** Variation of monthly accumulated precipitation (mm/month) (a), and average temperature ( $^{\circ}\text{C}$ ) (b) in the region of Urbana-Champaign (Illinois, USA) between 1901 to 2015.

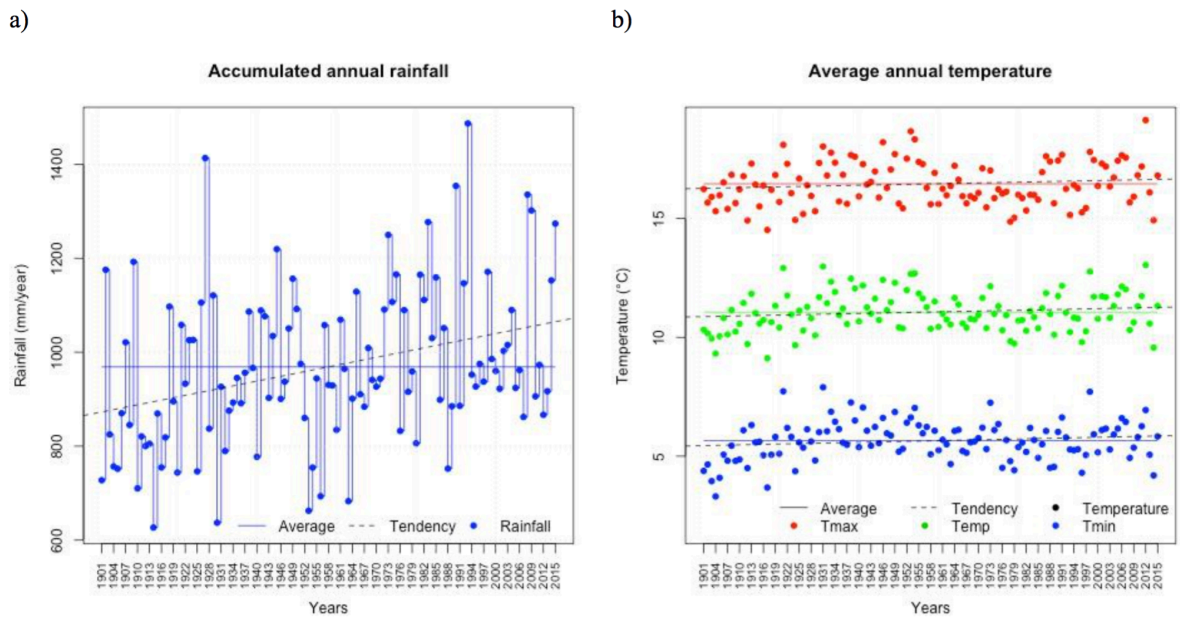


**Figure 19.** Variation of precipitation (a) and temperature (b) in the region of Urbana-Champaign (Illinois, USA), from 1901 to 2015.

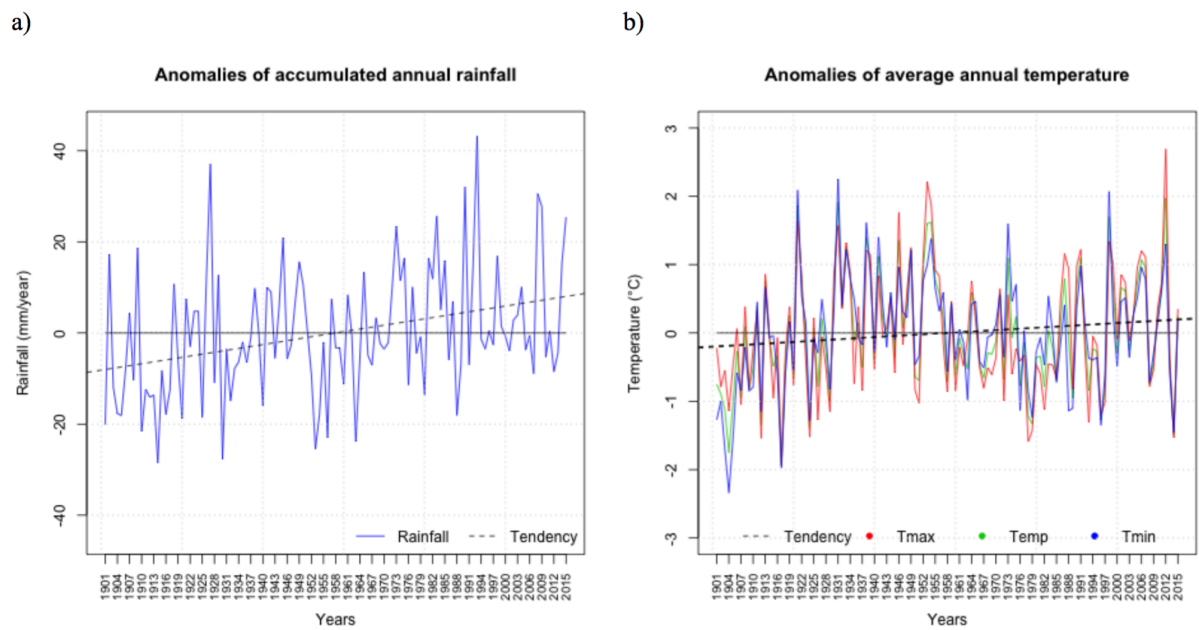


**Figure 20.** Anomalies of observed precipitation (a) accumulated per year and average temperature (b) per year (maximum, minimum and average) in Urbana-Champaign (IL, USA) between the period 1901 to 2015.

These results agree with the results presented by Hansen et al. (2001) which identifies global warming patterns between the years 1900 and 1940 and cooling between the years 1940 and 1965; although in this instance there was also a warming pattern from 1978 until the beginning of the 21<sup>st</sup> century.

#### 4.1.2. Extreme Events Occurrence

Indices of extreme precipitation and temperature events for the area, are given in Figure 21 and Figure 22. The accumulated one day (RX1DAY) and five consecutive days (RX5DAY) precipitation indices tend to increase over the years. The biggest RX1DAY and RX5DAY events occurred in 1993, and had a value of 135.13 millimeters and 192.53 millimeters, respectively. Ten years later (2003) the RX5DAY index reached the value of 176.23 millimeters. This value occur just once in the first 90 years of analysis, in 1927 with 177.03 millimeters. Thus the highest values occur in the last 30 years.

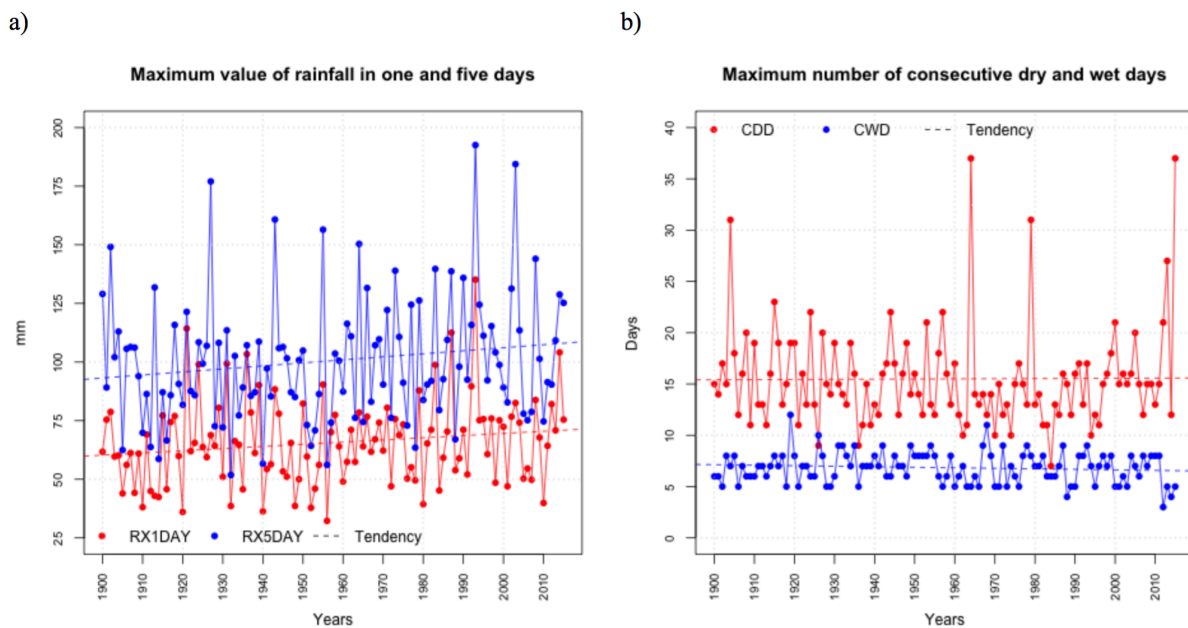


**Figure 21.** Extreme events of precipitation, considering observed data from 1901 to 2015. The dashed line means the tendency of each index, the letter a) presents the index of maximum value of rainfall in one and five days (RX1DAY, RX5DAY) and b) the maximum number of consecutive dry and wet days (CDD, CWD).

The consecutive wet days (CWD) index does not have a large variance. Before 1960, the consecutive dry days (CDD) index only exceeded 30 once (1904, 31 days). However, after 1960 it has exceeded 30 four times (1964-37 days, 1979-31 days, 2002-33 days, 2015-37 days). These results may be indicative that the case of years with long period without rainfall is increasing, which could be a problem for sectors such as agriculture and energy.

Extreme temperatures are represented by the minimum value of minimum and maximum temperature ( $TN_n$  and  $TX_n$ ), maximum value of minimum and maximum temperature ( $TN_x$  and  $TX_x$ ), daily temperature range (DTR), number of summer days (SU), number of frost days (FD), number of icing days (ID) indices. There is no tendency for  $TN_x$  and  $TN_n$  to increase or decrease in this region (Figure 22).  $TX_x$  exceeded  $40^\circ\text{C}$  four times before 1954 but not once since then. SU exceeded 130 days nine times in the whole period studied (1901-2015), seven of which were in the last 30 years (2015, 2012, 2010, 2007, 2005, 1991, 1986). This tendency of increasing frequency of SU could be indicative of global warming. SU is defined as the sum of the days in a year with daily temperature higher than  $25^\circ\text{C}$ .

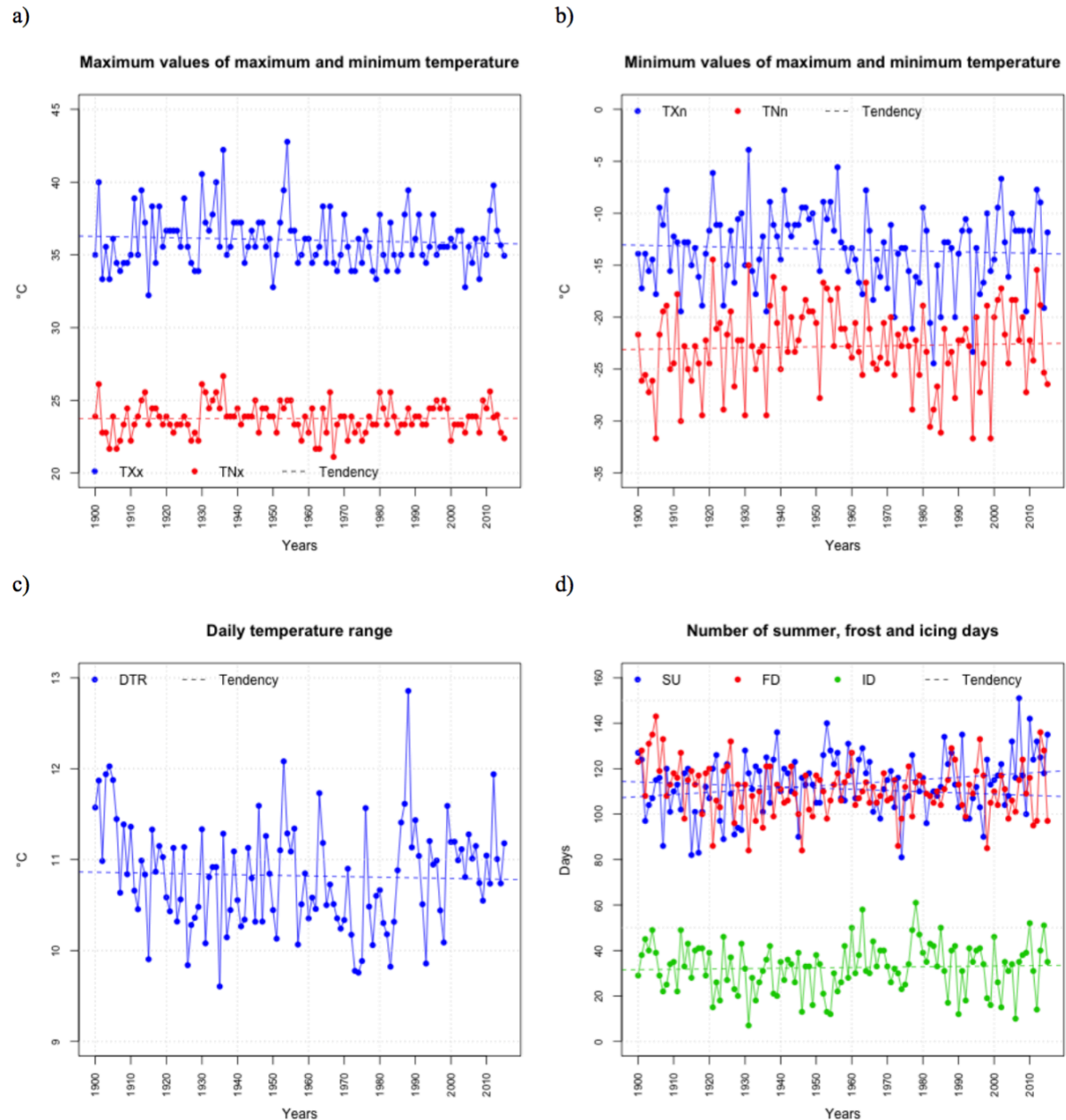


**Figure 22.** Extreme events of temperature, considering observed data from 1901 to 2015. The dashed line means the tendency of each index, the letter a) presents the index of maximum value of maximum and minimum temperature (TXx, TNx), b) minimum value of maximum and minimum temperature (TXn, TNn), c) daily temperature range (DTR) and d) number of summer, frost and icing days (SU, FD and ID).

Based on the number of frozen days (annual count of days when  $TN < 0^{\circ}\text{C}$ ) it was possible to identify a decreasing trend for this index. There were more than 130 frozen days in a year five times between 1900 and 1926, but only once since then (2013). This fact may be indicative that the region is not as cold as it is used to be. Tx exceed 50 days six times, all during or after 1960 (1960, 1963, 1978, 1985, 2010, 2014). The amplitude of daily temperature is decreasing although in 1988 was the highest value.

### 4.1.3. Statistical Analysis Of Errors

The statistical analysis of the climate in the region can be used to identify the model which most accurately represents the study region. It should be noted that the statistical analysis can be used to identify the models that best match observed data, but this is not directly related to the representation of the physical processes. This analysis can also help other researchers choose the most accurate model for the region, in order to apply other techniques, such as downscaling or agricultural applications.

Goodness-of-fit statistics for maximum, minimum and average temperature, and also for precipitation are shown in Figures 23, 24 and 25. Based on the negative values of the Mean Bias Error (MBE), the models have a tendency to underestimate the precipitation (Figure 23). Those models also tends to underestimate the maximum and average temperature ( $T_{max}$ ,  $T_{med}$ ) and overestimate the minimum temperature ( $T_{min}$ ) in the historical simulation. Based on Mean Absolute Error (MAE), maximum temperature and precipitation have the lowest values of error. The model with the lowest MAE was IPSL-CM5-MR and the model with highest value was CANESM2. IPSL-CM5-MR underestimates of  $T_{max}$ ,  $T_{med}$  and precipitation, while CANESM2 generally overestimates temperature (maximum, minimum and average) and precipitation.

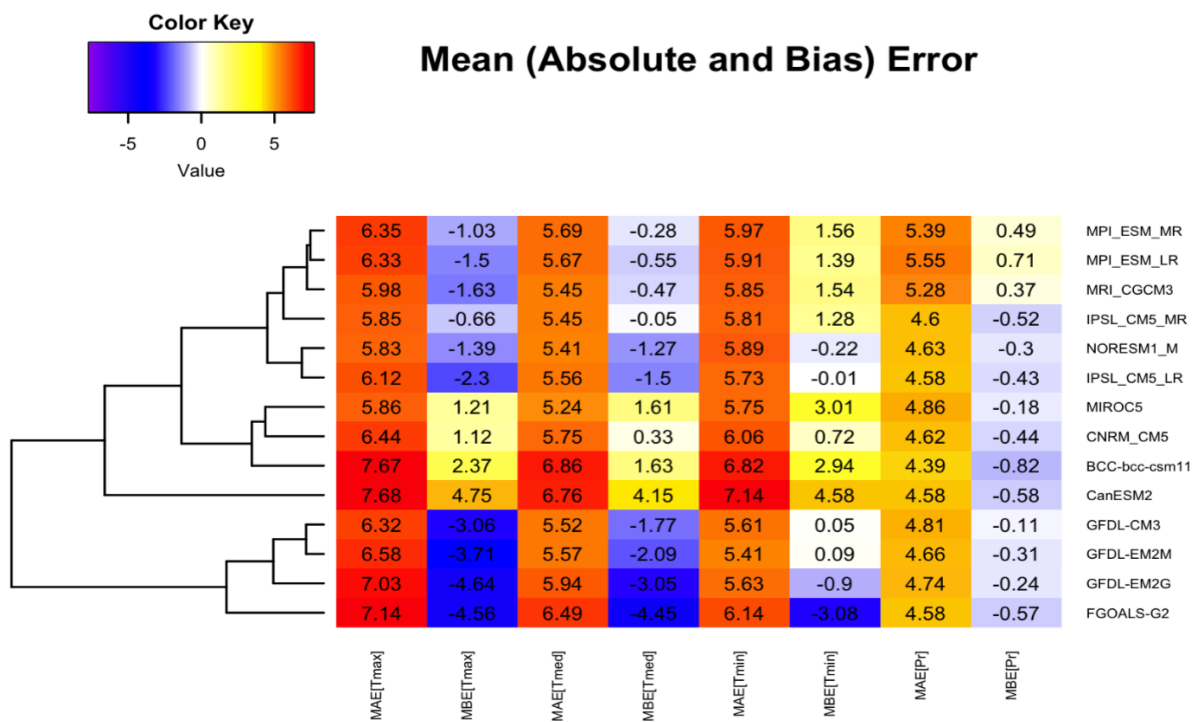


**Figure 23.** Statistical analysis of errors of temperature (maximum, average and minimum, °C) and precipitation (mm) in the climate models, based on mean (absolute and bias) error (MAE, MBE) considering systematic and unsystematic errors.

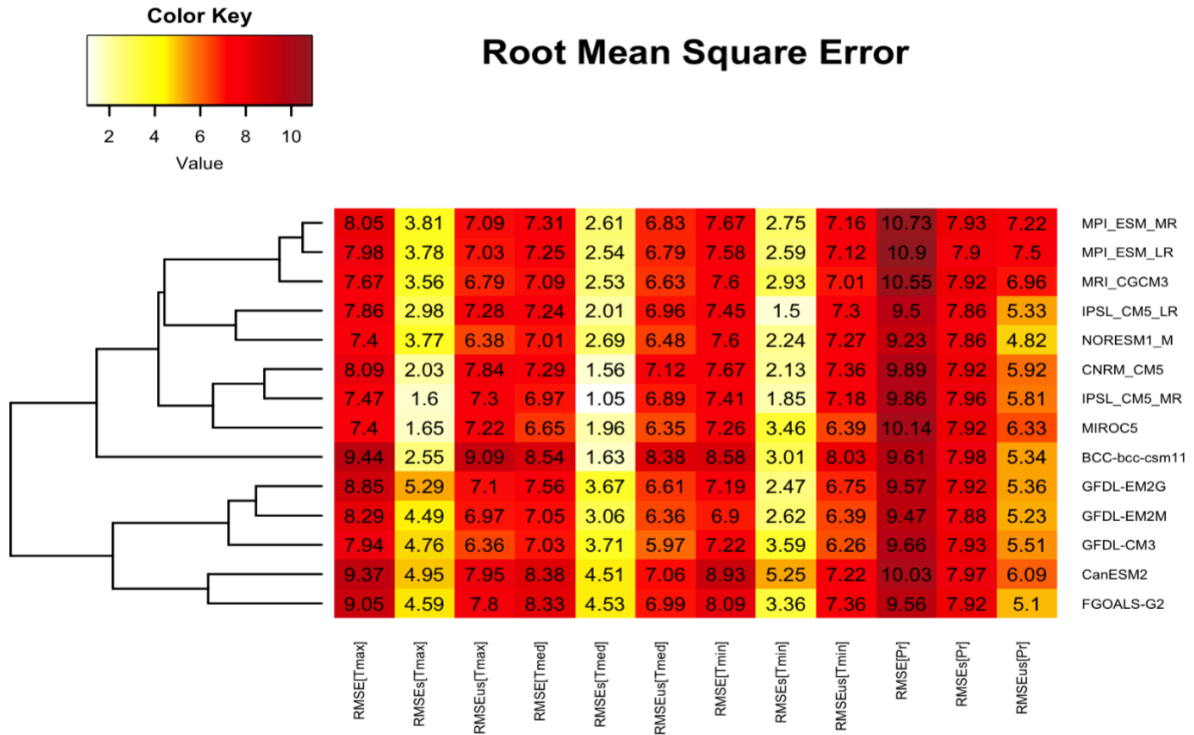


**Figure 24.** Statistical analysis of errors of temperature (maximum, average and minimum, °C) and precipitation (mm) in the climate models, based on root mean square error (RMSE) considering systematic and unsystematic errors.

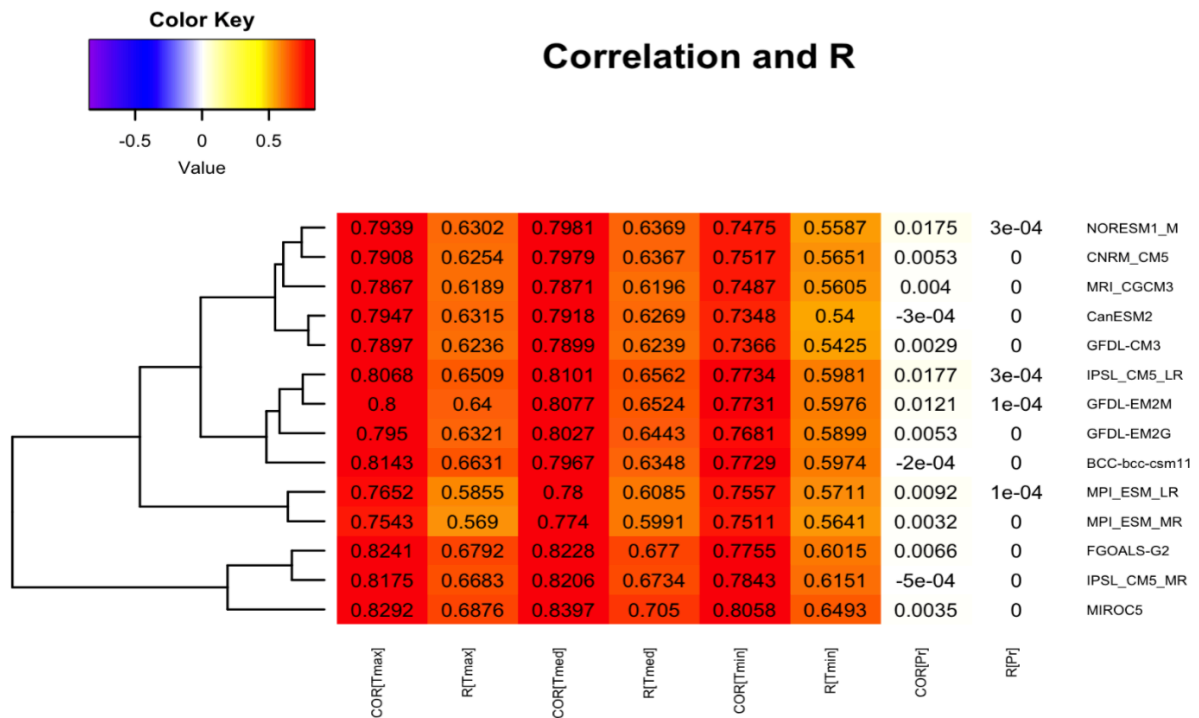


**Figure 25.** Statistical analysis of errors of temperature (maximum, average and minimum) and precipitation in the climate models, based on correlation and coefficient of determination  $R^2$ .

RMSE (Figure 24) can be divided into systematic  $RMSE_s$  and unsystematic  $RMSE_{us}$  components. The unsystematic part is, in most cases, higher than the systematic part. This fact makes the removal of the errors difficult. In the case of precipitation,  $RMSE_s$  is not much larger than  $RMSE_{us}$ . However,  $RMSE_s$  it was not removed due to the difficulty of doing this removal in a punctual variable. Precipitation had the highest total RMSE, and

average temperature, the lowest. The model with lowest and highest values of RMSE were NORESM1-M and CANESM2, respectively.

Correlation (C) and coefficient of determination ( $R^2$ ) are extremely low for precipitation (Figure 25). These low values may be due to the fact that precipitation is a punctual variable. Such variables are difficult to predict. For example, a delay of one day in predicting precipitation could lead to a very low correlation, even if the predicted values were extremely accurate. In a long term, is very difficult to predict the exact day of a large rainfall, but it is important that the tendency having large rainfall events is correct. Temperatures are normally is easier to predict, which might explain why temperature variables have higher C and  $R^2$ . The correlation between observed and simulated temperatures exceed 0.7, with average temperature having the highest correlation. The MIROC5 model had the highest C and  $R^2$  values.

It is more important to match extreme events that average values since the effects of these extremes are more devastating. The Figures 26 and 27 shows the boxplot for the extreme events of precipitation and temperature.

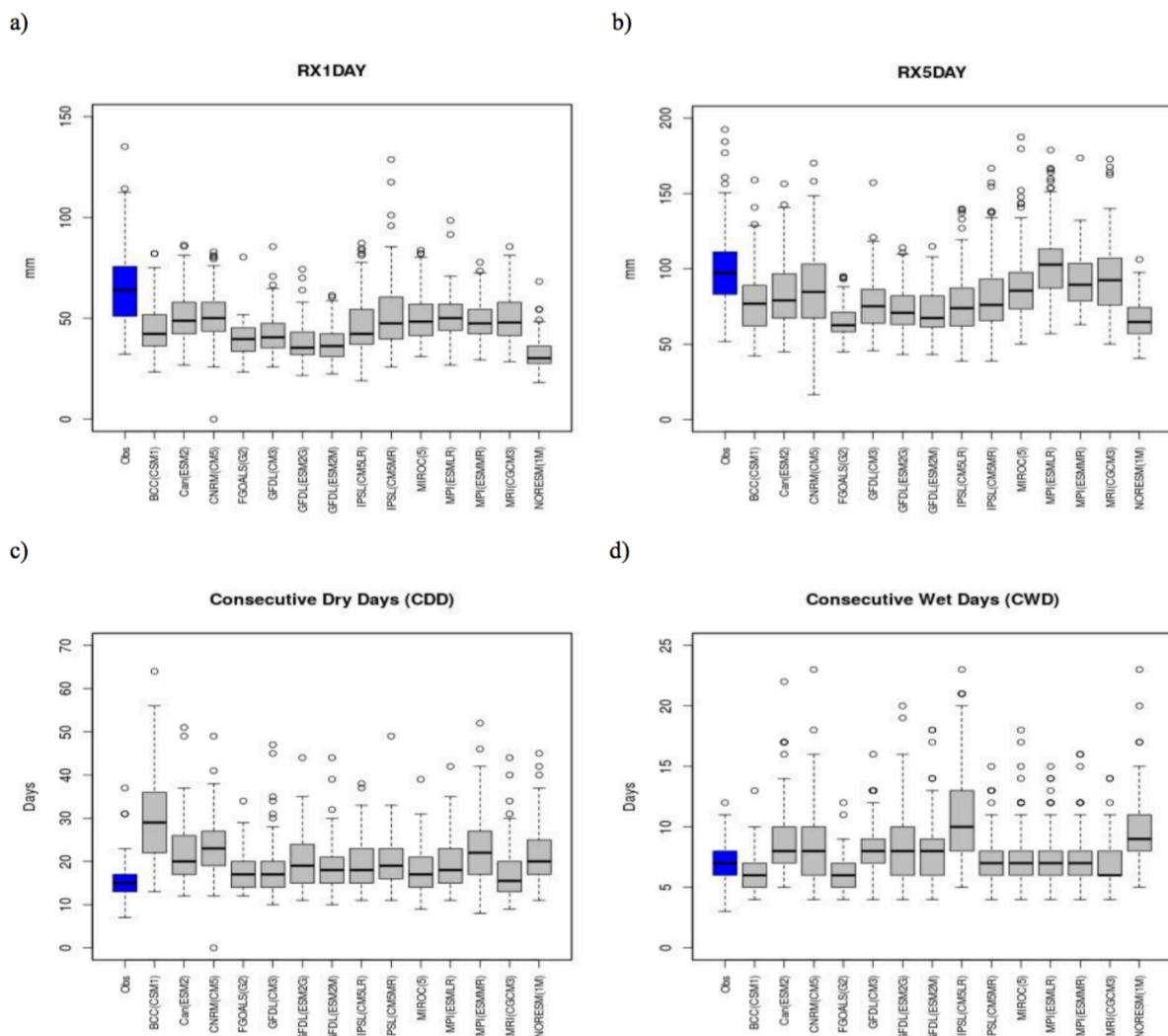


**Figure 26.** Occurrence of extreme events of precipitation according to observed data (blue box) and climate models (grey box), between 1901 and 2015. The indices are a) Maximum value of rainfall in one day (RX1DAY), b) Maximum value of rainfall in five days (RX5DAY), c) consecutive dry days (CDD), d) consecutive wet days (CWD).

Most of models underestimate RX1DAY, particularly the IPSL(CM5MR) model. The FGOALS(G2) and NORESM(1M) models had the lowest values of the RX5DAY index. The IPSL(CM5MR) model once again, along with the MIROC5, MPI(ESMLR), MPI(ESMMR) and MRI(CGCM3) models, best replicated the observed data. CDD and CWD (consecutive dry and wet days) were overestimation in the simulations, particularly when outliers are considered. The BCC(CSM1) model most overestimated CDD, while the IPSL(CM5LR) model most overestimated CWD. The IPSL(CM5MR), MIROC5, MPI(ESMLR), MPI(ESMMR) and MRI(CGCM3) models best replicated these two indices.

While some of the models overestimated  $TX_x$  and  $TN_x$ , but there was not an overarching tendency. The BCC(CSM1), Can(ESM2) and CNRM(CM5) most overestimated these indices. The CNRM(CM5) and MIROC5 models had higher values of both extremes than the observed data. The FGOALS(G2) and BCC(CSM1) models had the lowest values of  $TX_n$  and  $TN_n$ .

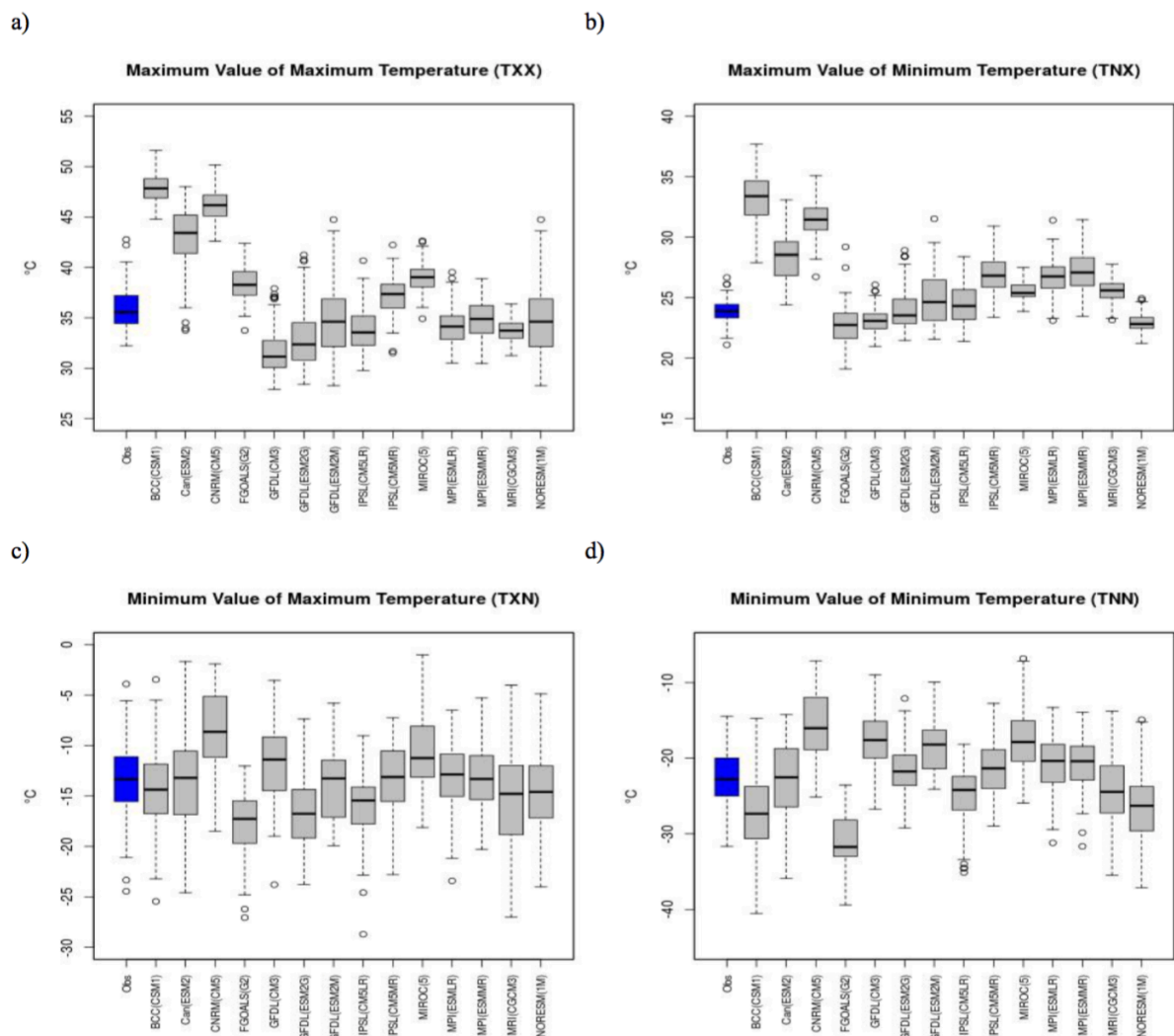


**Figure 27.** Occurrence of extreme events of temperature according to observed data (blue box) and climate models (grey box), between 1901 and 2015. The indices are maximum value of a) maximum ( $TX_x$ ) and b) minimum temperature ( $TN_x$ ), minimum value of c) maximum ( $TX_n$ ) and d) minimum temperature ( $TN_n$ ).

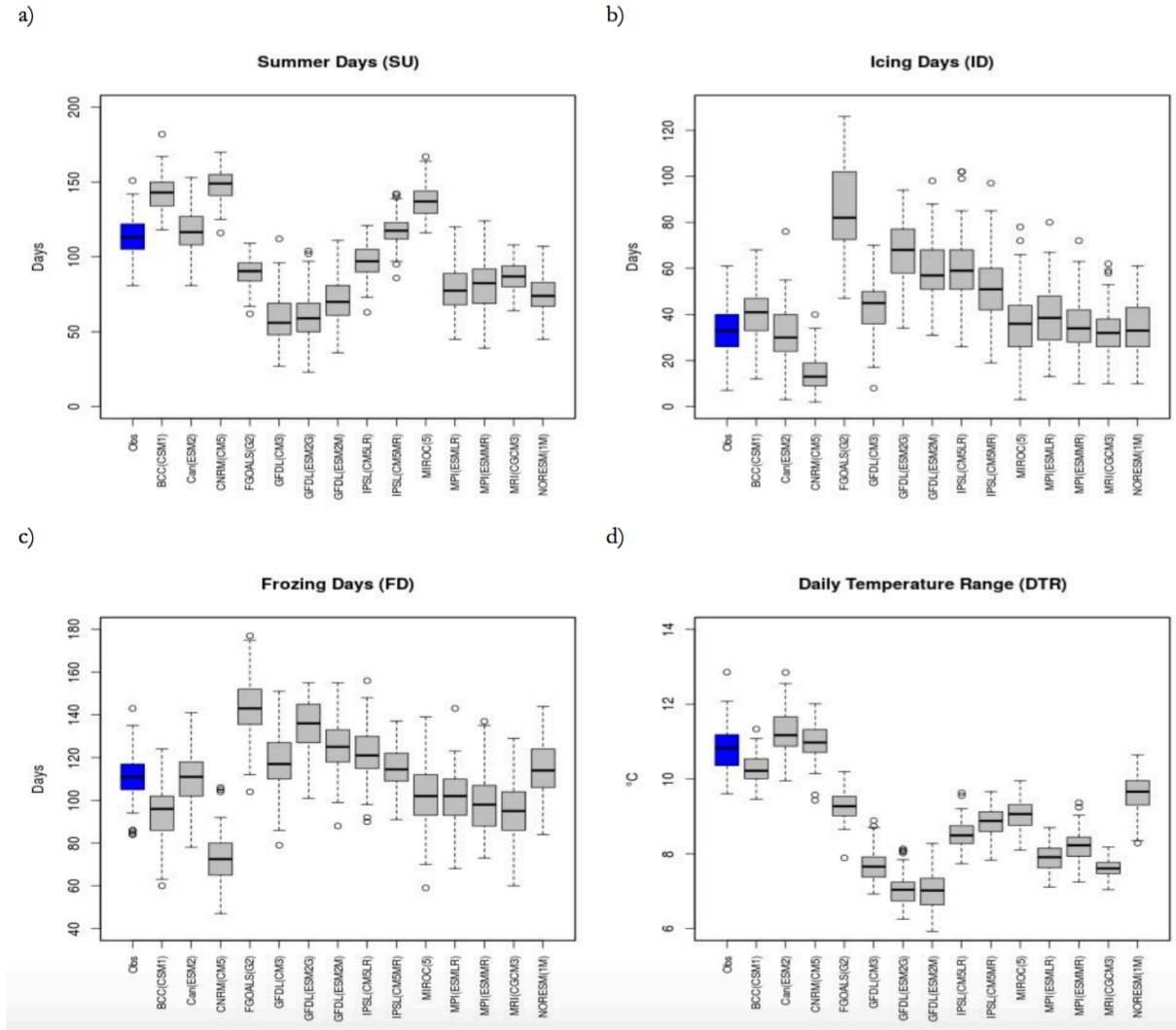


**Figure 28.** Occurrence of extreme events of temperature according to observed data (blue box) and climate models (grey box), between 1901 and 2015. The indices are maximum value of a) summer days (SU), b) icing days (ID), c) freezing days (FD) and d) daily temperature range (DTR).

Figure 28 shows the occurrence of extreme events of SU, ID, FD and DTR. The model FGOALS(G2) most overestimated ID. Some models tended to overestimate DTR. The IPSL(CM5MR) and Can(ESM2) models best replicated SU. When compared to the observed data, the CNRM(CM5) and FGOALS(G2) models underestimated and overestimated FD, respectively.

#### 4.1.4. Climate Projections Scenarios

As can be inferred from the previous section, the choice of a model to use in a specific location is not easy. There is a lot of factors that can influence this choice, depending mostly of the application of this data. In this case, for the region of Urbana-Champaign in Illinois state (USA) the IPSL(CM5MR) model was good at replicating both meteorological variables and extreme events. This IPSL model includes an interactive carbon cycle, a representation of tropospheric and stratospheric chemistry, and a comprehensive representation of aerosols. A fully description of this model can be found at Dusfrene et al. (2013).

IPSL(CM5MR) was developed in France by the *Institut Pierre-Simon Laplace*. The horizontal grade is 1.3°x 2.5°. More information about this model can be found at <https://verc.enes.org/models/earthsystem->

models/ipsl/ipslesm. This model tends to underestimate precipitation, average and maximum temperature and overestimate minimum temperature. It accurately estimated the indices for extreme events in general, but overestimated ID and underestimated DTR.

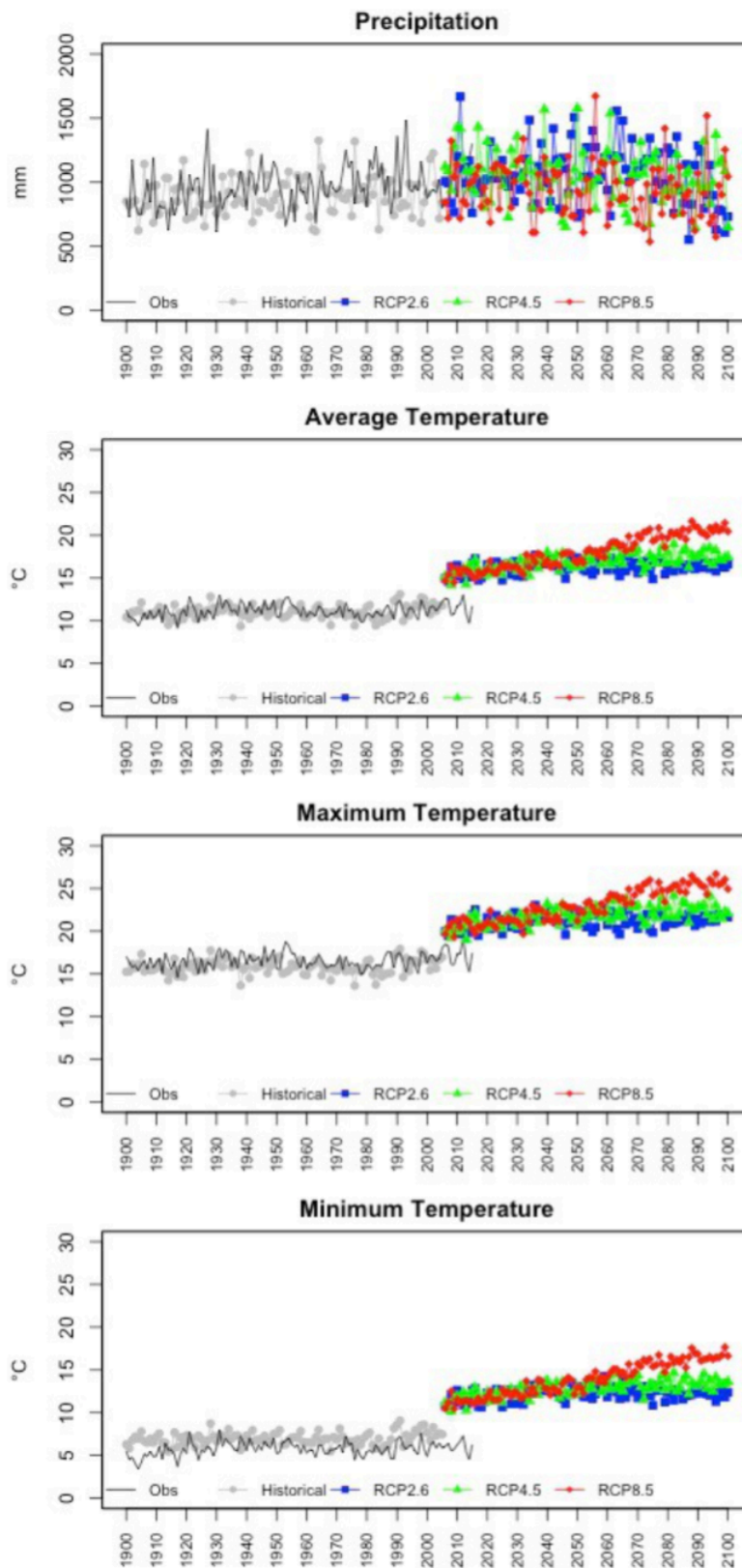
Climate projections scenarios for the IPSL(CM5MR) model are given by Figure 29. The simulated data are divided into historical (1901 to 2005) and RCP2.6, RCP4.5 and RCP8.5 (2006 to 2100).

Regarding to precipitation, the climate scenarios does not show any pattern. But it is also presented that the accumulated values can be higher in specific years. At the end of the 21<sup>th</sup> century, it is notice the more often occurrence of low values of accumulated precipitation. All scenarios of temperature projections indicates that this variable may increase in future. The scenario with higher increase was RCP8.5, which was expected considering that this scenario is the most pessimist in the analyzed projections. The scenario with lower increase was RCP2.6, the optimist scenario. The same pattern is observed in maximum and minimum temperature, however, with different magnitudes.

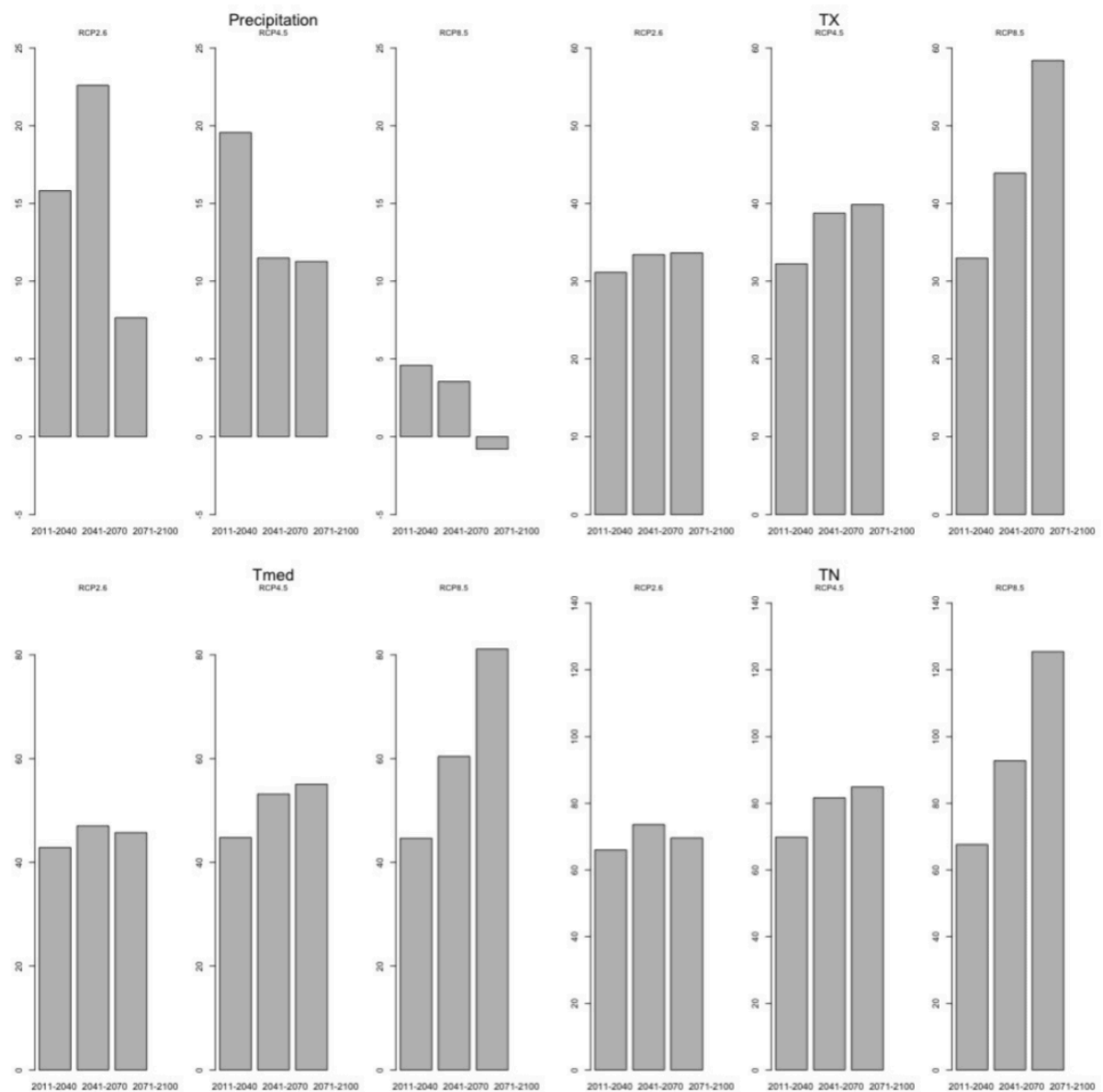
This variables and indices were also analyzed in terms of percentile. In order to make this analysis it was made the average of the index/variable for the period. The period was divided into 3 ranges: 2011 to 2040, 2041 to 2070 and 2071 to 2100. These values were compared to the average values of 1976 to 2005, considering this period as a period of reference, representing the current conditions of extreme events in the region. The total period of historical simulation was not considered, because of the difference in extreme events founded between the beginning and ending of 20<sup>th</sup> century.

Figure 30 shows the changes on precipitation, maximum, average and minimum temperature, considering the percentile of difference between climate projections (divided into periods: 2011-2040, 2041-2070, 2071-2100) and the reference period of 1976 to 2005.

The RCP2.6 scenario indicated the highest values of changes in precipitation and this changes tends to be more expressive in the period of 2041 to 2070, with 22.61% of change when compared to observed data. The tendency of decreasing of precipitation, compared to the reference, are founded only in the RCP8.5 for the final period of the 21<sup>th</sup> century (2071 to 2100), and it is around -0.8% of change. Also, in agreement with Figure 29, Figure 30 presents an increase of changes in maximum, mean and minimum temperature in all climate scenarios. This changes in maximum, minimum and average temperature are higher in the last period (2071-2100) of RCP8.5 scenario. This change can reach the value of 58.4% for maximum, 81.1% for mean temperature and 125.4% for minimum temperature.



**Figure 29.** Observed and simulated data of precipitation and maximum, average, and minimum temperature (projected by IPSL(CM5MR)) for 1901 to 2100. The simulated data includes historical simulation (grey) and RCP2.6 (blue), RCP4.5 (green) and RCP8.5 (red).



**Figure 30.** Changes on precipitation, maximum, average and minimum temperature, considering the percentile of difference between climate projections (divided into periods: 2011-2040, 2041-2070, 2071-2100) and the reference period of 1976 to 2005. These changes were calculated for the scenarios RCP2.6, RCP4.5 and RCP8.5.

Figure 31 shows that the RX1DAY index was underestimated by the historical simulation. Also, the projected scenarios presents the increase of frequency of extreme events of precipitation in one day (RX1DAY), mostly in RCP2.6 and RCP8.5 scenarios. Same pattern is presented for the RX5DAY index, which underestimate the observed data. This index (RX5DAY) also presents a tendency of occurrence of high values in all scenarios. The highest value is simulated by the RCP2.6 simulation. CDD index calculated by historical projection overestimate the index calculated with observed data. Projections also shows the occurrence of extreme events with high values of CDD. CWD index is also expected to be higher on future, considering all scenarios of climate projections.

From Figure 32 we observed that all scenarios shows increasing of RX1DAY in future and RCP8.5 shows higher increase at the end of the century (up to 50.1%). Same pattern is found in RX5DAY, although the percentile of increasing of the index for the RCP8.5 (2071 to 2100) was 32.01%.

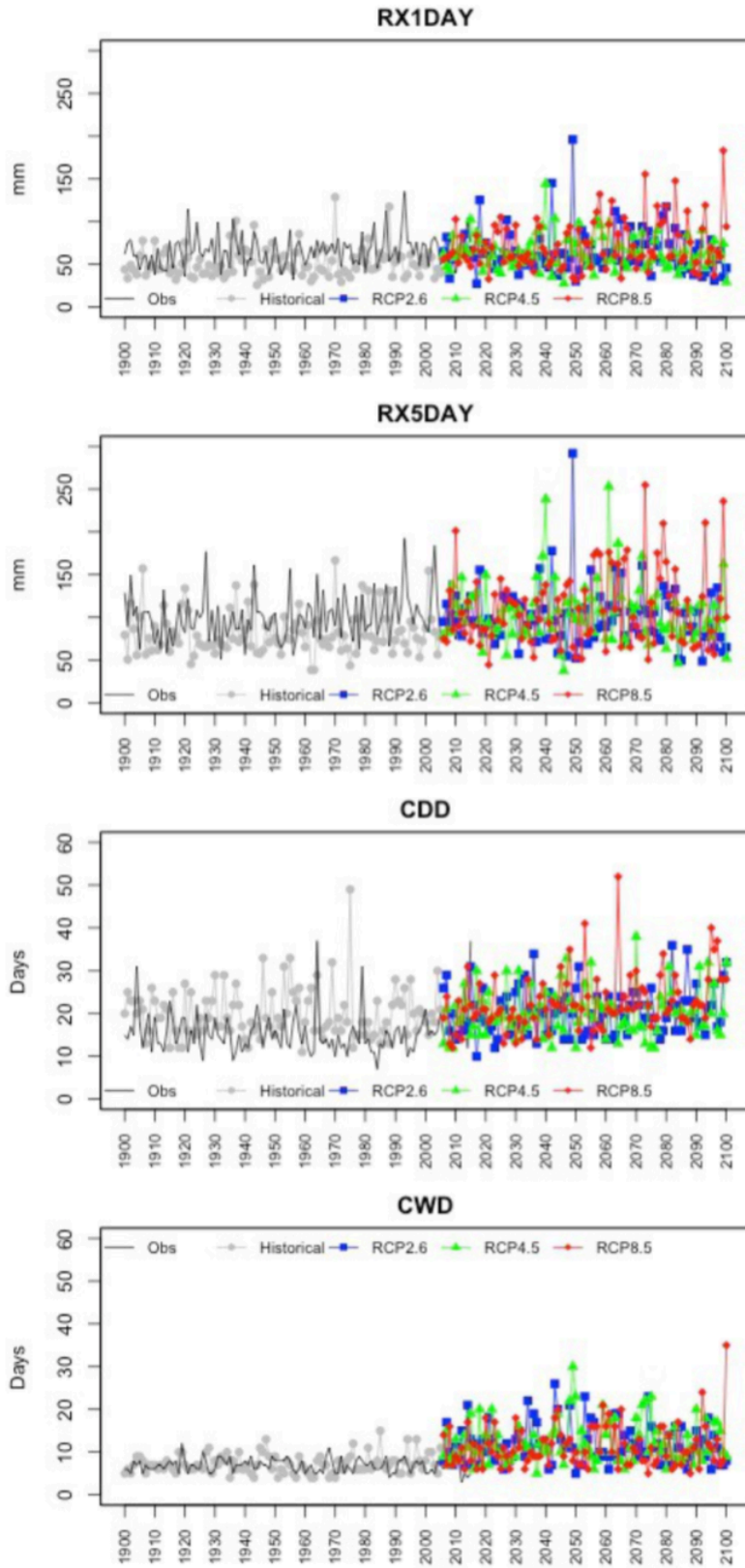


**Figure 31.** Indices of extreme events of precipitation calculated based on observed and simulated data (projected by IPSL(CM5MR)) for 1901 to 2100. The indices calculated are maximum value of rainfall in one (RX1DAY) and five days (RX5DAY) and consecutive dry (CDD) and wet days (CWD). The simulated data includes historical simulation (grey) and RCP2.6 (blue), RCP4.5 (green) and RCP8.5 (red).

CWD and CDD also presented patterns of positive change in the percentile of the indices.

CWD and CDD also presented patterns of positive change in the percentile of the indices. CWD indicates the period of 2041 to 2070 as the more intense in terms of changes in the consecutive wet days, and the RCP4.5 presents the worst scenario (increase of 62.08%). The trend considering the consecutive dry days (CDD) is increase of the index and the worst scenario is that this index could reach 29.05% of change in RCP8.5 (2071-2100).

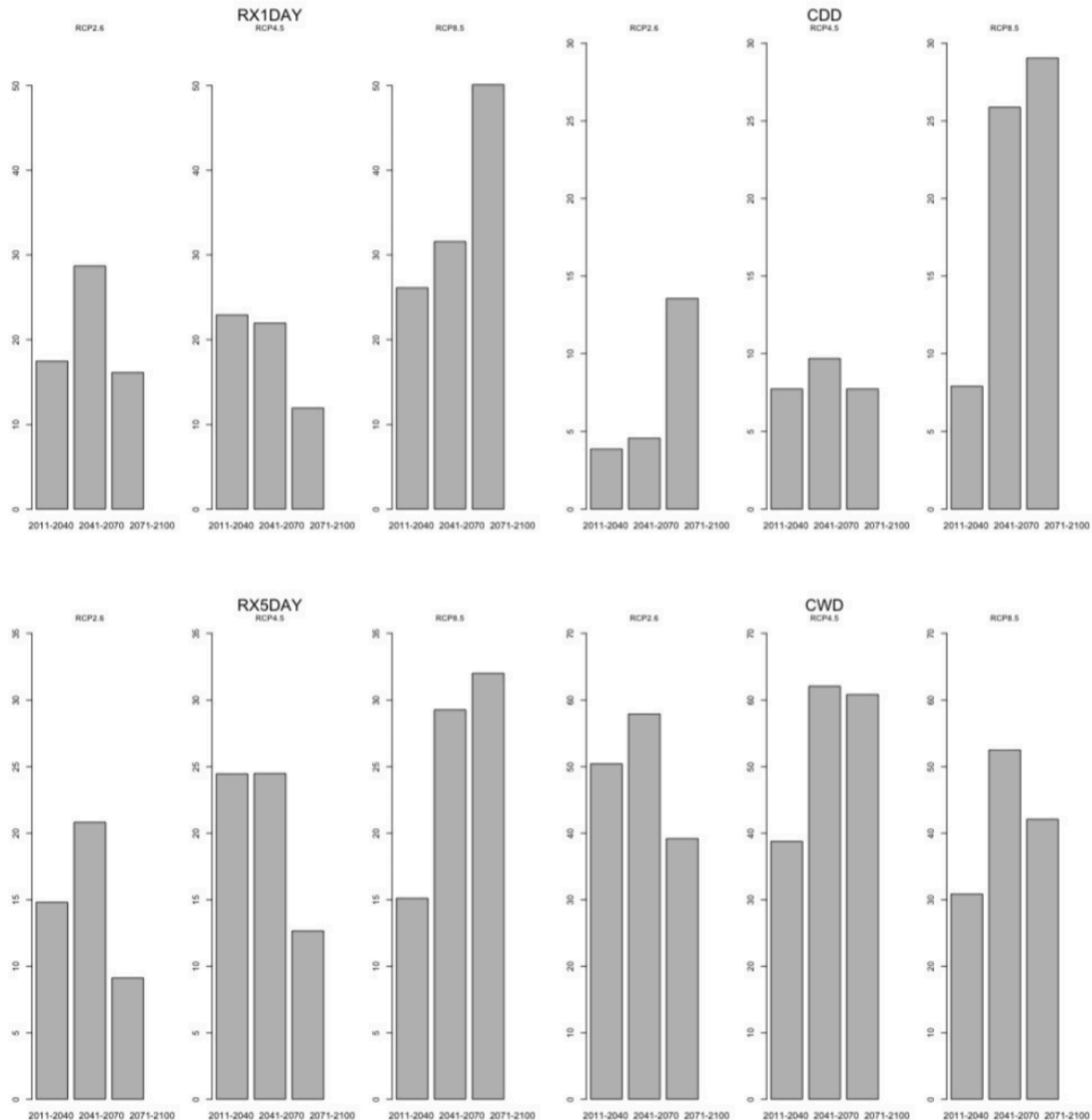


**Figure 32.** Changes on index of extreme precipitation, as RX1DAY, RX5DAY, CDD and CWD, considering the percentile of difference between climate projections (divided into periods: 2011-2040, 2041-2070, 2071-2100) and the reference period of 1976 to 2005. These changes were calculated for the scenarios RCP2.6, RCP4.5 and RCP8.5.

From Figure 33 and the indices of extreme events of temperature, it is noticed again the tendency of increase of temperature on future. The projections indicates that the maximum values of maximum and minimum temperature may increase until 2100.

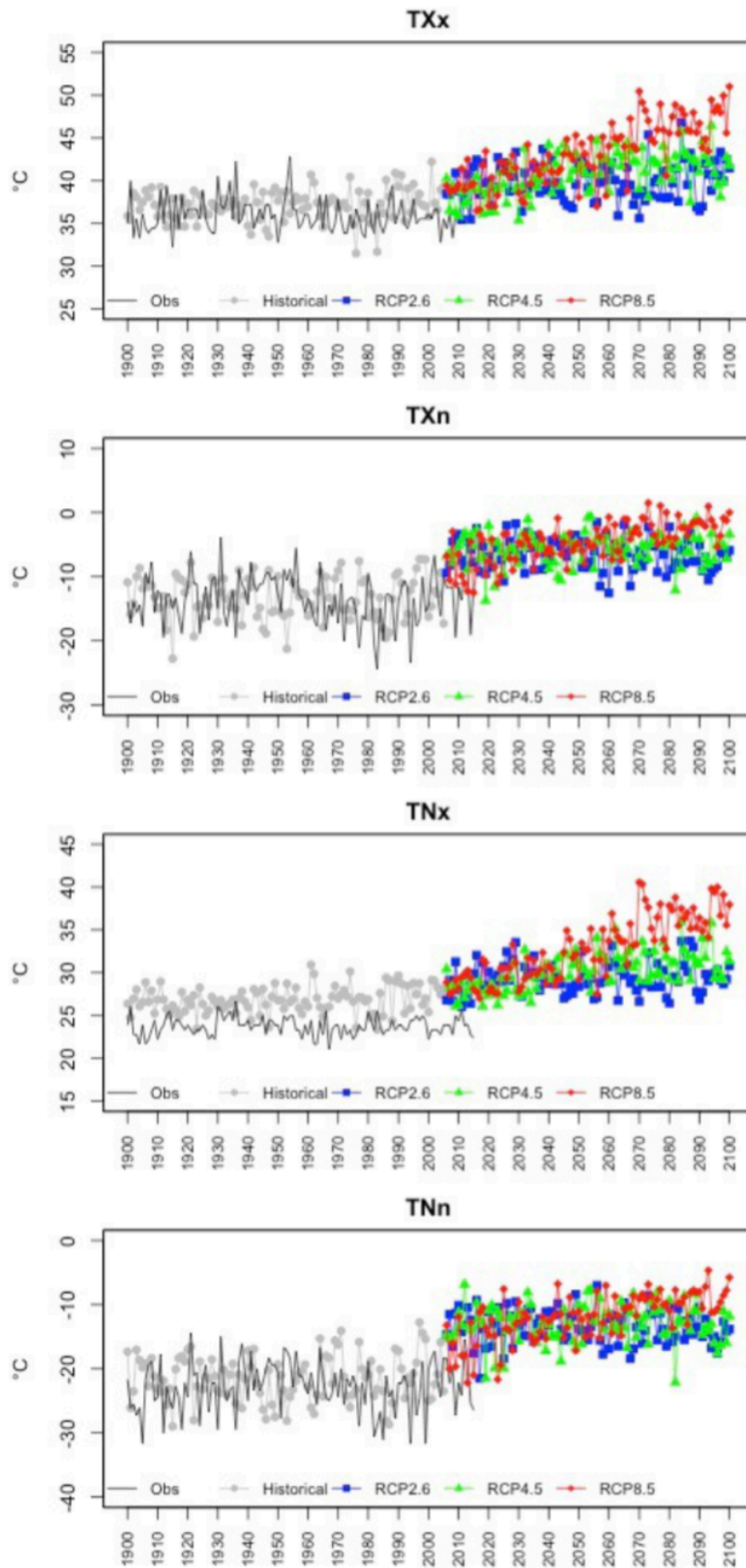


**Figure 33.** Indices of extreme events of temperature calculated based on observed and simulated data (projected by IPSL(CM5MR)) for 1901 to 2100. The index are maximum value of maximum ( $TX_x$ ) and minimum temperature ( $TN_x$ ), minimum value of maximum ( $TX_n$ ) and minimum temperature ( $TN_n$ ). The simulated data includes historical simulation (grey) and RCP2.6 (blue), RCP4.5 (green) and RCP8.5 (red).

This tendency of increase can be noticed in the increase of percentile of change (Figure 34). Thus, the minimum value of maximum and minimum temperature shows the same trend. The highest changes were in RCP8.5 in the period of 2071 to 2100. The values of the percentile of changes were: 24.92% (TXx), 35.82% (TNx), 56.66% (TNn) and 84.48% (TXn). The lowest values of changes for TXx and TNn were in RCP4.5 in the period of 2011 to 2040 (4.83% and 5.35%, respectively). For the indices TNn and TXn the lowest values were found for same period but in RCP8.5 (30.46% and 46.87%).

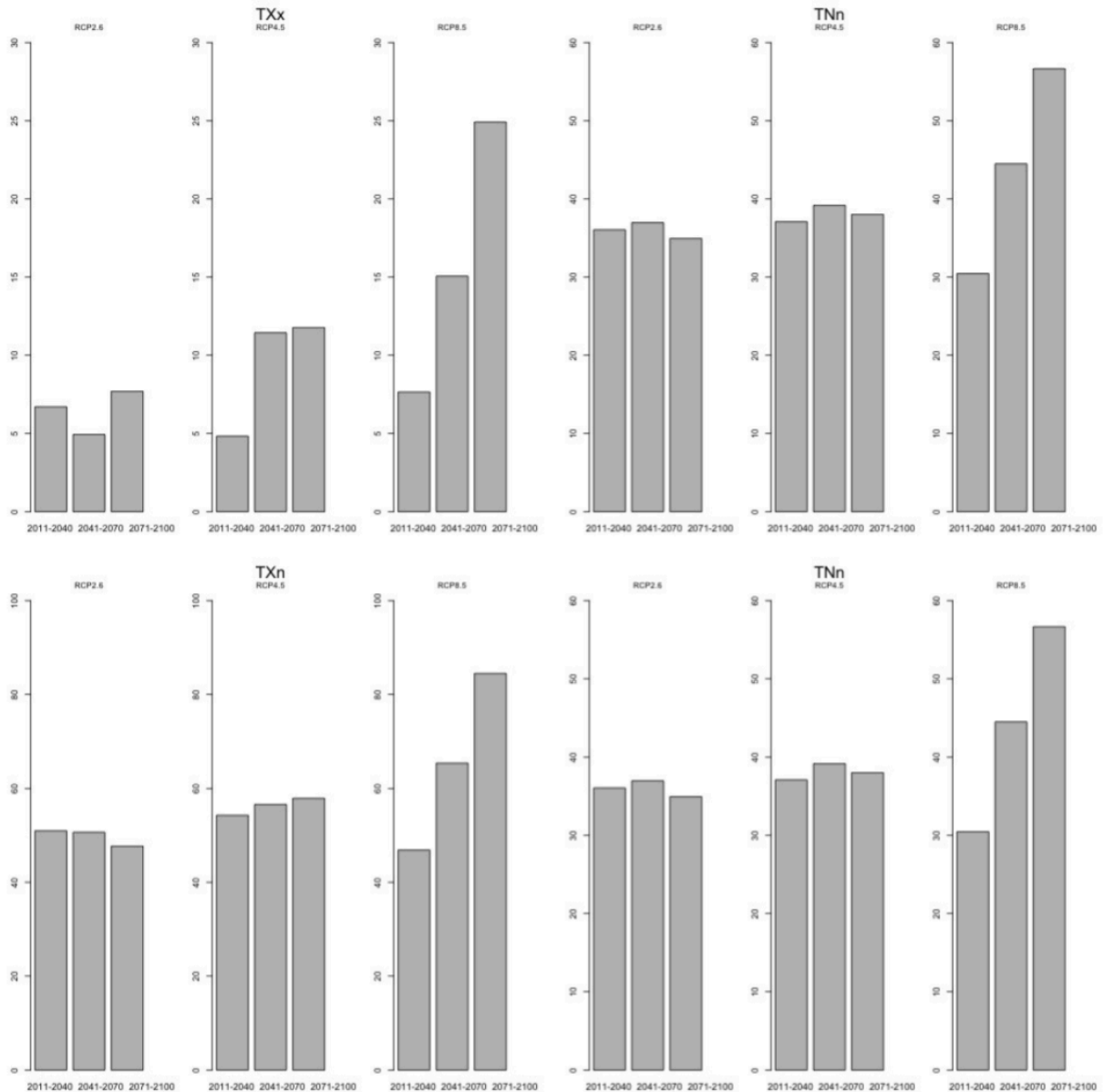


**Figure 34.** Changes on extreme indices, as TXx, TNx, TXn and TNn considering the percentile of difference between climate projections (divided into periods: 2011-2040, 2041-2070, 2071-2100) and the reference period of 1976 to 2005. These changes were calculated for the scenarios RCP2.6, RCP4.5 and RCP8.5.

An interesting point is related to the SU, DTR, ID and FD indices, presented in Figure 35. SU was well simulated in historical projection when compared to the observed simulation. However, in future scenarios the projections shows increase of summer days, which is also observed in the percentile of changes in this indices (Figure 36).

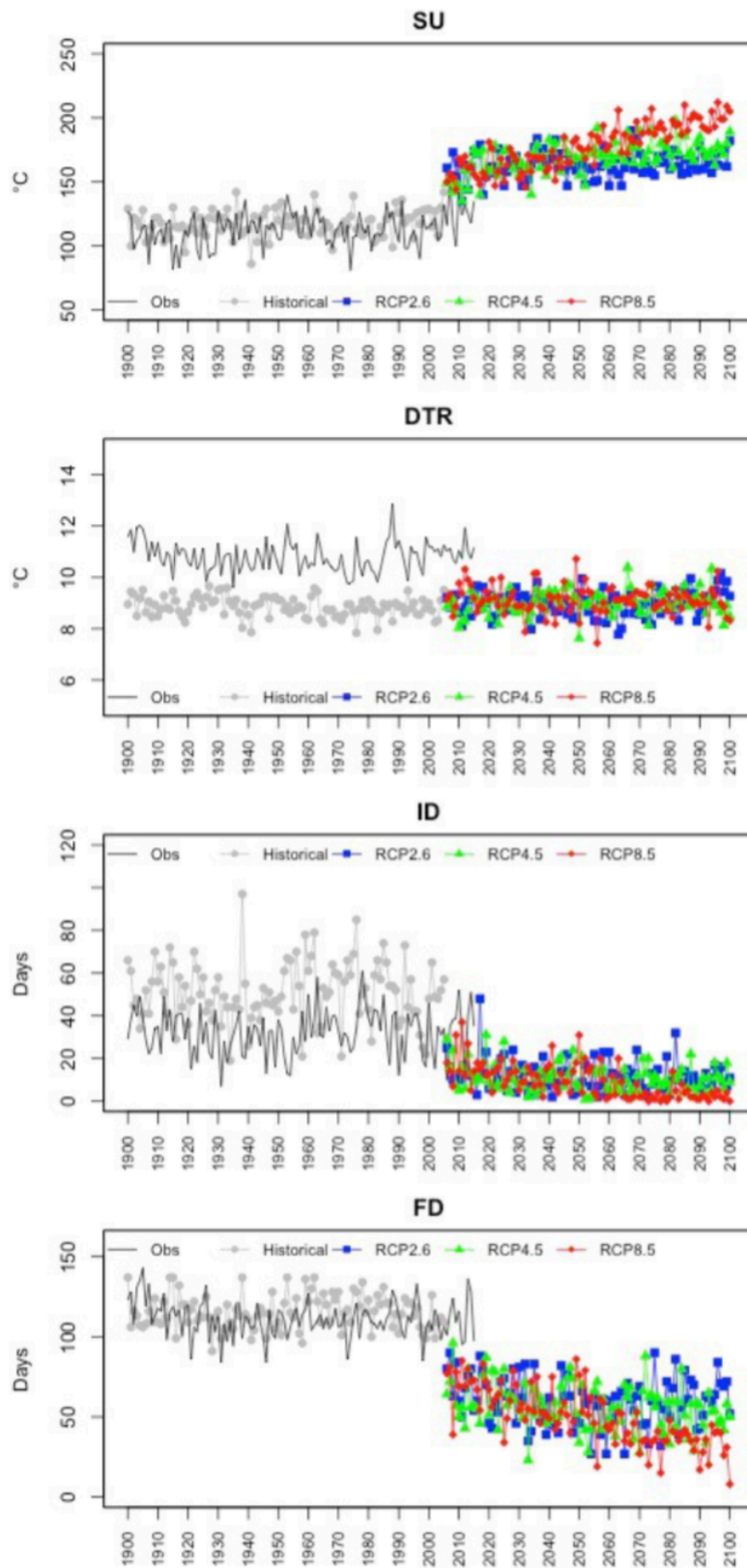


**Figure 35.** Indices of extreme events of temperature calculated based on observed and simulated data (projected by IPSL(CM5MR)) for 1901 to 2100. The index are maximum value of maximum ( $TX_x$ ) and minimum temperature ( $TN_x$ ), minimum value of maximum ( $TX_n$ ) and minimum temperature ( $TN_n$ ), summer days (SU), icing days (ID), daily temperature range (DTR) and freezing days (FD). The simulated data includes historical simulation (grey) and RCP2.6 (blue), RCP4.5 (green) and RCP8.5 (red).

Also, in Figure 35 we noticed the higher increasing of SU in RCP8.5 and lowest in RCP2.6. Figure 36 shows that this increase is around 35.67 % in the period of 2011-2040 (RCP2.6) and goes up to 64.77% in the period of 2071-2100 (RCP8.5). Regarding to DTR index, although the model has good capacity in simulate the weather in the study region, the index was largely underestimated by the model in historical simulation and future projection does not show any visible pattern from Figure 35. Based on Figure 36 it is possible to infer that this change is around 4% in the end of the century. However, there is no agreement between the climate scenarios regarding to the simulation of the index DTR in the period of 2011-2040 (RCP2.6 simulates positive changes of 2.58%, and RCP8.5 simulates negative changes around -4.9%).

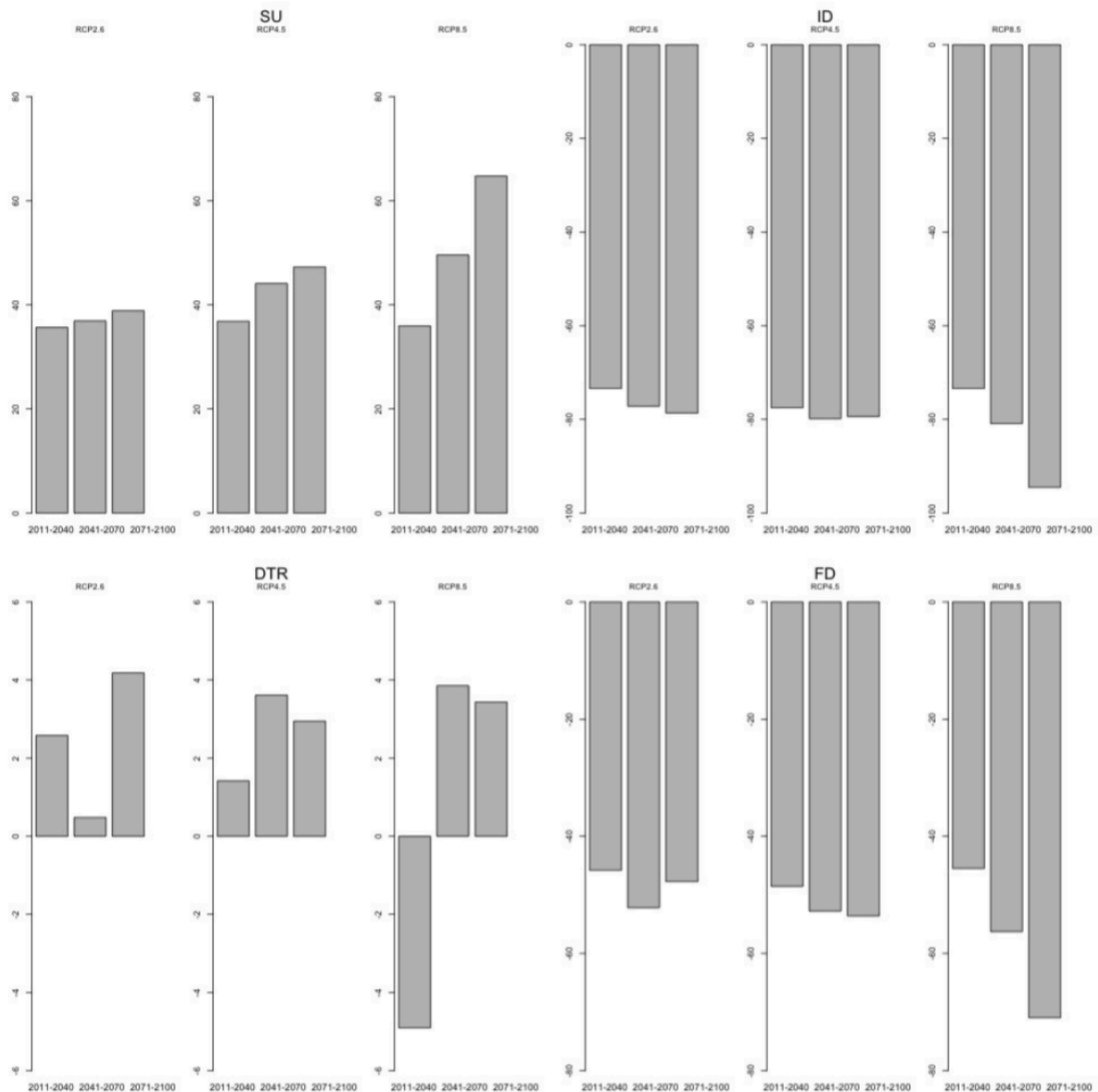


**Figure 36.** Changes on extreme indices, as SU, ID, DTR and FD, considering the percentile of difference between climate projections (divided into periods: 2011-2040, 2041-2070, 2071-2100) and the reference period of 1976 to 2005. These changes were calculated for the scenarios RCP2.6, RCP4.5 and RCP8.5.

The ID index were overestimated by historical projection and there is a tendency of decreasing of the values of this index in all projection. This tendency of decreasing is also founded considering the index FD, and is

more proeminente in RCP8.5 (Figure 35). This decreasing is reflected in the percentile of changes (Figure 36), which is negative in both index. This changes ranges -45.49% in the period of 2011-2040 to -70.95% in the period of 2071-2100 (FD, RCP8.5). For the index ID, this values are -73.43% to -94.5%, respectively.

The appendix A1, A2, A3 and A4 presents the values of this percentile of changes for all variables and indices.

In this first part of the research it was identified the climate change in the region (from 1901 to 2015). The model IPSL(CM5MR) was founded as the most accurate for the analyzed region. However, the model presented tendency of underestimation of precipitation and average and maximum temperature between 1901 to 2005. Regarding to minimum temperature this models has tendency to overestimation. Regarding to the indices of extreme events, we noticed that most of them showed good performance.

As a partial conclusion of this results we can highlight that the variation of precipitation in the future may cause increasing of the RX1DAY, RX5DAY, CDD and CWD. This evidence can be specially noticed observing the period of 2071 to 2100 in RCP8.5. In this projection, the increasing of 0.8% in precipitation (compared to the period of reference) will reflect an increase of 50.1% (RX1DAY), 29.05% (RX5DAY), 29.05% (CDD) and 42.08% in CWD. From this result we can conclude that the changes are more proeminente in maximum values of precipitation in 1 day (than the accumulated precipitation in a year or in the accumulated precipitation in 5 days). Also, the changes in the consecutive wet days (CWD) are larger than the changes in consecutive dry days (CDD). This situation representes a risk for agriculture, considering that the less distributed rainfall and scenarios of higher values of rainfall, increases for example the potential risk of runoff in the field which can compromise the production due to moisture stress. The consequences of this changes in climate conditions will be analyzed in next section.

Considering the extreme events of temperature, we noticed that the increasing of average, maximum and minimum temperature will be reflected as an increasing of the indices TN<sub>n</sub>, TN<sub>x</sub>, TX<sub>n</sub>, TX<sub>x</sub> and SU; and decreasing of the index ID and FD. Based on the simulation of RCP8.5 in the period of 2071 to 2100, is importante to highlight the increase of 125.42% of the minimum temperature and the increase of 56.66% and 84.48% in the minimum values of minimum and maximum temperature. This increase in temperatures will represent a risk for agriculture considering the evapotranspiration, which will increase the water necessity of the plants and can create a hydric stress. Also, the indices ID and FD tends to decrease (-94.5% and -70.92%), which can be good considering a possibility to switch the dates of planting and harvest as a mitigation measure.

## 4.2. Hydrus Model Simulation

### 4.2.1. Meteorological Analysis And Sensitivity Of Drainage Parameters

The drainage parameters play an important role in the dynamic of water and solutes in soil. In order to analyze the sensitivity of drainage parameters, is also necessary study the weather conditions in the experiment.

Figure 37 presents the meteorological fluxes simulated by Hydrus mode during April to September, 2015. The analyzed period correspond to the period between planting (April) and harvest (September) of maize, in 2015. The highest events of precipitation during the experiment occur in 05/30/15, 06/25/15 and 09/18/15 with values of 75.438, 73.914 and 60.198 millimeters, respectively.

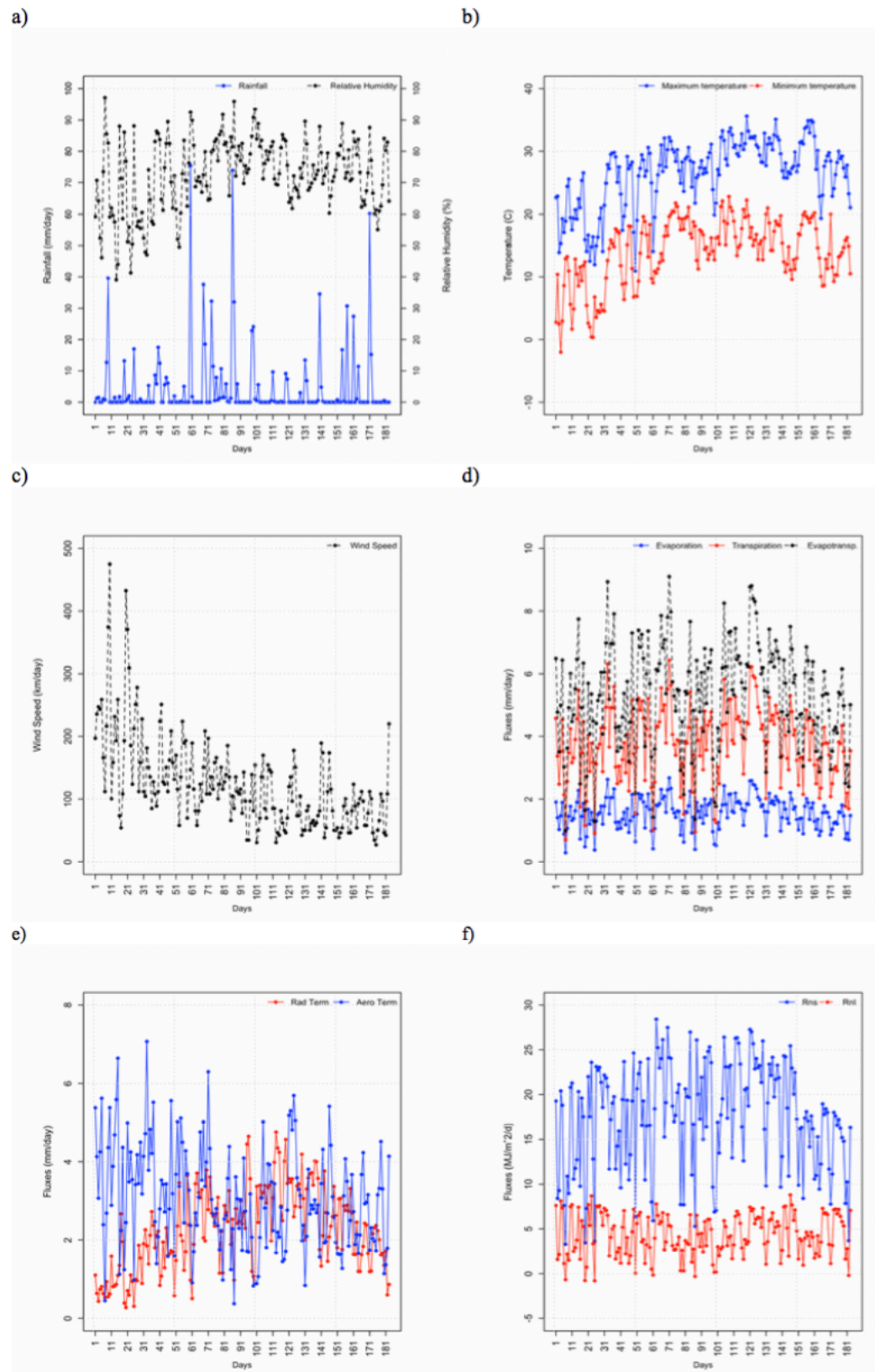


**Figure 37.** Meteorological fluxes, between April to September, 2015. The fluxes are divided into a) rainfall (blue) and relative humidity (black), b) maximum (blue) and minimum temperature (red), c) wind speed (black), d) evaporation (blue), transpiration (red) and evapotranspiration (black), e) radiative term (red) and aerodynamic term (blue), f) net short wave radiation (Rns, blue) and net out-going long wave radiation (Rnl, red).

Maximum and minimum temperature increased during the experiment with the approach of summer. We observed that the intensity of wind tends to decrease all over the days. This reflects in the aerodynamic term, which follow same pattern of decreasing. This pattern can be explained by the resistance of the crop to wind flow. The radiation term follow the increase and decrease of temperature during the cycle. Figure 37 indicate that most part of the evapotranspiration is due to the transpiration of the corn crop although the evaporation has some part in the total evapotranspiration.

After the precipitation, there is a reduction of values of maximum and minimum temperature, which reflect in reduction of fluxes of evapotranspiration, evaporation and transpiration. Regarding to the net short wave radiation (Rns) and net out-going long wave radiation (Rnl) we noticed that Rnl does not show larger variation in the studied period. However, Rns presents variation related with the variation of temperature.

Figure 38 shows the potential root water uptake of the crop. This potential was calculated from Hydrus and depends of the climate conditions, considering that the root water uptake is the response of the plant of thermal and water stress.

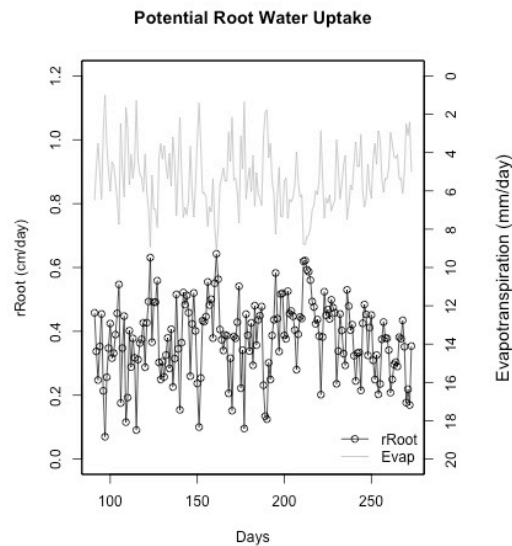


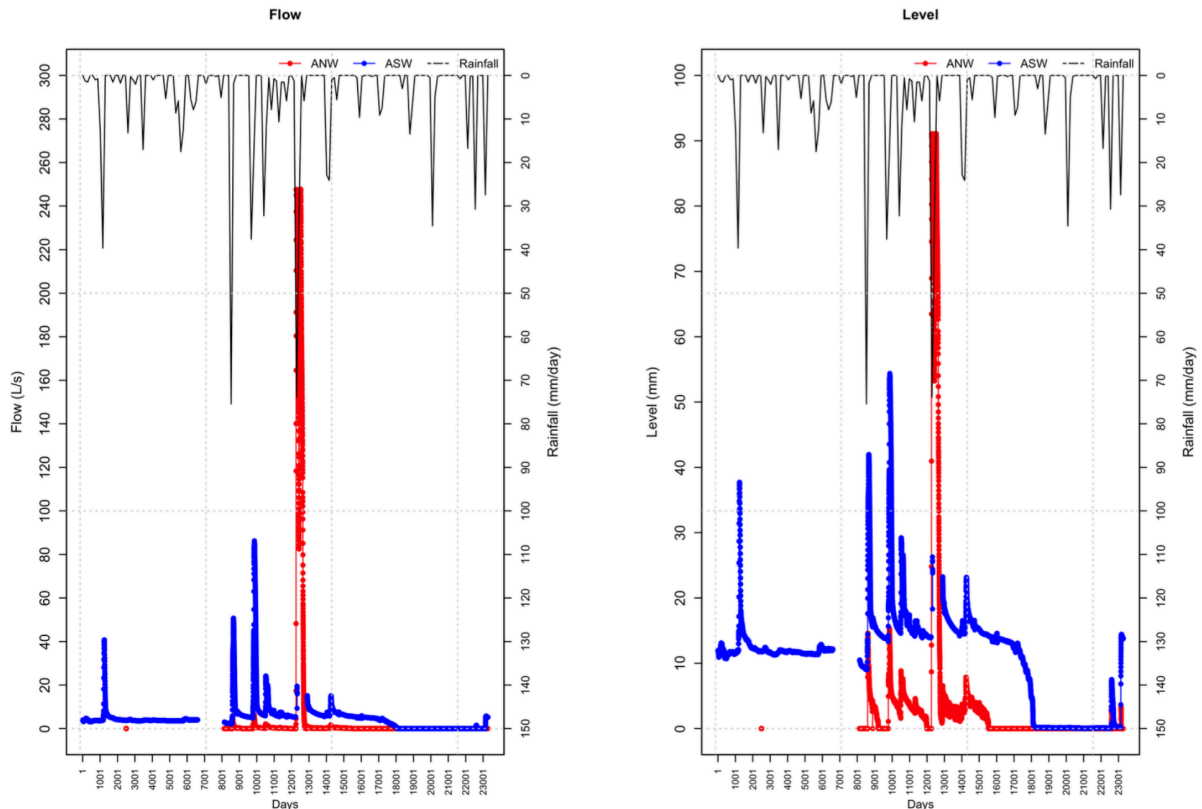
**Figure 38.** Potential root water uptake, considering the corn crop in the experimental field, from April to September (2015).

From Figure 38 we noticed that the changes in potential root water uptake is associated to changes in evapotranspiration. In this meteorological conditions were analyzed the flow in the experimental fields (ANW and ASW). The variation of flow and level according to the field is presented in Figure 39.

Figure 39 shows that level and flow have similar behavior, considering that the flow is the level of water after a V-Notch calibration. Analyzing the values of spacing between drains and depth of this drains in each field it is possible to explain the behavior of the level and flow founded in Figure 39. The field ANW and ASW has similar behavior, however, the values of level and flow are different in magnitude. As presented in Table 11, the field ANW is the one with drains near to surface (0.76 meters) and spacing between drains with 18.3 meters. So normally the field do not have large values of flow, and after a heavy precipitation (as happened in 06/25/2015) the system is capable to a flow large amount of water. This is the ideal condition for drainage system considering that this system does not allow large amount of water in the field and withdraws this water from the field, avoiding problems due to poor drainage.

Considering the field ASW (the one with higher spacing between drains), the system normally have some amount of flow, with immediate response after rainfall events and more susceptible to atmospheric conditions. However, when a large amount of water is introduced in the field, the drains need more time to drain the water from the field.

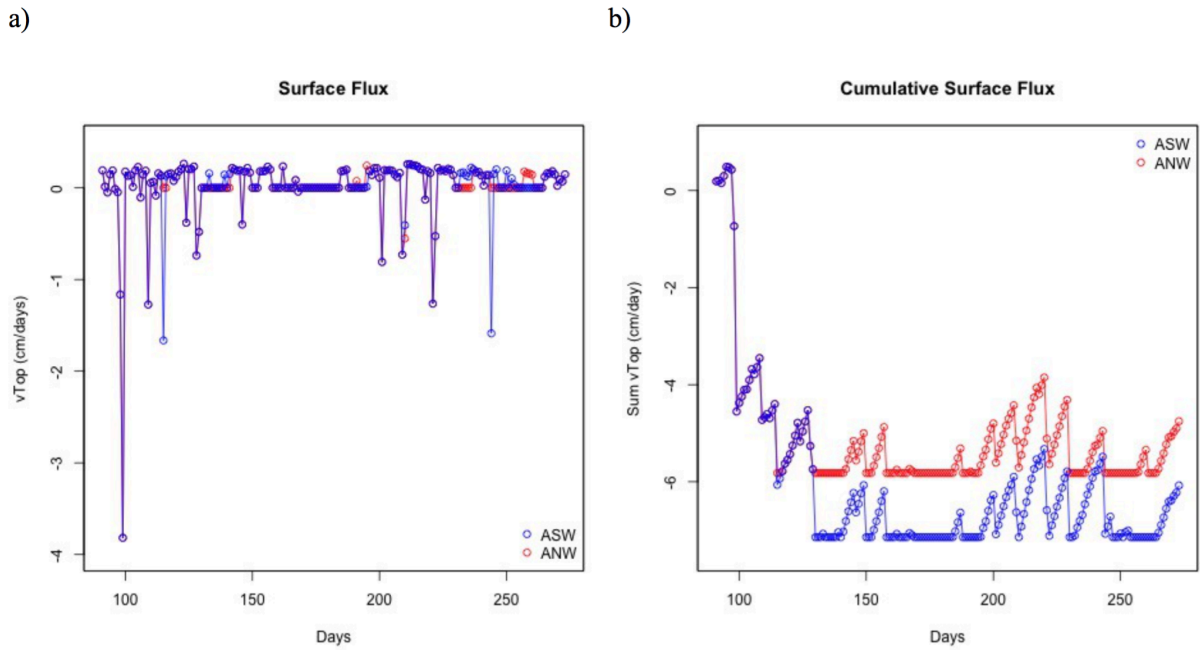
Hydraulic properties of this soil (as hydraulic conductivity, hydraulic capacity, water content and effective water content) can be found at Apendix B.1, and were based in Badiger et al (2001).



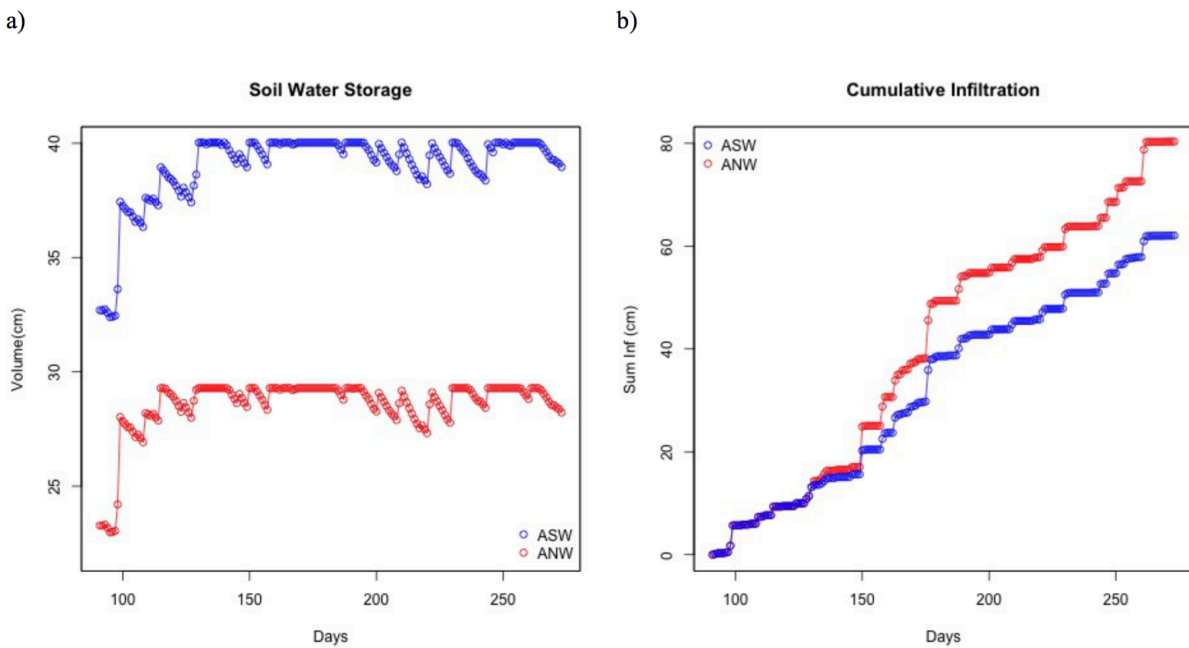
**Figure 39.** Meteorological fluxes, between April to September (2015). The data was collect in ANW (red) and ASW (blue) field.

Figure 40 and 41 shows the profile information in each field (ANW and ASW).

Figure 40 shows the water fluxes considering the variables surface flux ( $v_{Top}$ ,  $cm.day^{-1}$ ) and cumulative actual surface flux ( $Sumv_{Top}$ ,  $cm.day^{-1}$ ), over the different designs of drainage systems. To analyze this variables is necessary first state that the negative values is due to the direction of the flux). In other words, the negative flux is due to the direction of the flux to the soil or, the flux flowing into the drains, and are influenced by the drainage system parameters. In order to facilitate the understanding of these variables it will be treated as absolute values. The cumulative surface flux ( $sumv_{Top}$ ,  $cm.day^{-1}$ ) has same pattern of the surface flux with the lowest (absolute) values in the field with drains near surface (ANW) and highest (absolut) values in ASW field. Considering the surface flux ( $v_{Top}$ ,  $cm.day^{-1}$ ) it is noticeable that during an extreme event of precipitation there is always a large negative flux, following by a high value of flux. This relation can be confirmed when analyzed the events of large precipitation occurred in 05/30/2015, 06/25/2015 and 09/18/2015. ANW shows the lowest absolute values, and this flux is related to the proximity of the drain to surface.



**Figure 40.** Profile information of: a) surface flux ( $v_{Top}$ , cm.day<sup>-1</sup>) and b) cumulative surface flux (Sum  $v_{Top}$ , cm.day<sup>-1</sup>) in the fields ANW (red) and ASW (blue) in Illinois (USA), between April to September, 2015.



**Figure 41.** Profile information of: a) soil water storage (volume, cm) and c) cumulative infiltration (Sum Inf, cm.day<sup>-1</sup>) in the fields ANW (red) and ASW (blue) in Illinois (USA), between April to September, 2015.

Water storage (volume, cm) is the fundamental state variable of hydrological systems, as the water storage changes. The soil water storage indicated on Figure 41 shows that the field ANW presented lower value of soil water storage which is explained by the lowest spacing between drains and drains near to surface. ASW has higher values of water storage due to the higher spacing between drains, higher depth of the drains and consequently the difficulty to drain the water in the soil. This condition of ASW field may cause problems in future due to excess of water in the soil.

Both fields presented same pattern due to the relation of water storage with climate condition and plant growth, which are the same in both fields. Also, cumulative infiltration was higher in ANW than ASW. This occurs most likely due to the large spacing between drains used in the ASW field.

Infiltration (SumInf, cm) has long been a focus of agriculture and water research because of its fundamental role in land-surface and sub-surface hydrology, and agricultural irrigation (Milla & Kish, 2006). The infiltration value gives an idea if the root of the plant is receiving the necessary amount of water to maintain the production. ANW has highest values of infiltration also because of the smaller depth of the drains which facilitate the infiltration into the soil, when compared to the other field. Since ASW has high values of spacing between drains, it is noticeable that the infiltration in this field is smaller.

Figure 42 shows the profile information, considering the variables: surface runoff (Flux, cm.day<sup>-1</sup>) and cumulative surface runoff (CumFlux, cm), between April to September, 2015. Regarding to surface runoff (Flux, cm.day<sup>-1</sup>), Figure 42 shows that the ASW field presents higher values which indicates that there is a large flux over the surface due to the condition of drains installed and the incapability to infiltrate the water. Figure 42 also shows that considering the cumulative surface runoff (CumFlux, cm) there is no large difference between the fields. Also, as expected, the highest values of CumFlux are related to extreme events of precipitation (days 150, 176 and 261).

Also was simulated by Hydrus model the profile information of water content ( $\theta$ , -), water flux ( $v$ , cm.day<sup>-1</sup>), pressure head ( $h$ , cm), hydraulic conductivity ( $k$ , cm.day<sup>-1</sup>) and hydraulic capacity ( $C$ , 1.cm<sup>-1</sup>). Those parameters were simulated in different time. The Figure 43 shows the parameters simulated in 4 prints: T1 (day 91), T2 (150), T3 (200) and T4 (273). Before analyzing this figure it is important to highlight some information regarding the climate conditions of these specific days printed. In the day 91 the precipitation was zero and the model did not have enough time to adjust simulation. In the day 150, the region experimented an extreme event of precipitation (around 75.438 mm in a day) after a dry period. In day 200, the soil was humid, not because of the rainfall of the day (which was 0.508 mm) but because of the sequence of wet days presented in the week. The final time (day 273) did not have precipitation events. As expected (and showed in Figure 43), the print 2, which represents the day when occurred an event of intense precipitation, had the higher values of hydraulic conductivity, pressure head and water contents. This fact indicates the necessity of studying the climate conditions and the effects of future climate changes over hydrological parameters.

The yield of the both fields, ANW and ASW, were equal and around 216.06 bu/acre. This yield can be related to a lot of factors, and not only because of the drainage system. This makes it difficult to compare yield with any other variable.

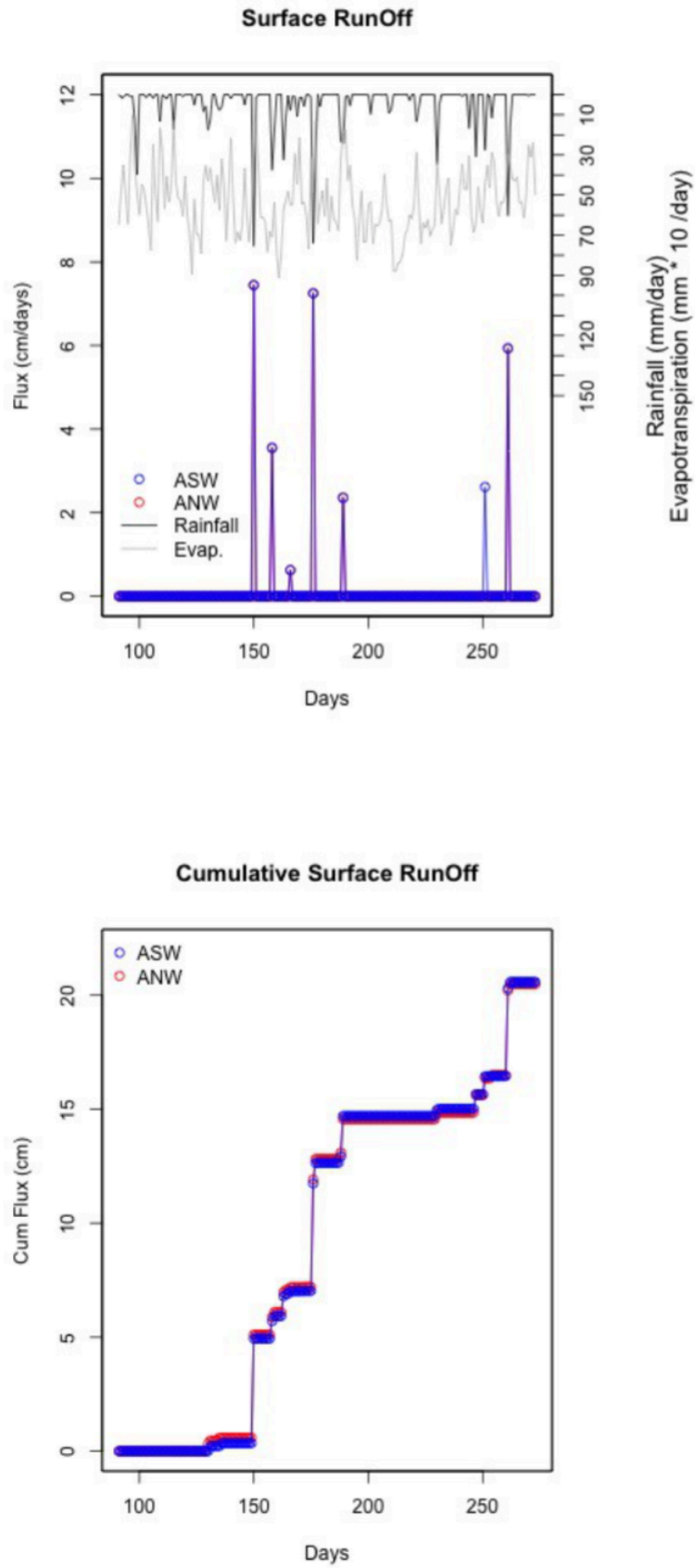


**Figure 42.** Profile information of surface runoff (flux, cm/day) and cumulative surface runoff (Sum Inf, cm) in the fields ANW (red) and ASW (blue) in Illinois (USA), between April to September, 2015.

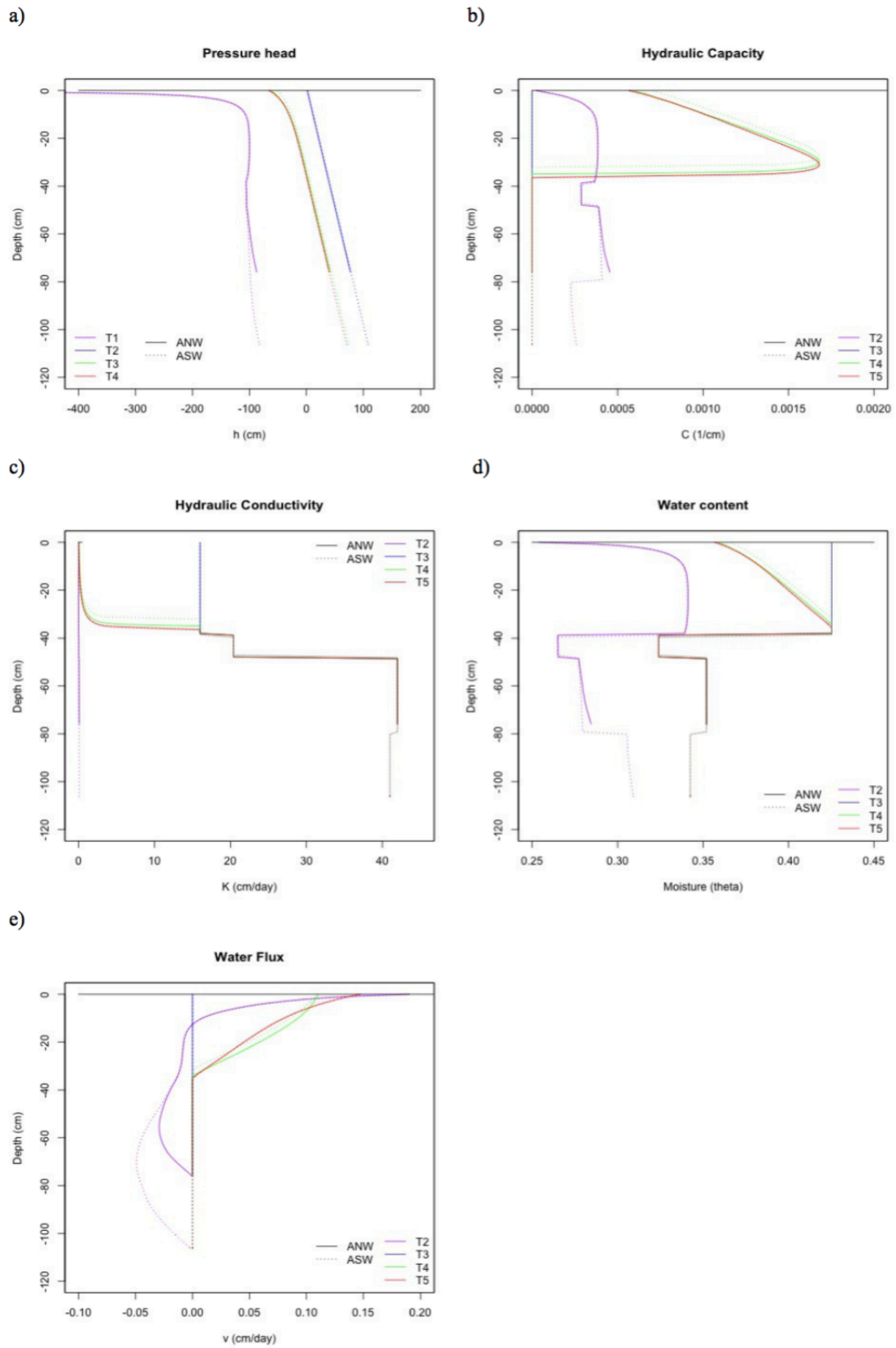


**Figure 43.** Profile information of a) water flux, b) hydraulic conductivity, c) hydraulic capacity, d) pressure head and e) water content, in a soil in Illinois (USA), between April to September, 2015. The variables were simulated for three fields (ANW and ASW) showed with different line types and were simulated in five different times showed with different colors.

## 4.2.2. Applications In Climate Projections

In this section is presented the results of hydrus simulation, using climate data from different climate projection scenarios. This section is divided into past analysis and future climate projection (presented for short, medium and long term integration).

### 4.2.2.1. Past Analysis

The past analysis were made considering the period of 30 years from 1976 to 2005. This period was chosen after the initial results of climate section, which indicates changes of patterns all over the 20<sup>th</sup> century. So it was assumed that this period represents better the current climate. The length of 30 years were considered in order to have same length of time series as the simulations for future (RCP2.6, RCP4.5 and RCP8.5). For this reason, it is showed just the simulations from 1976 to 2005 to consider as a baseline for the following steps of the research.

Figure 44 indicates the surface flux and cumulative surface flux simulated for both fields. Considering the historical simulation it was observed same pattern as the presented with observed data, where the field ASW presented lowest (absolute) values of surface flux and cumulative surface flux (Figure 44). This result agreed with the results founded in Figure 40.

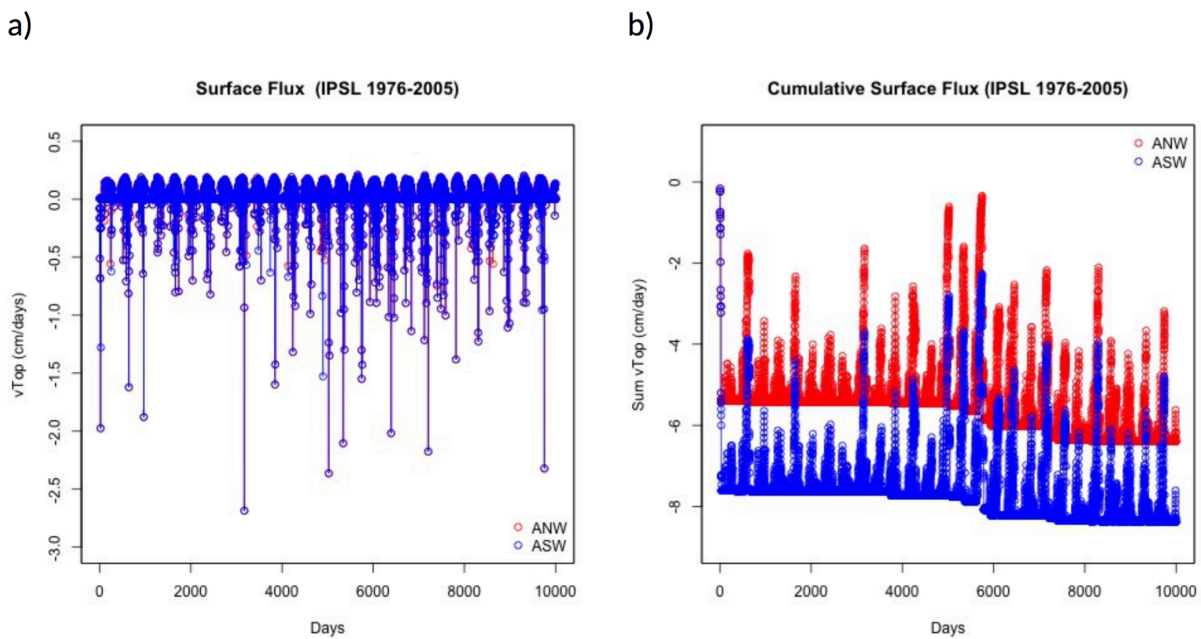


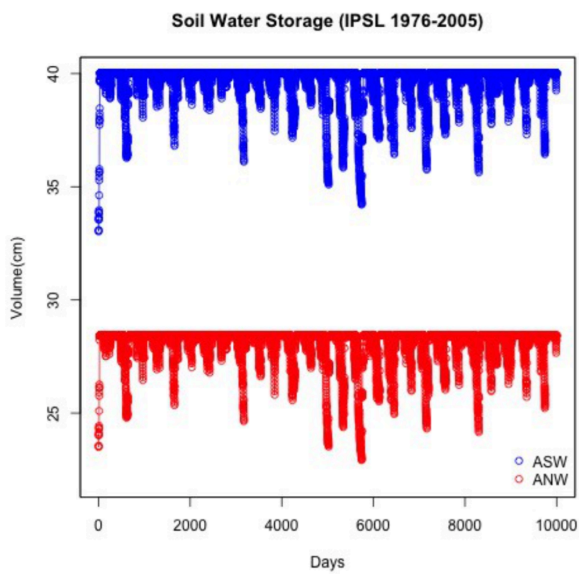
**Figure 44.** Profile information of: a) surface flux ( $v_{Top}$ , cm.day<sup>-1</sup>) and b) cumulative surface flux ( $Sum v_{Top}$ , cm.day<sup>-1</sup>) in the fields ANW (red) and ASW (blue) in Illinois (USA), considering the period of 1976 to 2005 in the historical simulation of IPSL model.

Also, observing the cumulative surface flux it is noticeable an increase of this value in the last 15 years of analysis. This can be analyzed in the context of extreme events indices, which indicate increase of extreme events of precipitation in same period (for example, as showed in Figure 21, RX1DAY).

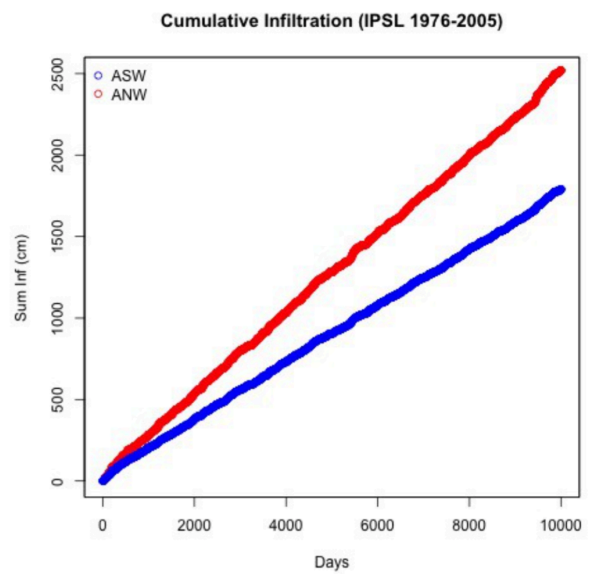
Figure 45 present the historical simulation of the soil water storage and cummulative infiltration, and shows also the same trend as Figure 41 (observed simulation). However it is also noticeable from Figure 42 that the soil water storage tended to reduce in the last 15 years.

Figure 46 shows the runoff and cumulative runoff for the historical simulation in both fields. However, this figure does not indicates visible changes in runoff or cumulative runoff considering the selected drainage systems. So further steps of this studies will present valuable explanation regarding to the behavior of runoff in both fields.

a)



b)



**Figure 45.** Profile information of: a) soil water storage (Volume, cm) and b) cumulative infiltration (Sum Inf, cm.day-1) in the fields ANW (red) and ASW (blue) in Illinois (USA), considering the periof of 1976 to 2005 in the historical simulation of IPSL model.

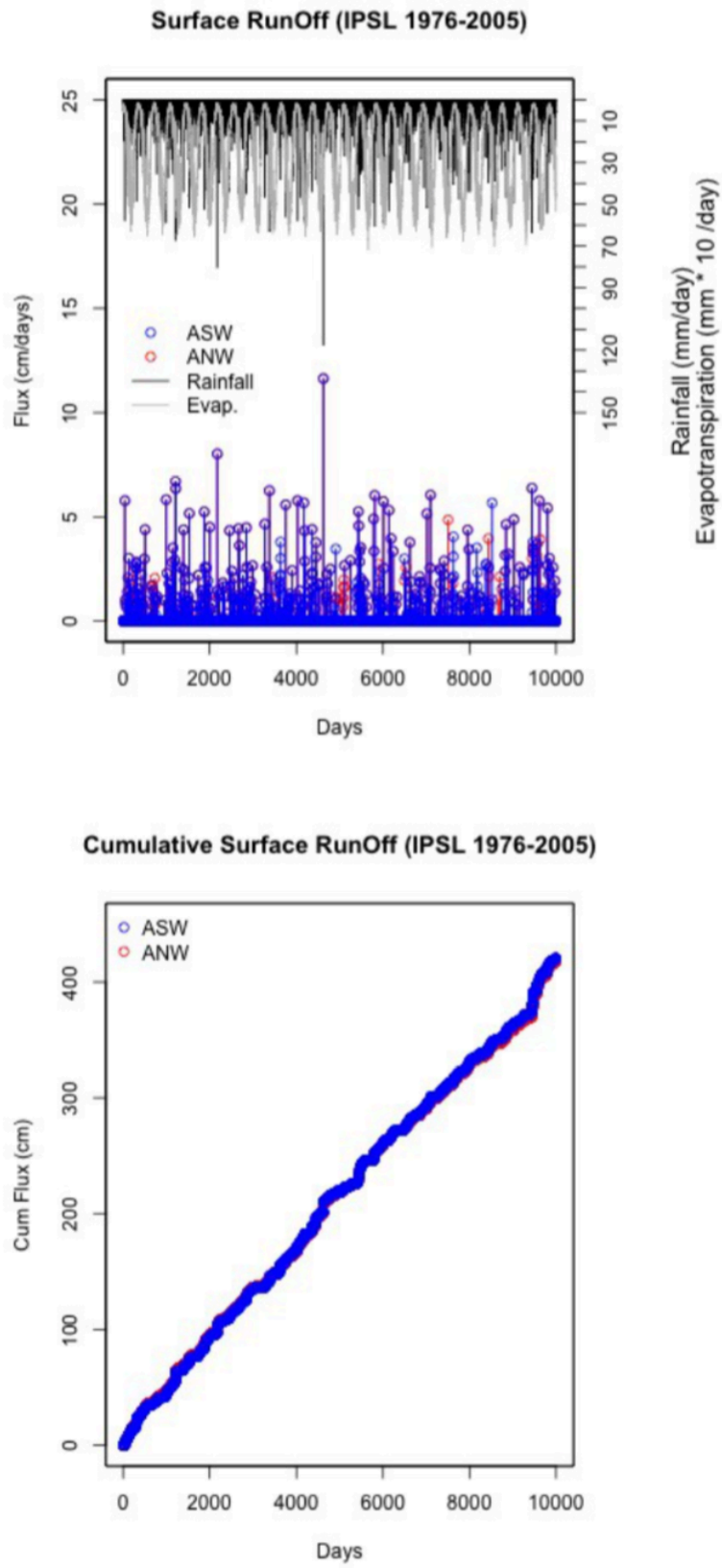


**Figure 46.** Profile information of: a) surface runoff (flux, cm/day) and c) cumulative surface runoff (Sum Inf, cm) in the fields ANW (red) and ASW (blue) in Illinois (USA), considering the period of 1976 to 2005 in the historical simulation of IPSL model.

#### 4.2.2.2. Short, Medium and Long Time Variations

Climate changes is likely to have significant effects on the hydrological cycle. In this section is presented the simulations of dynamic of water in soil under different climate projections, using IPSL\_CM5 model. This model was chosen after the errors of a set of models for this specific region were analyzed. The hydrological cycle it will respond to the differences in climate variations, which will also contribute to the evapotranspiration and also will define the necessity of the crop, in terms of water and temperature. Those differences in climate projections were already studied in the section 4.1, which showed the increasing of annual average of maximum and minimum temperature and annual accumulated precipitation. It was also showed the increasing of indices of extreme events of precipitation (CDD, CWD, Rx1DAY, Rx5DAY) and temperature (SU, TXx and others), and decreasing of some temperature indices (ID, FD).

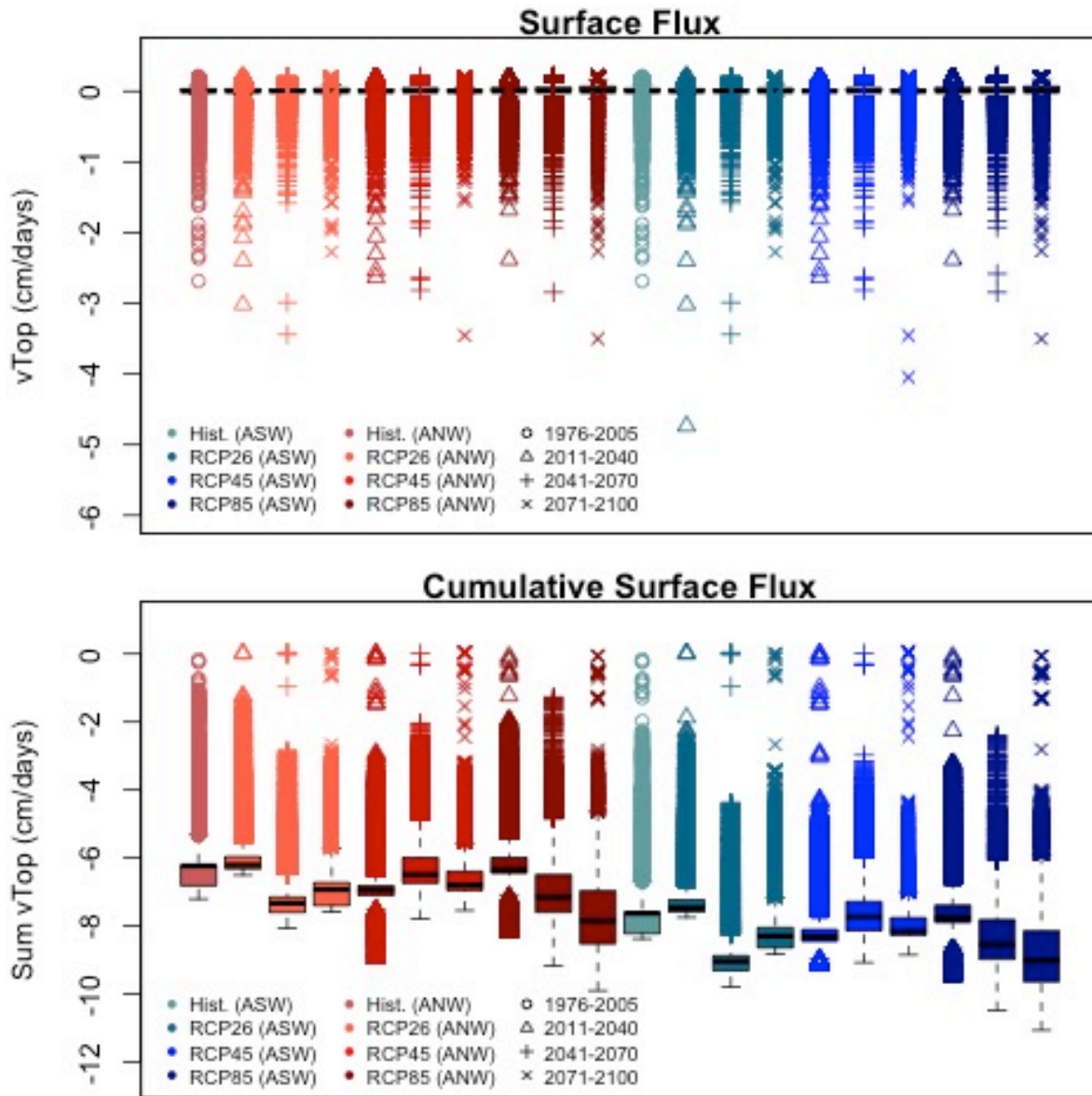
This unequal distribution of precipitation, as changes in the timing of wet and dry season can lead in both drought and flood, which makes important studies about effect of climate changes in dynamic of water. Also, as indicated in Appendix C 1, IPSL model integrated with Hydrus model presented an increase of evapotranspiration all over the analyzed periods. The period with higher percentile change in evapotranspiration is 2071-2100, and this changes are more pronounced in RCP8.5 scenario (around 19% of increasing of evapotranspiration). Also, as presented in the previous sections the hydrological cycle will be intensified, with more evaporation and more precipitation. But the increase in the precipitation it is unequal, by the occurrence of extreme events of precipitation.

Simulations were made in order to describe the variations of hydrological and climatological variables under scenarios of climate changes. The scenarios was chosen to represent the optimistic, regular and pessimist projection (RCP2.6, RCP4.5 and RCP8.5) for each field. The next figures presents the simulations of IPSL model applied in Hydrus model to simulate surface pressure head, cumulative surface pressure head, soil water storage, cumulative infiltration, considering this variables really important in a crop corn production. This part of this research intend to describe changes in hydrological characteristic at this particular region located in Champaign (Illinois). The model is run to simulate 30 years (1976-2005, 2011-2040, 2041-2070, 2071-2100) in a daily time step.

The data simulated in Hydrus using climate projections were compared with a baseline climatology (circle), from 1976 to 2005. The simulation were plotted as a boxplot (Figures 47, 49 and 51), in order to verify the outliers of the series, considering this outliers as extreme events, which are more dangerous to agricultural processes. Also was plotted the percentile of average changes in different scenarios of projections and period, as presented in Figures 48, 50 and 52.

From figure 47 it is possible infer about how climate change may affect the surface flux. The negative signal of the surface flux were used to indicate the direction of the flux and the values will be explained as absolut values. On the top of the figure, the field ANW (red) presented lower values (module) comparing to ASW (blue). This indicates that the risk associated in ASW drainage system is higher than ANW, which is related to the higher spacing between drains and the difficulty in this case in drainage the necessary amount of water. Considering both fields, the simulations normally indicates more oliers (high values, or in other words, extreme events of surface flux) in the future projections when compared to the period of reference (mostly the simulations of 2011-2040 and 2041-2100). It is not possible to indentify a pattern of variation in terms of average values of surface flux within the fields or within the periods od simulation. To analyze this average values, Figure 38 shows the percentile of change in the average values. This analysis were made using the average values of the period and compared to the values of the reference period. This changes shows the uncertainty of the projected hydrological variables. This values are also

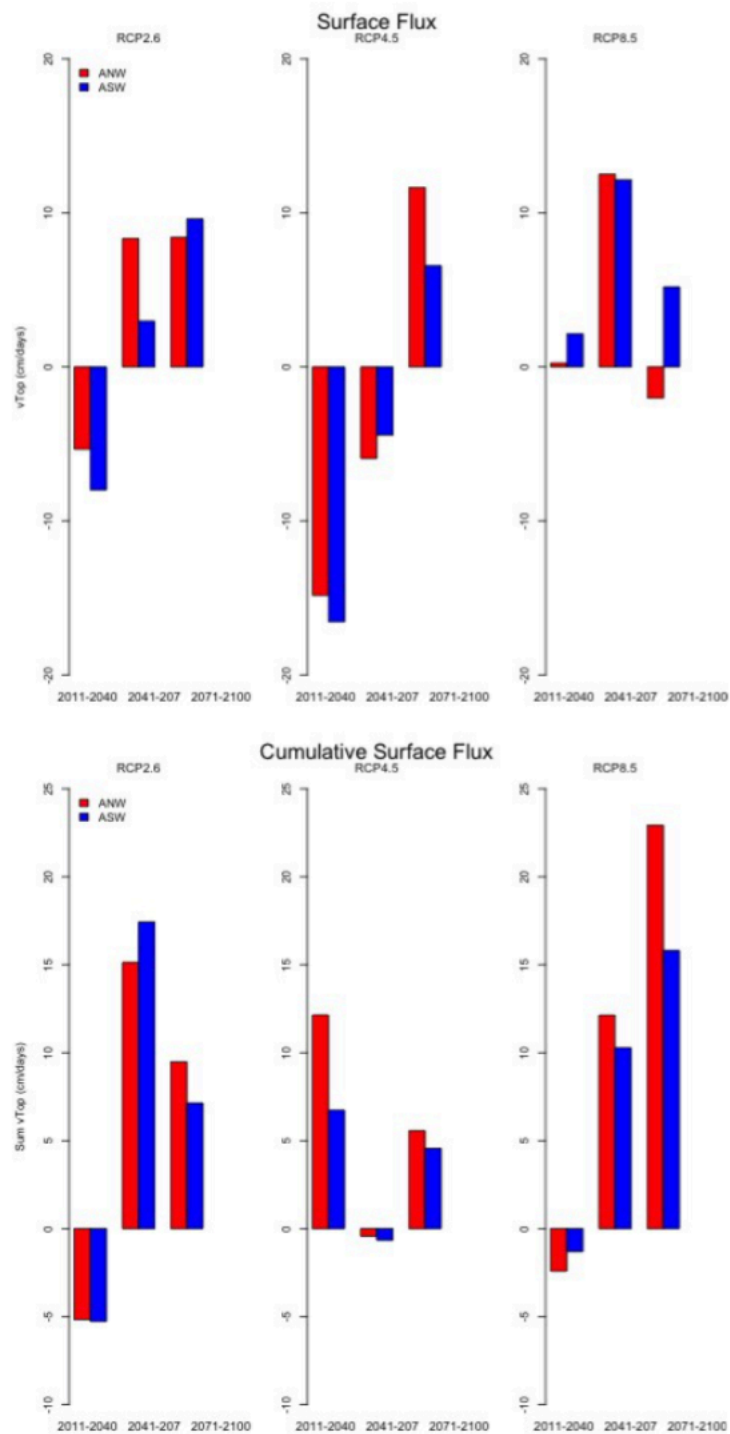
presented in Appendix D, as a table. From the top of Figure 38 we observed that in terms of average values the simulations shows a tendency of decreasing of surface flux in the beginning of the century (20011-2040, RCP2.6 and RCP4.5) and increasing in middle and end of century (2041-2070 and 2071-2100, RCP2.6 and RCP4.5).



**Figure 47.** Climate scenarios applied to simulations of surface flux (top) and cumulative surface flux (bottom), considering the fields ANW (shades of red) and ASW (shades of blue). Scenarios were divided into historical (1976-2005, circle symbol) and short (2011-2040, triangle symbol), medium (2041-2070, cross symbol) and long time variation (2071-2100, x symbol)

In the bottom of Figure 47 it is also noticed that the cumulative surface flux, in general is higher in ASW. Since the values of cumulative surface flux in ANW is close to ASW, we can conclude from this figure that ANW have small values of surface flux more often, which indicates that the system is well designed. We also observed that in ANW simulation most simulations have higher average values of cumulative surface flux than the average of the period of reference (except in 2011-2040, RCP2.6 and RCP8.5 simulation). Also, the simulations indicate increasing of maximum values of acumulated surface flux. Considering the ASW field, same pattern is founded. As in ANW, the only period that the average value of simulation were lower than the average value of the reference period was in

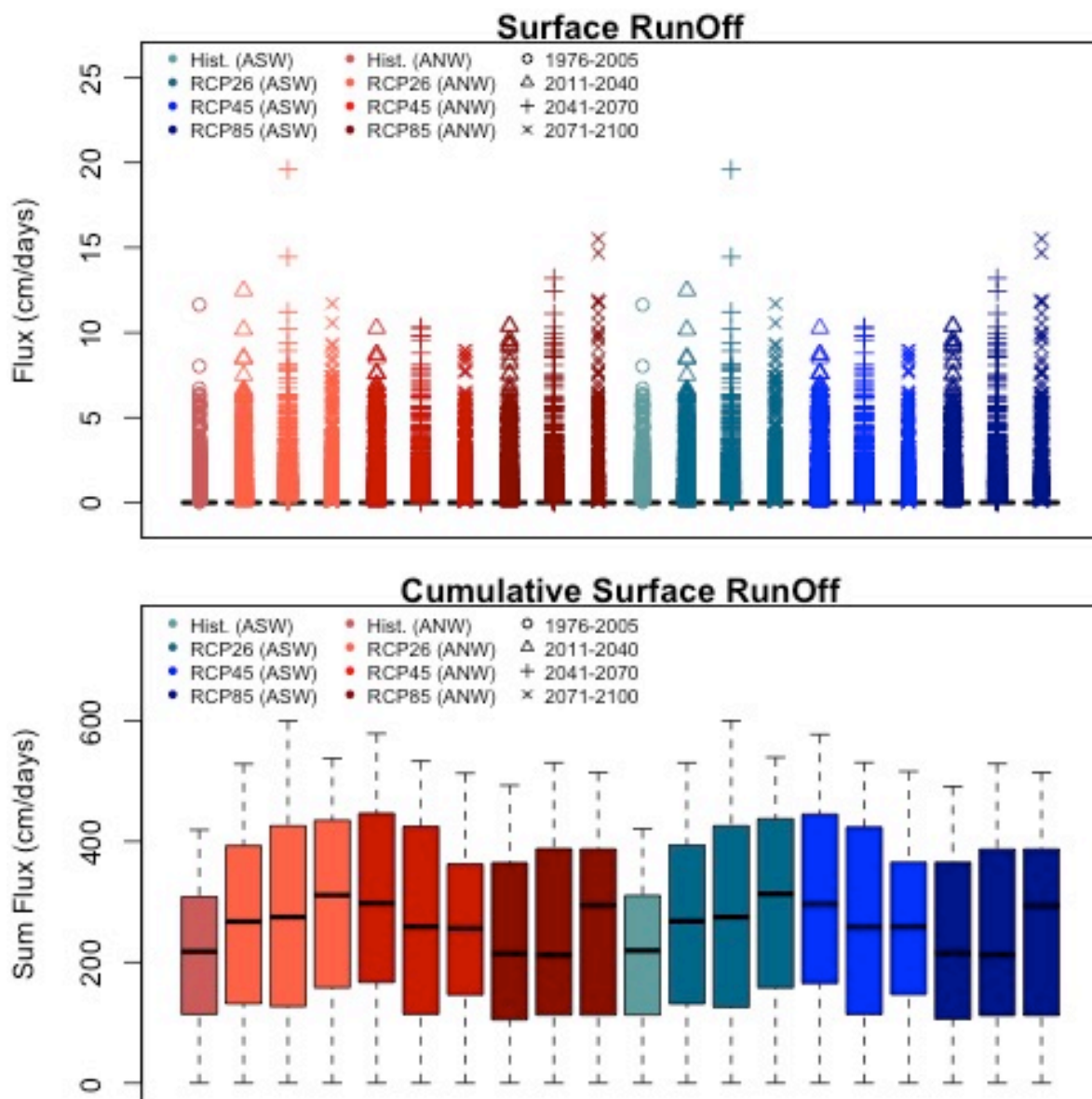
2011-2040, considering the scenarios RCP2.6 and RCP8.5. So, the tendency of the variables surface flux and cumulative surface flux, is in general, increasing over scenarios of climate changes (in maximum and average values). This tendency can also be noticed in Figure 38. This figure indicates that the changes in average cumulative surface can reach 22.92% in the end of century (RCP8.5), considering ANW field. This percentile changes in cumulative surface flux tends to be higher in ANW, which indicates that in future it will be necessary some adaptations in the “ideal” drainage system in order to maintain the good performance of the system.



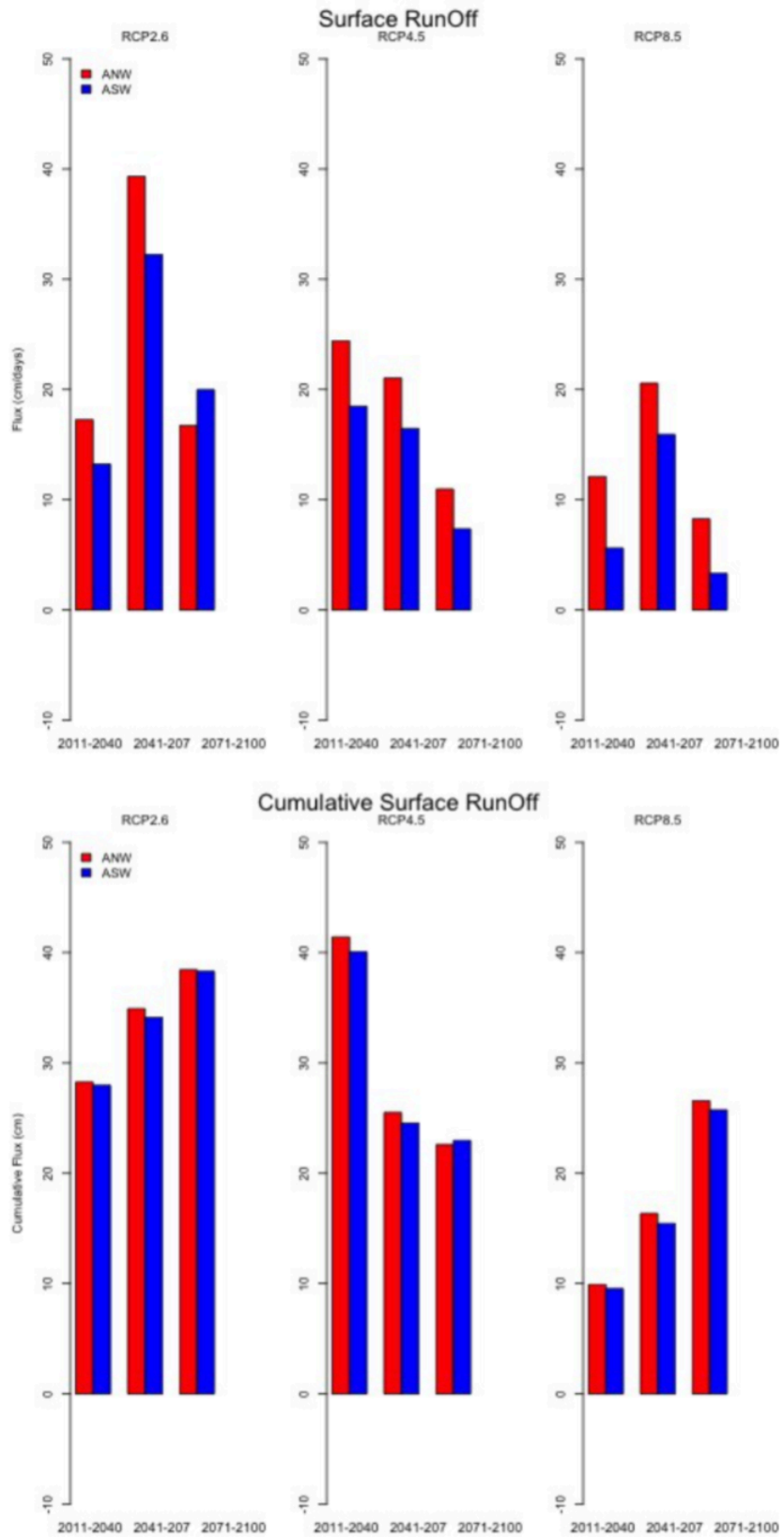
**Figure 48.** Percentile of changes in surface flux and cumulative surface flux, considering ANW (red) and ASW (blue) field. The percentile was calculated for the climate projections RCP2.6, RCP4.5 and RCP8.5, considering the periods of 2011-4040; 2041-2070 and 2071-2100, compared to the reference period (1976-2005).

Figure 49 shows the change in average daily runoff over the study region, by the different projections and scenarios. This difference was calculated from the data simulated to ANW and ASW field, and considering the baseline as the period of 1976 to 2005.

Considering the surface runoff (Figure 49) it is observed that there is a large amount of days considered as an outlier. This is especially important, considering this outliers as extreme events of runoff which can cause intense damages on agriculture and affect the local economy. It is important to highlight that the outliers of runoff over the period of 2041-2070 under RCP2.6 is the worst possible scenario in both fields. The values of cumulative surface runoff presented in Figure 46 seems to be similar. Also it is noticeable that the all simulation indicates increasing of surface runoff and cumulative surface runoff in terms of maximum values. The percentile of changes of average values of runoff and cumulative runoff are presented in Figure 50.



**Figure 49.** Climate scenarios applied to simulations of surface runoff (top) and cumulative surface runoff (bottom), considering the fields ANW (shades of red) and ASW (shades of blue). Scenarios were divided into historical (1976-2005, circle symbol) and short (2011-2040, triangle symbol), medium (2041-2070, cross symbol) and long time variation (2071-2100, x symbol).



**Figure 50.** Percentile of changes in surface runoff and cumulative surface runoff, considering ANW (red) and ASW (blue) field. The percentile was calculated for the climate projections RCP2.6, RCP4.5 and RCP8.5, considering the periods of 2011-4040; 2041-2070 and 2071-2100, compared to the reference period (1976-2005).

Figure 50 shows that the climate projection tends to increase the surface runoff in different scenarios of simulation. This increasing range from 5.61% to 24.4% in 2011-2040, compared to historical simulation. This range is around 16.45 to 39.32%, considering 2041 to 2070 and finally 3.32 to 19.98% for 2071 to 2100.

Soil water storage and cumulative infiltration can be an indicative of water stress and for this reason is really important to analyze this variable in future projections under climate changes. The ideal condition of soil water storage depends of the phase of the crop cycle, cultivars, soil, among other variables. Although estimate the ideal condition is difficult, and requires experimental researches, the changes of this values of soil water storage turns to be an important factor that needs to be studied. Those changes highlight the fact that is necessary to create mitigation measures to deal with this variability.

The soil water storage has large variability, so we can notice a presence of large amount of outliers (Figure 51).

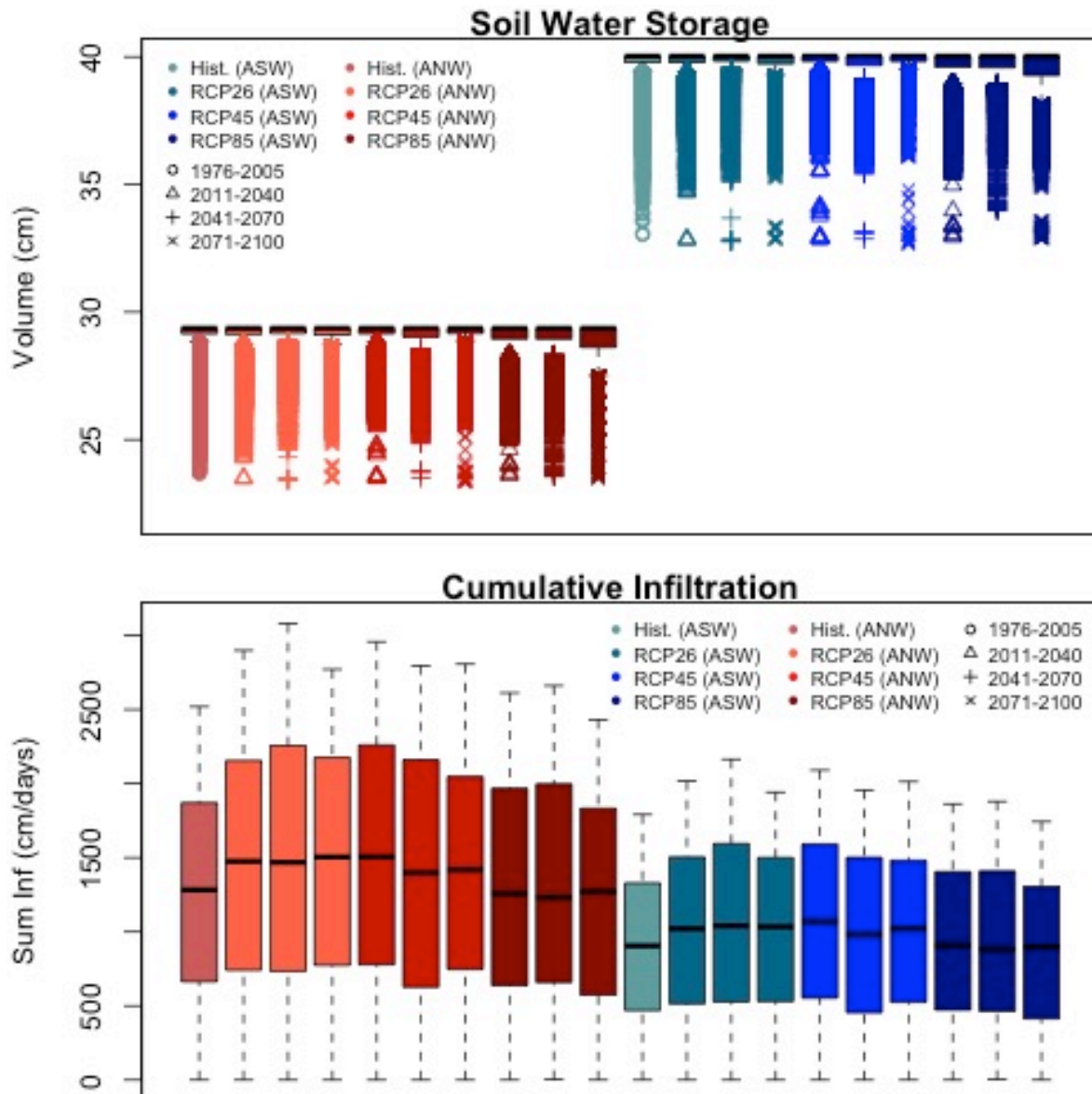


**Figure 51.** Climate scenarios applied to simulations of soil water storage (top) and cumulative infiltration (bottom), considering the fields ANW (shades of red) and ASW (shades of blue). Scenarios were divided into historical (1976-2005, circle symbol) and short (2011-2040, triangle symbol), medium (2041-2070, cross symbol) and long time variation (2071-2100, x symbol).

This outlier is even more expressive when we consider the historical simulation, which represents the current climate. This explains the fact that we are already having problems under soil water storage, as explicit in literature review section. The soil water storage is larger in ASW field, which agrees with previous results and again, is explained by the higher depth of the soil profile, permitting a bigger amount of water in soil.

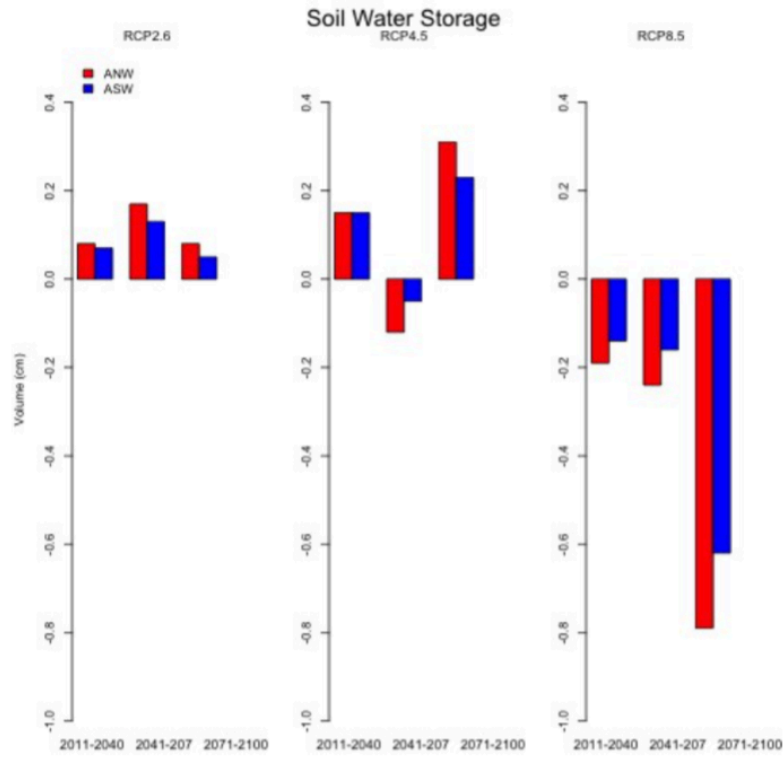
In the bottom of Figure 51 is indicated the cumulative infiltration. The cumulative infiltration is lower in ASW, due to the difficulty of the drainage system of this field to drain the water and promote higher infiltration. The maximum values of infiltration tend to be higher in all simulations when compared to the period of reference (in both fields). Figure 52 shows the percentile of changes for soil water storage and cumulative infiltration.

From Figure 52 we observe gradual decreasing of soil water storage in RCP8.5, although the differences are lower than 1%. RCP's 2.6 and 4.5 indicate different behavior, as present an increase of the percentile change in soil water storage in long term. Again, changes in soil water storage is small, comparing to other variables. Also, changes in cumulative infiltration indicate that scenarios RCP2.6 and RCP4.5 simulate positive changes, as the infiltration tends to increase in future. RCP8.5 simulates a small increasing in short and medium term and small decrease in long term simulation.

In order to summarize some results founded in this section, Figure 53 shows the values of surface flux and runoff all over the years, compared to precipitation. These results were displayed for both fields and different RCPs. From Figure 53 we observed changes in the values of precipitation, with more often high values of daily rainfall. Also, we noticed, mostly in RCP2.6 and RCP8.5 increasing of runoff all over the years. From RCP4.5 and RCP8.5 we can also notice increasing of surface flux all over the years.

To conclude this section, Figure 54 indicates the percentile of changes (considering climate scenarios and historical simulations) of extreme events and hydrological variables. In this Figure the variables with hatch presented significant difference at the level of 5% of significance (also showed in Appendix D4). The tendency of the surface flux and cumulative surface flux, is in general, increasing over scenarios of climate changes (in maximum and average values). This tendency can also be due to the changes in average cumulative surface that can reach 22.92% in the end of century (RCP8.5), considering ANW field. This percentile changes in cumulative surface flux tends to be higher in ANW, which indicates that in future it will be necessary some adaptations in the "ideal" drainage system in order to maintain the good performance of the system. The percentile of changes of average values of runoff and cumulative runoff shows that the climate projection tends to increase the surface runoff in different scenarios of simulation. This increasing range from 5.61% to 24.4% in 2011-2040, compared to historical simulation. This range is around 16.45 to 39.32%, considering 2041 to 2070 and finally 3.32 to 19.98% for 2071 to 2100. From the percentile of changes for soil water storage and cumulative infiltration we observe gradual decreasing of soil water storage in RCP8.5, although the differences are lower than 1%. RCP's 2.6 and 4.5 indicate different behavior, as present an increase of the percentile change in soil water storage in long term. Again, changes in soil water storage is small, comparing to other variables. Also, changes in cumulative infiltration indicate that scenarios RCP2.6 and RCP4.5 simulate positive changes, as the infiltration tends to increase in future. RCP8.5 simulates a small increasing in short and medium term and small decrease in long term simulation.

a)



b)

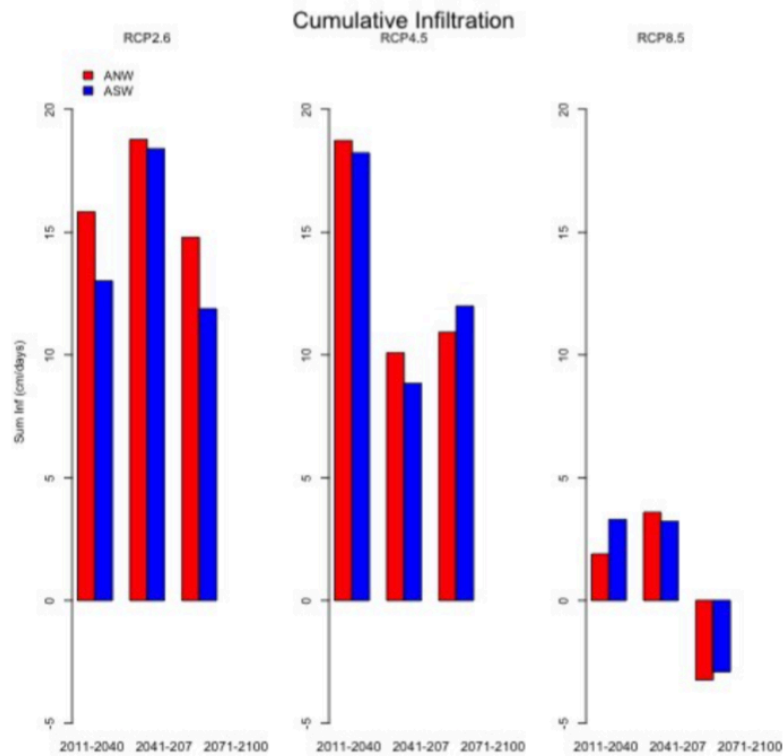


**Figure 52.** Percentile of changes in soil water storage and cumulative infiltration, considering ANW (red) and ASW (blue) field. The percentile was calculated for the climate projections RCP2.6, RCP4.5 and RCP8.5, considering the periods of 2011-4040; 2041-2070 and 2071-2100, compared to the reference period (1976-2005).

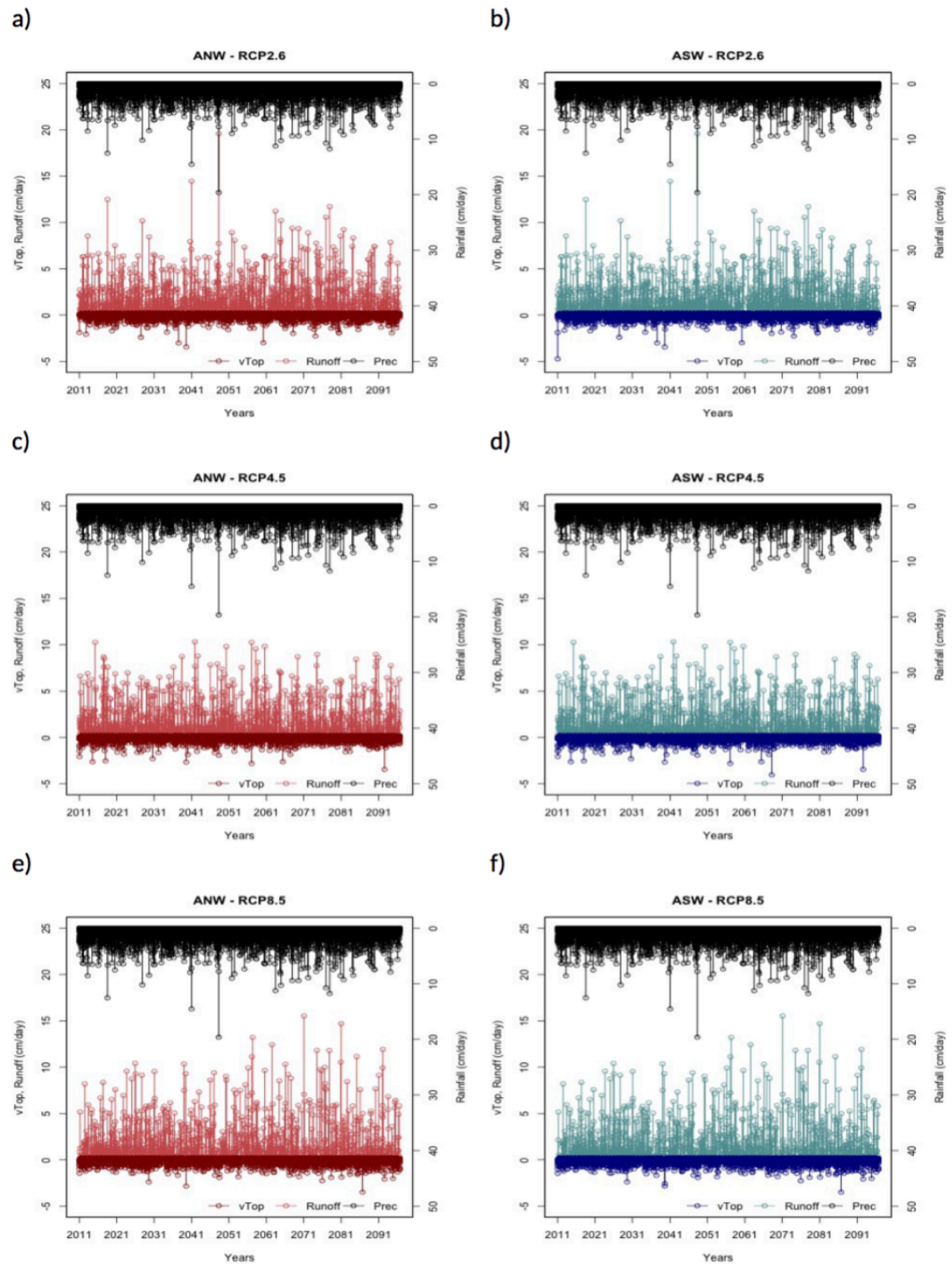


**Figure 53.** Surface flux, surface runoff and precipitation, considering the fields ANW (red) and ASW (blue), in the RCP2.6 (a, b), RCP4.5 (c, d) and RCP8.5 (e, f). The analyzed period was from 2011 to 2100.

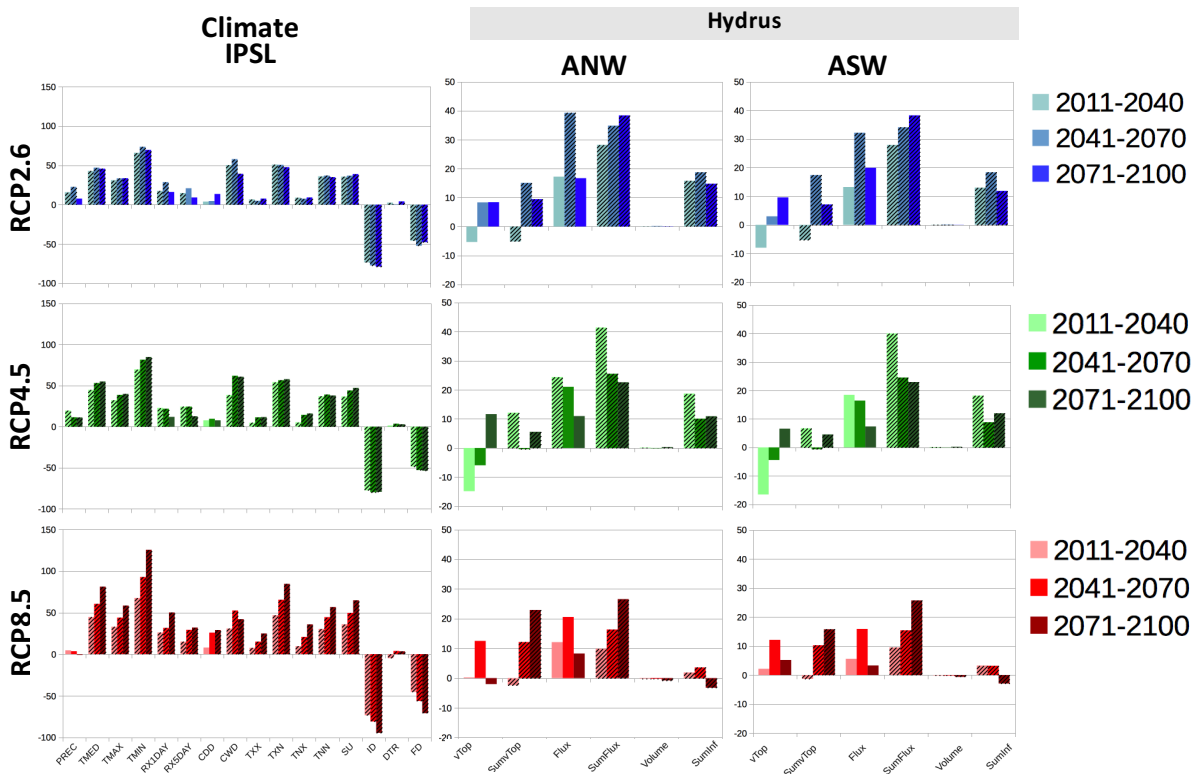


**Figure 54.** Summary of percentile fo changes (considering climate scenarios and historical simulations) of extreme events and hydrological variables. Variables with hatch is considered statistically different, considering a significant level of 5%.

From Figure 54 it is also possible to identify that extreme events can have a large impact over these hydrological variables. Considering, for example, the simulation RCP8.5 in the short term (2011-2040) we can notice that a small increasing of precipitation (0.8%) can lead to a large increasing of extreme events of precipitation (50.1% in RX1DAY, 32% in RX5DAY, 29.1%\* in CDD and 42.1% in CWD) resulting in changes in the dynamic of water in soil. For both fields these changes are increasing of cumulative surface flux (22.92% in ANW and 15.8% in ASW), runoff (8.26%\* in ANW and 6.32%\* in ASW), and cumulative runoff (26.57% in ANW and 25.75% in ASW) and decreasing of soil water storage (-0.79% in ANW and -0.62% in ASW) and infiltration (-3.24% in ANW and -2.91% in ASW). Percentiles with \* are non significant in a 5% level of significance.

### 4.2.3. Correlation between hydrological variables and extreme climatic events

The changes in the hydrological variables can be related to the changes in extreme events studied in the section 4.1.

Figure 55 shows the correlation between maximum values of surface flux in (ANW and ASW field) with extreme events of precipitation and temperature. Regarding to ANW field, it is found different correlations in different scenarios. In scenario RCP2.6 the surface flux tends to have higher correlation with CDD and DTR (0.45 and 0.43, respectively). For the scenarios RCP4.5 and RCP8.5 the correlation is higher for the indices DTR (0.44) and SU (0.41), respectively. These correlations seem to be even lower in ASW field. For ASW fields, the correlations higher than 0.4 were only found in RCP8.5, which indicates that the surface flux is inversely correlated with precipitation (-0.44) and correlated with SU (0.4).

Considering the Figure 56, which shows the correlation between runoff and extreme events, the correlation seems to be higher. All simulations indicated that the correlation between runoff and extreme events of precipitation

RX1DAY (ranges between 0.76 and 0.78) and RX5DAY (ranges between 0.5 and 0.66) are higher than the correlation between runoff and precipitation (ranges between 0.31 and 0.43). This pattern is founded in both fields.

The results agree with Arnel et al (1999) which studied the effect of climate change on hydrological regimes at the global scale and conclude that the variations in change reflect not only the patterns of change, but also the changes in evaporation and runoff. However, Arnel et al (1999) found a general increase in potential evaporation and reduction in annual runoff, although in this work we concluded that the runoff tends to increase for the soils in the studied region.

As a partial conclusion of this section it is possible to infer that climate changes is likely to have significant effects on the hydrological cycle as the surface flux, cumulative surface flux, runoff, cumulaive runoff, soil water storage and cumulative infiltration. Those variables are critical in a corn production, determining the available water and heat available to the crop. It is also importante to highlight that more than the relation of climate changes with dangerous events for agriculture (due to moisture and temperature stress), it was also founded the relation of climate extremes with those events.

From this section it is concluded that, in general, changes in maximum values of of surface flux and runoff, which represents a risk for agriculture, will increase and are related to the increasing of the occurence of extreme events. As a summary, it is noticeable that climate changes and the consequently changes in the occurrence of extreme events might cause changes in the pattern of surface flux, increasing of runoff and infiltration, although the soil water storage might have small decreasing. This will likely affect the corn production, which is a concern, due to the importance of this crop not only for USA, but for all the world.

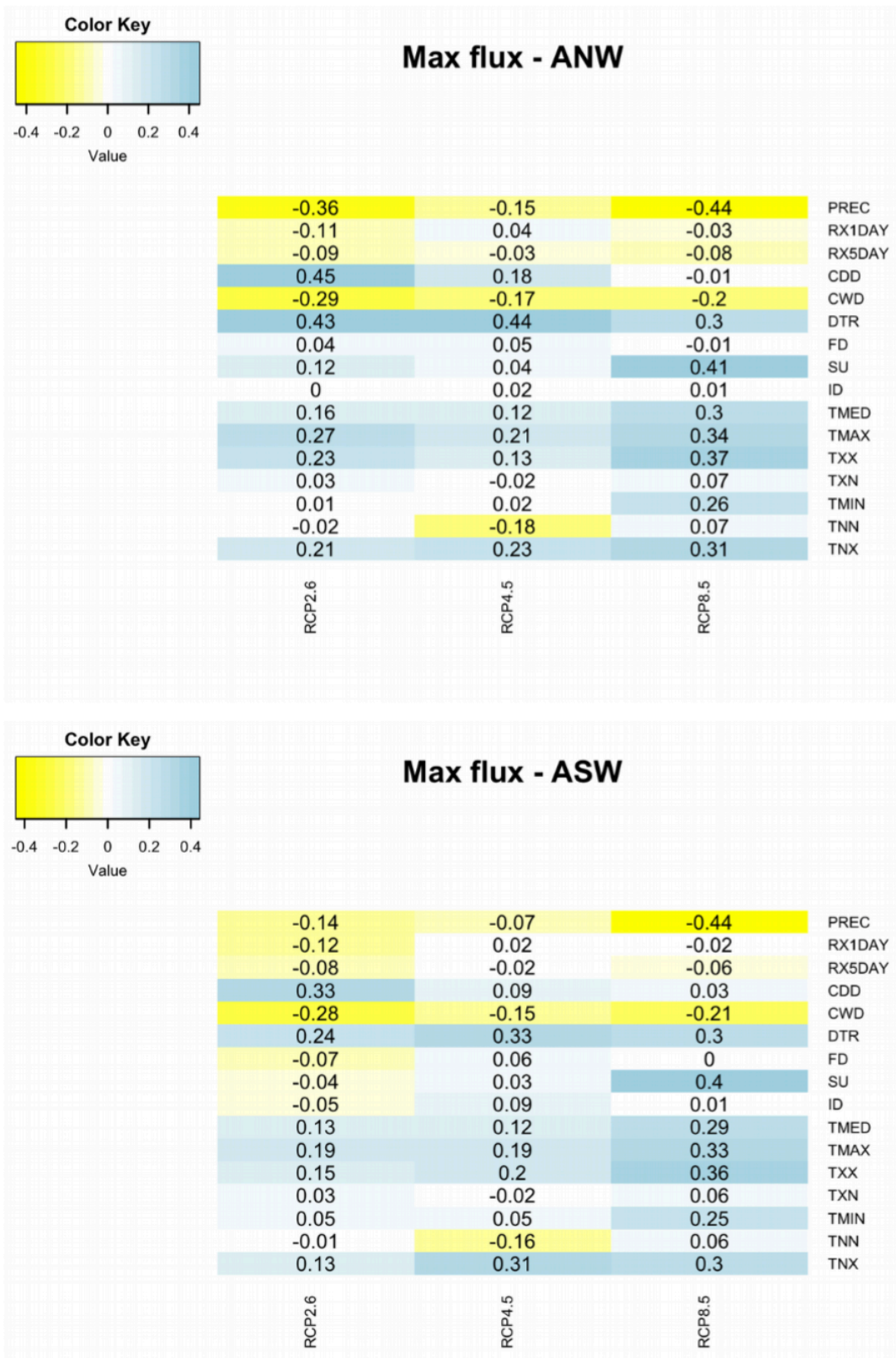


Figure 55. Correlation between climate indices and maximum values of surface flux in ANW (top) and ASW (bottom) fields, considering the climate scenarios of RCP2.6, RCP4.5 and RCP8.5.

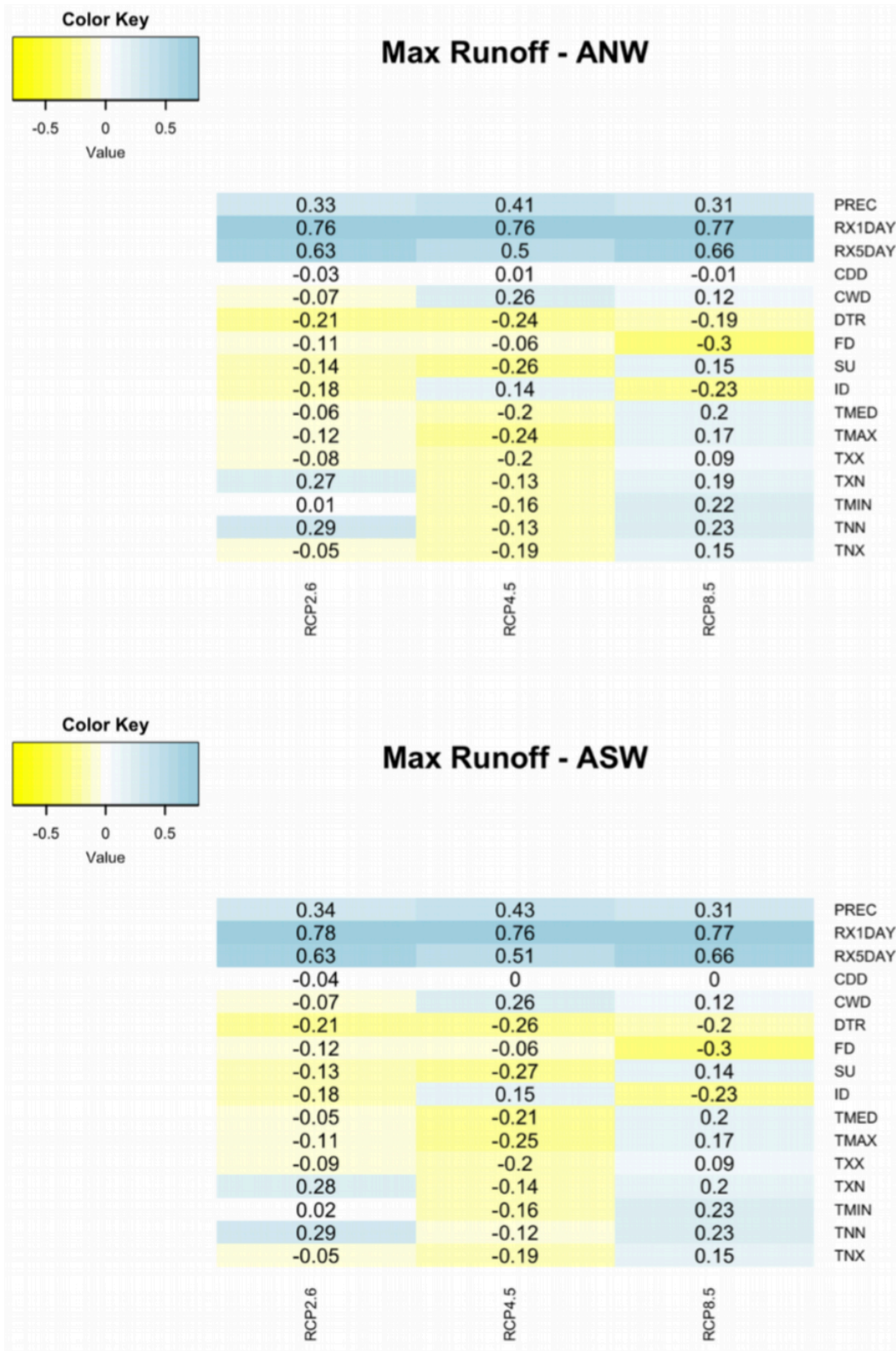


Figure 56. Correlation between climate indices and maximum values of surface runoff in ANW (top) and ASW (bottom) fields, considering the climate scenarios of RCP2.6, RCP4.5 and RCP8.5.



## 5. CONCLUSIONS

The study identified the climate change patterns in the region (from 1901 to 2015) and the occurrence of extreme events of temperature and precipitation. The model IPSL(CM5MR) was found as the most accurate for the analyzed region. However, the model presented tendency to underestimation of precipitation and average and maximum temperature between 1901 to 2005. Regarding to this model has a tendency to overestimate the minimum temperature. Regarding to the indices of extreme events, we noticed that most of them showed good performance.

As a conclusion of this results we can highlight that the variation of precipitation in the future may cause increasing of the RX1DAY, RX5DAY, CDD and CWD. This evidence can be specially noticed observing the period of 2071 to 2100 in RCP8.5. In this projection, the increasing of 0.8% in precipitation (compared to the period of reference) will reflect an increase of 50.1% (RX1DAY), 32.01% (RX5DAY), 29.05% (CDD) and 42.08% in CWD. This situation represents a risk for agriculture, considering that the less distributed rainfall and scenarios of higher values of rainfall, increases for example the potential risk of runoff in the field which can compromise the production. The consequences of this changes in climate conditions it was also explored. Considering the extreme events of temperature, we noticed that the increase in average, maximum and minimum temperature will be reflected as increases of the indices TNn, TNx, TXn, TXx and SU; and the decrease in the index ID and FD. Based on the simulation of RCP8.5 in the period of 2071 to 2100, it is importante to highlight the increase of 125.42% of the minimum temperature and the increasing of 56.66% and 84.48% in the minimum values of minimum and maximum temperature. This increasing temperatures will represent a risk for agriculture considering the evapotranspiration, which will increase the water necessity of the plants and can create a hydric stress. Also, the indices ID and FD tends to decrease (-94.5% and -70.92%), which can be good considering a possibility to switch the dates of planting and harvest as a mitigation measure. The period with higher percentile change in evapotranspiration is 2071-2100, and this changes are more pronounced in RCP8.5 scenario (around 19% of increasing of evapotranspiration).

The research presents the simulations of IPSL model applied in Hydrus model to simulate, surface flux, cumulative surface flux, runoff, cumulative runoff, soil water storage and cumulative infiltration, considering these variables is really important in corn production. The field ANW presented lower values of surface flux and cumulative (module) comparing to ASW, which indicates that the risk associated in ASW drainage system is higher than ANW, which is related to the higher spacing between drains and the difficulty in this case in drainage the necessary amount of water. Considering both fields, the simulations normally indicate more outliers (high values, or in other words, extreme events of surface flux) in the future projections when compared to the period of reference (mostly the simulations of 2011-2040 and 2041-2100). The tendency of the surface flux and cumulative surface flux, is in general, increasing over scenarios of climate changes (in maximum and average values). This tendency can also be due to the changes in average cumulative surface that can reach 22.92% in the end of century (RCP8.5), considering ANW field. This percentile changes in cumulative surface flux tends to be higher in ANW, which indicates that in future it will be necessary some adaptations in the “ideal” drainage system in order to maintain the good performance of the system.

Considering the surface runoff it is observed that there is a large amount of days considered as an outlier. This is especially important, considering this outliers as extreme events of runoff which can cause intense damages on agriculture and affect the local economy. It is important to highlight that the outliers of runoff over the period of 2041-2070 under RCP2.6 is the worst possible scenario in both fields. The values of cumulative surface runoff also seems to be similar. Also it is noticeable that the all simulation indicates increasing of surface runoff and cumulative

surface runoff in terms of maximum values. The percentile of changes of average values of runoff and cumulative runoff shows that the climate projection tends to increase the surface runoff in different scenarios of simulation. This increasing range from 5.61% to 24.4% in 2011-2040, compared to historical simulation. This range is around 16.45 to 39.32%, considering 2041 to 2070 and finally 3.32 to 19.98% for 2071 to 2100.

The soil water storage has largely variability, so we can notice a presence of large amount of outliers. These outliers is even more expressive when we consider the historical simulation. The soil water storage is larger in ASW field, which is explained by the higher depth of the soil profile, permitting a bigger amount of water in soil. The cumulative infiltration is lower in ASW, due to the difficulty of the drainage system of this field to drain the water and promote higher infiltration. The maximum values of infiltration tend to be higher in all simulations when compared to the period of reference (in both fields). From the percentile of changes for soil water storage and cumulative infiltration we observe gradual decreasing of soil water storage in RCP8.5, although the differences are lower than 1%. RCP's 2.6 and 4.5 indicates different behavior, as present an increase of the percentile change in soil water storage in long term. Again, changes in soil water storage is small, comparing to other variables. Also, changes in cumulative infiltration indicates that scenarios RCP2.6 and RCP4.5 simulates positive changes, as the infiltration tends to increase in future. RCP8.5 simulates a small increasing in short and medium term and small decrease in long term simulation.

The correlation between maximum values of surface flux in (ANW and ASW field) with extreme events of precipitation and temperature was analyzed. In scenario RCP2.6 the surface flux tends to have higher correlation with CDD and DTR (0.45 and 0.43, respectively). For the scenarios RCP4.5 and RCP8.5 the correclation is higher for the indices DTR (0.44) and SU (0.41), respectively. This correlations seems to be even lower in ASW field. For ASW fields, the correlations higher than 0.4 were only founded in RCP8.5, which indicates that the surface flux is inversely correlated with precipitation (-0.44) and correlated with SU (0.4). Considering the correlation between runoff and extreme events, the correlation seems to be higher. All simulations indicated that the correlation between runoff and extreme events of precipitation RX1DAY (ranges between 0.76 and 0.78) and RX5DAY (ranges between 0.5 and 0.66) are higher than the correlation between runoff and precipitation (ranges between 0.31 and 0.43). This pattern is founded in both fields.

The studied shows that different indications of the impact of climate change on water resource is obtained using different projections. This approach can improve the understanding of climate changes impacts on sustainable groundwater management based on adaptive management.

## 6. FINAL REMARKS

By defining the occurrence of changes in patterns in the climatology and also in the occurrence of extreme events the authors believe that more researches need to be done about the climate change subject in order to define the local effect of climate change in different sectors. Other researches can be stimulated by this work. The author suggests to apply the same methodology to a regional climate model (RCM) in order to describe the major source of uncertainty for the study region. We believe that it is important to apply this knowledge in specific areas, so it is possible to create mitigation measures, according to the forecast.

Also, it is important to highlight that the results of the simulations are a function of climate variables, soil conditions and parameters of the study region, drainage system, characteristics of crop and others. So the results found in this section are applied for a specific study case. However, the understanding of the mechanisms which bring to these results and also the consequences of those in the crop is really important in order to create mitigation measures. Also, the results may be applied to regions with similar climate patterns and soil.

These results can lead to a discussion about the effect of climate in the agriculture of the region. Thus, it is needed to have more studies regarding to this effect in corn production. A difficulty of the research is regarding the large amount of data and the necessity of daily step time to integration of variables. This approach can improve the understanding of climate changes impacts on sustainable groundwater management based on adaptive management.



## REFERENCES

- Adams, R. M., Hurd, B. H., & Reilly, J. (1999). Agriculture and Global Climate Change a Review of Impacts to US Agricultural Resources.
- Alcamo, J., Dronin, N., Endejan, M., Golubev, G., & Kirilenko, A. (2007). A new assessment of climate change impacts on food production shortfalls and water availability in Russia. *Global Environmental Change*, 17(3), 429-444.
- Allen, R. G., Pereira, L. S., Raes, D., & Smith, M. (1998). Crop evapotranspiration-Guidelines for computing crop water requirements-FAO Irrigation and drainage paper 56. *FAO, Rome*, 300(9), D05109.
- Arnell, N. W. (1999). Climate change and global water resources. *Global environmental change*, 9, S31-S49.
- Ashraf, M. (1999). Interactive effects of nitrate and long-term waterlogging on growth, water relations, and gaseous exchange properties of maize (*Zea mays* L.). *Plant Science*, 144(1), 35-43.
- Badiger, S. M. (2001). Integrated numerical modeling of spatial and time-variant hydrologic response in subsurface drained watersheds (Doctoral dissertation, University of Illinois at Urbana-Champaign).
- Basistha, A., Arya, D. S., & Goel, N. K. (2008). Spatial distribution of rainfall in Indian Himalayas—a case study of Uttarakhand region. *Water Resources Management*, 22(10), 1325-1346.
- Beven, K. J. (2001). *Rainfall–Runoff Modeling: The Primer* Wiley. Chichester, UK.
- Borah, D. K., Bera, M., & Shaw, S. (2003). Water, sediment, nutrient, and pesticide measurements in an agricultural watershed in Illinois during storm events. *Transactions of the ASAE*, 46(3), 657-674.
- Boughton, W., & Chiew, F. (2007). Estimating runoff in ungauged catchments from rainfall, PET and the AWBM model. *Environmental Modelling & Software*, 22(4), 476-487.
- Brunt, D. (2011). *Physical and dynamical meteorology*. Cambridge University Press.
- Carsel, R. F., Imhoff, J. C., Hummel, P. R., Cheplick, J. M., & Donigian Jr, A. S. (1998). PRZM-3, a model for predicting pesticide and nitrogen fate in the crop root and unsaturated soil zones: users manual for release 3.0. *National Exposure Research Laboratory, Office of Research and Development, US Environmental Protection Agency, Athens, GA*, 30605-2720.
- Carvalho, L. C., Oliveira Bernardo, S. D., Costa, P. D., Orgaz, M. D. M., & Yamasaki, Y. (2008). Validação da Temperatura da Superfície do Mar a partir de medições de satélite.
- Carvalho, L. M., Jones, C., & Liebmann, B. (2004). The South Atlantic convergence zone: Intensity, form, persistence, and relationships with intraseasonal to interannual activity and extreme rainfall. *Journal of Climate*, 17(1), 88-108.
- Changnon, S. A., Changnon, D., Fosse, E. R., Hoganson, D. C., Roth Sr, R. J., & Totsch, J. M. (1997). Effects of recent weather extremes on the insurance industry: major implications for the atmospheric sciences. *Bulletin of the American Meteorological Society*, 78(3), 425-435.
- Chiew, F. H. (2006). Estimation of rainfall elasticity of streamflow in Australia. *Hydrological Sciences Journal*, 51(4), 613-625.
- Chiotti, Q. P., & Johnston, T. (1995). Extending the boundaries of climate change research: a discussion on agriculture. *Journal of Rural Studies*, 11(3), 335-350.
- Chou, C., Neelin, J. D., Chen, C. A., & Tu, J. Y. (2009). Evaluating the “rich-get-richer” mechanism in tropical precipitation change under global warming. *Journal of Climate*, 22(8), 1982-2005.

- Cooke, R., & Verma, S. (2012). Performance of drainage water management systems in Illinois, United States. *Journal of Soil and Water Conservation*, 67(6), 453-464.
- Cordeiro, M. R., Krahn, V., Ranjan, R. S., & Sager, S. (2015). Water table contribution and diurnal water redistribution within the corn root zone. *Canadian Biosystems Engineering*, 57.
- Crosbie, R. S., Dawes, W. R., Charles, S. P., Mpelasoka, F. S., Aryal, S., Barron, O., & Summerell, G. K. (2011). Differences in future recharge estimates due to GCMs, downscaling methods and hydrological models. *Geophysical Research Letters*, 38(11).
- Crosbie, R. S., Pickett, T., Mpelasoka, F. S., Hodgson, G., Charles, S. P., & Barron, O. V. (2013). An assessment of the climate change impacts on groundwater recharge at a continental scale using a probabilistic approach with an ensemble of GCMs. *Climatic Change*, 117(1-2), 41-53.
- Cuculeanu, V., Tuinea, P., & Bălteanu, D. (2002). Climate change impacts in Romania: Vulnerability and adaptation options. *GeoJournal*, 57(3), 203-209.
- Daly, C., Gibson, W. P., Taylor, G. H., Johnson, G. L., & Pasteris, P. (2002). A knowledge-based approach to the statistical mapping of climate. *Climate research*, 22(2), 99-113.
- De Silva, C. S., Weatherhead, E. K., Knox, J. W., & Rodriguez-Diaz, J. A. (2007). Predicting the impacts of climate change—A case study of paddy irrigation water requirements in Sri Lanka. *Agricultural water management*, 93(1), 19-29.
- Diaz, S., Grime, J. P., Harris, J., & McPherson, E. (1993). Evidence of a feedback mechanism limiting plant response to elevated carbon dioxide. *Nature*, 364(6438), 616-617.
- Döll, P. (2009). Vulnerability to the impact of climate change on renewable groundwater resources: a global-scale assessment. *Environmental Research Letters*, 4(3), 035006.
- Dourado Neto, D. (1999). *Modelos fitotécnicos referentes á cultura do milho. 1999. 229f* (Doctoral dissertation, Tese (livre docência)-Escola Superior de Agricultura Luiz de Queiroz, Universidade de São Paulo, Piracicaba, SP.[Links]).
- Duarte, A. P., & Cruz, J. C. (2001). Manejo do solo e semeadura do milho safrinha. *SEMINÁRIO NACIONAL DE MILHO SAFRINHA*, 6, 45-71.
- Dufresne, J. L., Foujols, M. A., Denvil, S., Caubel, A., Marti, O., Aumont, O., ... & Bony, S. (2013). Climate change projections using the IPSL-CM5 Earth System Model: from CMIP3 to CMIP5. *Climate Dynamics*, 40(9-10), 2123-2165.
- Easterling, W. E., Aggarwal, P. K., Batima, P., Brander, K. M., Erda, L., Howden, S. M., ... & Tubiello, F. N. (2007). Food, fibre and forest products. *Climate change*, 273-313.
- Ernst, L. F. (1963). Groundwater Flow in the Saturated Zone and Its Calculation When Horizontal Parallel Open Conduits Are Present. *Soil Science*, 95(4), 288.
- Fancelli, A. L., Dourado Neto, D., Fancelli, A. L., & Dourado Neto, D. (2005). Produção de milho em terras baixas. *Milho: tecnologia e produção*, 21-33.
- Feddes, R. A., Bresler, E., & Neuman, S. P. (1974). Field test of a modified numerical model for water uptake by root systems. *Water Resources Research*, 10(6), 1199-1206.
- Fernandes, F. C. S., Libardi, P. L., & Carvalho, L. A. D. (2006). Internal drainage and nitrate leaching in a corn-black oat-corn succession with two split nitrogen applications. *Scientia Agricola*, 63(5), 483-492.
- Fowler, H. J., Blenkinsop, S., & Tebaldi, C. (2007). Linking climate change modelling to impacts studies: recent advances in downscaling techniques for hydrological modelling. *International journal of climatology*, 27(12), 1547-1578.

- Fuhrer, J., Beniston, M., Fischlin, A., Frei, C., Goyette, S., Jasper, K., & Pfister, C. (2006). Climate risks and their impact on agriculture and forests in Switzerland. In *Climate Variability, Predictability and Climate Risks* (pp. 79-102). Springer Netherlands.
- França G. E., Bahia Filho, A. V. C. (1985). Adubação nitrogenada no brasil. *SBCS*, 107–124.
- Frich, P., Alexander, L. V., Della-Marta, P., Gleason, B., Haylock, M., Tank, A. K., & Peterson, T. (2002). Observed coherent changes in climatic extremes during the second half of the twentieth century. *Climate research*, 19(3), 193-212.
- Friedlingstein, P., Meinshausen, M., Arora, V. K., Jones, C. D., Anav, A., Liddicoat, S. K., & Knutti, R. (2014). Uncertainties in CMIP5 climate projections due to carbon cycle feedbacks. *Journal of Climate*, 27(2), 511-526.
- Fujihara, Y., Tanaka, K., Watanabe, T., Nagano, T., & Kojiri, T. (2008). Assessing the impacts of climate change on the water resources of the Seyhan River Basin in Turkey: Use of dynamically downscaled data for hydrologic simulations. *Journal of Hydrology*, 353(1), 33-48.
- Gandolfi, C., Facchi, A., & Maggi, D. (2006). Comparison of 1D models of water flow in unsaturated soils. *Environmental Modelling & Software*, 21(12), 1759-1764.
- Garrigues, E., Doussan, C., & Pierret, A. (2006). Water uptake by plant roots: I–Formation and propagation of a water extraction front in mature root systems as evidenced by 2D light transmission imaging. *Plant and soil*, 283(1), 83-98.
- Green, T. R., Taniguchi, M., Kooi, H., Gurdak, J. J., Allen, D. M., Hiscock, K. M., ... & Aureli, A. (2011). Beneath the surface of global change: Impacts of climate change on groundwater. *Journal of Hydrology*, 405(3), 532-560.
- Groisman, P. Y., Knight, R. W., & Karl, T. R. (2001). Heavy precipitation and high streamflow in the contiguous United States: Trends in the twentieth century. *Bulletin of the American Meteorological Society*, 82(2), 219-246.
- Groisman, P. Y., Knight, R. W., Easterling, D. R., Karl, T. R., Hegerl, G. C., & Razuvaev, V. N. (2005). Trends in intense precipitation in the climate record. *Journal of climate*, 18(9), 1326-1350.
- Guo, S., Wang, J., Xiong, L., Ying, A., & Li, D. (2002). A macro-scale and semi-distributed monthly water balance model to predict climate change impacts in China. *Journal of Hydrology*, 268(1), 1-15.
- Hallema, D. W., Rousseau, A. N., Gumiere, S. J., Périard, Y., Hiemstra, P. H., Bouttier, L., ... & Olivier, A. (2014). Framework for studying the hydrological impact of climate change in an alley cropping system. *Journal of hydrology*, 517, 547-556.
- Handler, P. (1985). Possible association between the climatic effects of stratospheric aerosols and corn yields in the United States. *Agricultural and forest meteorology*, 35(1-4), 205-228.
- Hansen, J., Ruedy, R., Sato, M., Imhoff, M., Lawrence, W., Easterling, D., ... & Karl, T. (2001). A closer look at United States and global surface temperature change. *Journal of Geophysical Research: Atmospheres*, 106(D20), 23947-23963.
- Hayashi, M., & Rosenberry, D. O. (2002). Effects of ground water exchange on the hydrology and ecology of surface water. *Groundwater*, 40(3), 309-316.
- Haylock, M. R., Peterson, T. C., Alves, L. M., Ambrizzi, T., Anunciação, Y. M. T., Baez, J., ... & Corradi, V. (2006). Trends in total and extreme South American rainfall in 1960–2000 and links with sea surface temperature. *Journal of climate*, 19(8), 1490-1512.
- Hawkins, E., & Sutton, R. (2009). The potential to narrow uncertainty in regional climate predictions. *Bulletin of the American Meteorological Society*, 90(8), 1095-1107.

- Houghton, J. T., Y. Ding, D. J. Griggs, M. Noguer, P. J. van der Linden, X. Dai, K. Maskell, and C. A. Johnson (Eds.), *Climate Change 2001: The Scientific Basis. Contributions of Working Group 1 to the Third Assessment Report of the Intergovernmental Panel on Climate Change*. Cambridge Univ. Press, Cambridge, United Kingdom and New York, NY, USA, 881 pp., 2001.
- Holman, I. P., Allen, D. M., Cuthbert, M. O., & Goderniaux, P. (2012). Towards best practice for assessing the impacts of climate change on groundwater. *Hydrogeology Journal*, 20(1), 1-4.
- Holman, I. P., Tascone, D., & Hess, T. M. (2009). A comparison of stochastic and deterministic downscaling methods for modelling potential groundwater recharge under climate change in East Anglia, UK: implications for groundwater resource management. *Hydrogeology Journal*, 17(7), 1629-1641.
- Hooghoudt, S. B. (1940). General consideration of the problem of field drainage by parallel drains, ditches, watercourses, and channels. *Contribution to the Knowledge of Some Physical Parameters of the Soil*, (7).
- Howell, T. A. (2001). Enhancing water use efficiency in irrigated agriculture. *Agronomy journal*, 93(2), 281-289.
- Ines, A. V., Gupta, A. D., & Loof, R. (2002). Application of GIS and crop growth models in estimating water productivity. *Agricultural Water Management*, 54(3), 205-225.
- Ivanko, S. (1972). Recent progress in the use of <sup>15</sup>N in research on nitrogen balance studies in soil-plant relationship. In *Symposium on the Use of Isotopes and Radiation in Research on Soil plant Relat incl For, Vienna, 1971. Proc.*
- Jiang, T., Chen, Y. D., Xu, C. Y., Chen, X., Chen, X., & Singh, V. P. (2007). Comparison of hydrological impacts of climate change simulated by six hydrological models in the Dongjiang Basin, South China. *Journal of hydrology*, 336(3), 316-333.
- Jones, R. N., Chiew, F. H., Boughton, W. C., & Zhang, L. (2006). Estimating the sensitivity of mean annual runoff to climate change using selected hydrological models. *Advances in Water Resources*, 29(10), 1419-1429.
- Jones, P. G., & Thornton, P. K. (2003). The potential impacts of climate change on maize production in Africa and Latin America in 2055. *Global environmental change*, 13(1), 51-59.
- Kalnay, E., & Cai, M. (2003). Impact of urbanization and land-use change on climate. *Nature*, 423(6939), 528-531.
- Kane, S., Reilly, J., & Tobey, J. (1992). An empirical study of the economic effects of climate change on world agriculture. *Climatic change*, 21(1), 17-35.
- Kang, Y., Khan, S., & Ma, X. (2009). Climate change impacts on crop yield, crop water productivity and food security—A review. *Progress in Natural Science*, 19(12), 1665-1674.
- Kay, A. L., Davies, H. N., Bell, V. A., & Jones, R. G. (2009). Comparison of uncertainty sources for climate change impacts: flood frequency in England. *Climatic Change*, 92(1), 41-63.
- Kazmierczak, B., Kotowski, A., & Wdowikowski, M. (2014). Trend analysis of annual and seasonal precipitation amounts in the Upper Odra catchment. *Ochrona Srodowiska*, 36(3), 49-54.
- Katz, R. W., & Brown, B. G. (1992). Extreme events in a changing climate: variability is more important than averages. *Climatic change*, 21(3), 289-302.
- Kharin, V. V., Zwiers, F. W., Zhang, X., & Wehner, M. (2013). Changes in temperature and precipitation extremes in the CMIP5 ensemble. *Climatic Change*, 119(2), 345-357.
- Knutti, R., Masson, D., & Gettelman, A. (2013). Climate model genealogy: Generation CMIP5 and how we got there. *Geophysical Research Letters*, 40(6), 1194-1199.
- Knutti, R., & Sedláček, J. (2013). Robustness and uncertainties in the new CMIP5 climate model projections. *Nature Climate Change*, 3(4), 369-373.

- Kozdrój, J., & van Elsas, J. D. (2000). Response of the bacterial community to root exudates in soil polluted with heavy metals assessed by molecular and cultural approaches. *Soil Biology and Biochemistry*, 32(10), 1405-1417.
- Kroes, J. G., & Van Dam, J. C. (2003). Reference Manual SWAP; version 3.0. 3 (No. 773). Alterra.
- Kunkel, K. E., Easterling, D. R., Redmond, K., & Hubbard, K. (2003). Temporal variations of extreme precipitation events in the United States: 1895–2000. *Geophysical research letters*, 30(17).
- Kurylyk, B. L., MacQuarrie, K. T., & McKenzie, J. M. (2014). Climate change impacts on groundwater and soil temperatures in cold and temperate regions: Implications, mathematical theory, and emerging simulation tools. *Earth-Science Reviews*, 138, 313-334.
- Kurylyk, B. L., & MacQuarrie, K. T. (2013). The uncertainty associated with estimating future groundwater recharge: A summary of recent research and an example from a small unconfined aquifer in a northern humid-continental climate. *Journal of hydrology*, 492, 244-253.
- Leterme, B., & Mallants, D. I. R. K. (2011). Climate and land-use change impacts on groundwater recharge. Proc. ModelCARE2011: Models-Repositories of Knowledge.
- Marengo, J. A., & Valverde, M. C. (2007). Caracterização do clima no Século XX e Cenário de Mudanças de clima para o Brasil no Século XXI usando os modelos do IPCC-AR4. *Revista Multiciência*, 8, 5-28.
- Mati, B. M. (2000). The influence of climate change on maize production in the semi-humid–semi-arid areas of Kenya. *Journal of Arid Environments*, 46(4), 333-344.
- McCarthy, J.J., Canziani, O.K., Leary, N.A., Dokken, D.J., White, K.S. (2001). Impacts, Adaptation and vulnerability. Third Assessment Report of the Intergovernmental panel on climate change, working Group 2. Cambridge University Press, Cambridge, UK.
- McKeown, A., Warland, J., & McDonald, M. R. (2005). Long-term marketable yields of horticultural crops in southern Ontario in relation to seasonal climate. *Canadian journal of plant science*, 85(2), 431-438.
- Meehl, G. A., Goddard, L., Murphy, J., Stouffer, R. J., Boer, G., Danabasoglu, G., ... & Hegerl, G. (2009). Decadal prediction: can it be skillful?. *Bulletin of the American Meteorological Society*, 90(10), 1467-1485.
- Melo, T. M., & Louzada, J. A. (2013). Aplicação e avaliação dos modelos Swap e Hydrus 1D em diferentes cenários agrícolas. DOI: 10.7127/rbai. v6n400090. *REVISTA BRASILEIRA DE AGRICULTURA IRRIGADA-RBAI*, 6(4).
- Milla, K., & Kish, S. (2006). A low-cost microprocessor and infrared sensor system for automating water infiltration measurements. *Computers and electronics in agriculture*, 53(2), 122-129.
- Miranda, J. H., Duarte, S. N., Libardi, P. L., & Folegatti, M. V. (2005). Potassium displacement simulation in vertical columns of unsaturated soil. *Engenharia Agrícola*, 25(3), 677-685.
- Mirza, M. (2007). Climate change, adaptation and adaptive governance in water sector in South Asia. *Phys Sci Basis*, 1-19.
- Monteith, J. L. (1981). Evaporation and surface temperature. *Quarterly Journal of the Royal Meteorological Society*, 107(451), 1-27.
- Moss, R. H., Edmonds, J. A., Hibbard, K. A., Manning, M. R., Rose, S. K., Van Vuuren, D. P., ... & Meehl, G. A. (2010). The next generation of scenarios for climate change research and assessment. *Nature*, 463(7282), 747-756.
- Murray, F. W. (1966). *On the computation of saturation vapor pressure* (No. P-3423). RAND CORP SANTA MONICA CALIF.

- Neitsch, S. L., Arnold, J. G., Kiniry, J. R., & Williams, J. R. (2011). *Soil and water assessment tool theoretical documentation version 2009*. Texas Water Resources Institute.
- Nelson, G. C., Rosegrant, M. W., Koo, J., Robertson, R., Sulser, T., Zhu, T., ... & Magalhaes, M. (2009). *Climate change: Impact on agriculture and costs of adaptation* (Vol. 21). Intl Food Policy Res Inst.
- New, M., Todd, M., Hulme, M., & Jones, P. (2001). Precipitation measurements and trends in the twentieth century. *International Journal of Climatology*, 21(15), 1889-1922.
- Nobre, C. A., Young, A. F., Saldiva, P., Marengo, J. A., Nobre, A. D., Alves Jr, S., ... & Lombardo, M. (2010). Vulnerabilidades das megacidades brasileiras às mudanças climáticas: Região Metropolitana de São Paulo. *Embaixada Reino Unido, Rede Clima e Programa FAPESP em Mudanças Climáticas*.
- Nyenje, P. M., & Batelaan, O. (2009). Estimating the effects of climate change on groundwater recharge and baseflow in the upper Ssezibwa catchment, Uganda. *Hydrological sciences journal*, 54(4), 713-726.
- Palmer, T. N., & Räisänen, J. (2002). Quantifying the risk of extreme seasonal precipitation events in a changing climate. *Nature*, 415(6871), 512-514.
- Parry, M. L. (Ed.). (2007). *Climate change 2007-impacts, adaptation and vulnerability: Working group II contribution to the fourth assessment report of the IPCC* (Vol. 4). Cambridge University Press.
- Pielke Jr, R. A., & Downton, M. W. (2000). Precipitation and damaging floods: trends in the United States, 1932–97. *Journal of Climate*, 13(20), 3625-3637.
- Pinazza, L. A. (Ed.). (2007). *Cadeia produtiva do milho* (Vol. 1). Bib. Orton IICA/CATIE.
- Priestley, C. H. B., & Taylor, R. J. (1972). On the assessment of surface heat flux and evaporation using large-scale parameters. *Monthly weather review*, 100(2), 81-92.
- Reilly, J., Tubiello, F. N., McCarl, B., & Melillo, J. (2001). Impacts of climate change and variability on agriculture In: US National Assessment Foundation Document. *National Assessment Synthesis Team. Washington, DC. US Global Change Research Program*.
- Rienznner, M., de Maria, S. C., Facchi, A., Wassar, F., & Gandolfi, C. (2013). Estimating the contribution of rainfall, irrigation and upward soil water flux to crop water requirements of a maize agroecosystem in the Lombardy plain. *Journal of Agricultural Engineering*, 44(2s).
- Roberts, E. H., & Summerfield, R. J. (1987). Measurement and prediction of flowering in annual crops. *Manipulation of flowering*/JG Atherton, [editor].
- Roderick, M. L., & Farquhar, G. D. (2002). The cause of decreased pan evaporation over the past 50 years. *science*, 298(5597), 1410-1411.
- Rosenzweig, C. (1993). Agriculture in a greenhouse world. *Natl. Geographic Res. & Exploration*, 9, 208-221.
- Rosenzweig, C., & Hillel, D. (1998). *Climate change and the global harvest: potential impacts of the greenhouse effect on agriculture*. Oxford University Press.
- Rosenzweig, C., Tubiello, F. N., Goldberg, R., Mills, E., & Bloomfield, J. (2002). Increased crop damage in the US from excess precipitation under climate change. *Global Environmental Change*, 12(3), 197-202.
- Rowell, D. P. (2006). A demonstration of the uncertainty in projections of UK climate change resulting from regional model formulation. *Climatic Change*, 79(3), 243-257.
- Saarikko, R. A., & Carter, T. R. (1996). Estimating the development and regional thermal suitability of spring wheat in Finland under climatic warming. *Climate Research*, 243-252.
- Saghafian, B., & Bondarabadi, S. R. (2008). Validity of regional rainfall spatial distribution methods in mountainous areas. *Journal of Hydrologic Engineering*, 13(7), 531-540.

- Salati, E., Santos, A. D., & Nobre, C. (2004). As mudanças climáticas globais e seus efeitos nos ecossistemas brasileiros. Available in: <http://www.comciencia.br/reportagens/clima/clima14.htm>, 2.
- Sankarasubramanian, A., Vogel, R. M., & Limbrunner, J. F. (2001). Climate elasticity of streamflow in the United States. *Water Resources Research*, 37(6), 1771-1781.
- Serrat-Capdevila, A., Valdés, J. B., Pérez, J. G., Baird, K., Mata, L. J., & Maddock, T. (2007). Modeling climate change impacts—and uncertainty—on the hydrology of a riparian system: The San Pedro Basin (Arizona/Sonora). *Journal of Hydrology*, 347(1), 48-66.
- Schaake, J. C. (1990). From climate to flow. *Climate change and US water resources.*, 177-206.
- Shah, T., Burke, J., Villholth, K. G., Angelica, M., Custodio, E., Daibes, F., ... & Kendy, E. (2007). Groundwater: a global assessment of scale and significance.
- Sillmann, J., Kharin, V. V., Zhang, X., Zwiers, F. W., & Bronaugh, D. (2013). Climate extremes indices in the CMIP5 multimodel ensemble: Part 1. Model evaluation in the present climate. *Journal of Geophysical Research: Atmospheres*, 118(4), 1716-1733.
- Sillmann, J., Kharin, V. V., Zwiers, F. W., Zhang, X., & Bronaugh, D. (2013). Climate extremes indices in the CMIP5 multimodel ensemble: Part 2. Future climate projections. *Journal of Geophysical Research: Atmospheres*, 118(6), 2473-2493.
- Šimůnek, J., Suarez, D. L., & Šejna, M. (1996). The UNSATCHEM software package for simulating one-dimensional variably saturated water flow, heat transport, carbon dioxide production and transport, and multicomponent solute transport with major ion equilibrium and kinetic chemistry. *Res. Rep.*, 141, 186.
- Simunek, J., Van Genuchten, M. T., & Šejna, M. (2005). The HYDRUS-1D software package for simulating the one-dimensional movement of water, heat, and multiple solutes in variably-saturated media. *University of California-Riverside Research Reports*, 3, 1-240.
- Scoccimarro, E., Gualdi, S., Bellucci, A., Zampieri, M., & Navarra, A. (2013). Heavy precipitation events in a warmer climate: results from CMIP5 models. *Journal of climate*, 26(20), 7902-7911.
- Solomon, S. (Ed.). (2007). *Climate change 2007-the physical science basis: Working group I contribution to the fourth assessment report of the IPCC* (Vol. 4). Cambridge University Press.
- Southworth, J., Randolph, J. C., Habeck, M., Doering, O. C., Pfeifer, R. A., Rao, D. G., & Johnston, J. J. (2000). Consequences of future climate change and changing climate variability on maize yields in the midwestern United States. *Agriculture, Ecosystems & Environment*, 82(1), 139-158.
- Stocker, T. F., Qin, D., Plattner, G. K., Tignor, M., Allen, S. K., Boschung, J., ... & Midgley, P. M. (2014). Climate change 2013: The physical science basis.
- Stone, R. J. (1993). Improved statistical procedure for the evaluation of solar radiation estimation models. *Solar energy*, 51(4), 289-291.
- Tao, F., Yokozawa, M., Hayashi, Y., & Lin, E. (2003a). Changes in agricultural water demands and soil moisture in China over the last half-century and their effects on agricultural production. *Agricultural and Forest Meteorology*, 118(3), 251-261.
- Tao, F., Yokozawa, M., Hayashi, Y., & Lin, E. (2003b). Future climate change, the agricultural water cycle, and agricultural production in China. *Agriculture, ecosystems & environment*, 95(1), 203-215.
- Tao, F., Hayashi, Y., Zhang, Z., Sakamoto, T., & Yokozawa, M. (2008). Global warming, rice production, and water use in China: developing a probabilistic assessment. *Agricultural and forest meteorology*, 148(1), 94-110.

- Tao, F., & Zhang, Z. (2010). Adaptation of maize production to climate change in North China Plain: quantify the relative contributions of adaptation options. *European Journal of Agronomy*, 33(2), 103-116.
- Taylor, K. E., Stouffer, R. J., & Meehl, G. A. (2012). An overview of CMIP5 and the experiment design. *Bulletin of the American Meteorological Society*, 93(4), 485-498.
- Tegen, I. (1990). *Towards a global aerosol climatology: preliminary trends in tropospheric aerosol amounts and corresponding impact on radiative forcing between 1950 and 1990* (Doctoral dissertation, Max-Planck-Institute for Biogeochemistry, Jena, Germany).
- Teng, J., Vaze, J., Chiew, F. H., Wang, B., & Perraud, J. M. (2012). Estimating the relative uncertainties sourced from GCMs and hydrological models in modeling climate change impact on runoff. *Journal of Hydrometeorology*, 13(1), 122-139.
- Tetens, O. (1930). Über einige meteorologische Begriffe. *Z. Geophys.*, 6, 297-309.
- Terando, A., Keller, K., & Easterling, W. E. (2012). Probabilistic projections of agro-climate indices in North America. *Journal of Geophysical Research: Atmospheres*, 117(D8).
- Thomas, C. D., Cameron, A., Green, R. E., Bakkenes, M., Beaumont, L. J., Collingham, Y. C., ... & Hughes, L. (2004). Extinction risk from climate change. *Nature*, 427(6970), 145-148.
- Tuong, T. P., & Bhuiyan, S. I. (1999). Increasing water-use efficiency in rice production: farm-level perspectives. *Agricultural Water Management*, 40(1), 117-122.
- Wei, H., Li, J. L., & Liang, T. G. (2005). Study on the estimation of precipitation resources for rainwater harvesting agriculture in semi-arid land of China. *Agricultural Water Management*, 71(1), 33-45.
- Wesseling, J. G. (1991). *Meerjarige simulatie van grondwaterstroming voor verschillende bodemprofielen, grondwatertrappen en gewassen met het model SWATRE* (No. 152). DLO-Staring Centrum.
- Wheeler, T. R., Craufurd, P. Q., Ellis, R. H., Porter, J. R., & Prasad, P. V. (2000). Temperature variability and the yield of annual crops. *Agriculture, Ecosystems & Environment*, 82(1), 159-167.
- Wigley, T. M. L., & Jones, P. D. (1985). Influences of precipitation changes and direct CO<sub>2</sub> effects on streamflow. *Nature*, 314(6007), 149-152.
- Wilby, R. L., & Harris, I. (2006). A framework for assessing uncertainties in climate change impacts: Low-flow scenarios for the River Thames, UK. *Water Resources Research*, 42(2).
- Wuebbles, D., Meehl, G., Hayhoe, K., Karl, T. R., Kunkel, K., Santer, B., ... & Goodman, A. (2014). CMIP5 climate model analyses: climate extremes in the United States. *Bulletin of the American Meteorological Society*, 95(4), 571-583.
- Zhou, B., Wen, Q. H., Xu, Y., Song, L., & Zhang, X. (2014). Projected changes in temperature and precipitation extremes in China by the CMIP5 multimodel ensembles. *Journal of Climate*, 27(17), 6591-6611.

## APENDIX

**Appendix A 1.** Percentile of changes in precipitation, maximum, average and minimum temperature. The percentile was calculated for the climate projections RCP2.6, RCP4.5 and RCP8.5, considering the periods of 2011-4040; 2041-2070 and 2071-2100, compared to the reference period (1976-2005).

	Prec	Tmax	Tmed	Tmin
RCP2.6: 2011-2040	15.82	31.15	42.86	65.98
2041-2070	22.61	33.43	47.07	73.61
2071-2100	7.66	33.64	45.75	69.59
RCP4.5: 2011-2040	19.57	32.24	44.80	69.82
2041-2070	11.50	38.76	53.19	81.61
2071-2100	11.27	39.88	55.06	84.90
RCP8.5: 2011-2040	4.59	32.98	44.66	67.61
2041-2070	3.55	43.92	60.46	92.75
2071-2100	-0.80	58.40	81.13	125.42

**Appendix A 2.** Percentile of changes RX1DAY, RX5DAY, CDD and CWD. The percentile was calculated for the climate projections RCP2.6, RCP4.5 and RCP8.5, considering the periods of 2011-4040; 2041-2070 and 2071-2100, compared to the reference period (1976-2005).

	RX1DAY	RX5DAY	CDD	CWD
RCP2.6: 2011-2040	17.45	14.80	3.87	50.42
2041-2070	28.69	20.81	4.58	57.92
2071-2100	16.11	9.12	13.56	39.17
RCP4.5: 2011-2040	22.91	24.45	7.75	38.75
2041-2070	21.95	24.48	9.68	62.08
2071-2100	11.94	12.65	7.75	60.83
RCP8.5: 2011-2040	26.12	15.10	7.92	30.83
2041-2070	31.59	29.27	25.88	52.50
2071-2100	50.11	32.01	29.05	42.08

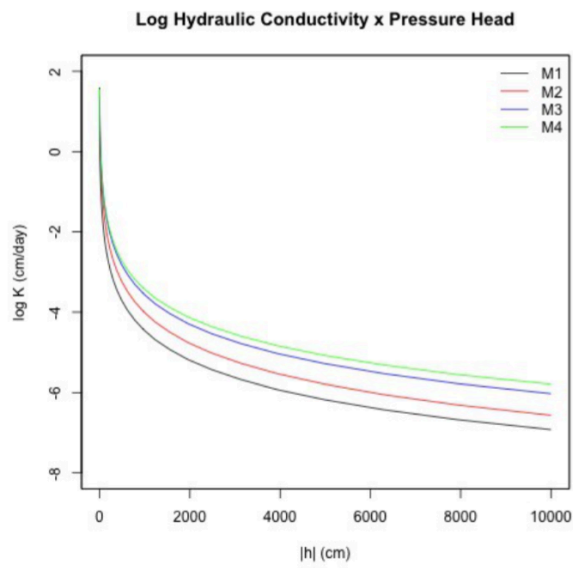
**Appendix A 3.** Percentile of changes in TXx, TXn, TNx and TNn. The percentile was calculated for the climate projections RCP2.6, RCP4.5 and RCP8.5, considering the periods of 2011-4040; 2041-2070 and 2071-2100, compared to the reference period (1976-2005).

	TXx	TXn	TNx	TNn
RCP2.6: 2011-2040	6.71	50.97	8.89	36.07
2041-2070	4.93	50.67	7.56	36.98
2071-2100	7.69	47.69	9.18	34.95
RCP4.5: 2011-2040	4.83	54.29	5.35	37.10
2041-2070	11.45	56.60	14.43	39.18
2071-2100	11.77	57.91	16.09	38.02
RCP8.5: 2011-2040	7.65	46.88	9.65	30.46
2041-2070	15.07	65.42	20.71	44.50
2071-2100	24.92	84.48	35.82	56.67

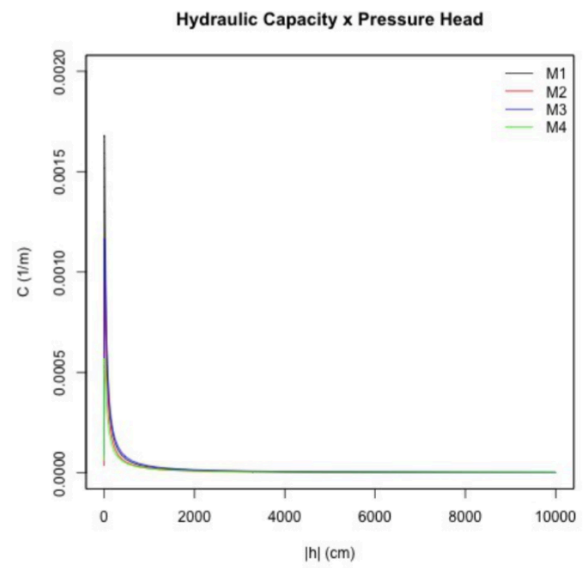
**Appendix A 4.** Percentile of changes in SU, DTR, ID and FD. The percentile was calculated for the climate projections RCP2.6, RCP4.5 and RCP8.5, considering the periods of 2011-2040; 2041-2070 and 2071-2100, compared to the reference period (1976-2005).

	SU	DTR	ID	FD
RCP2.6: 2011-2040	35.67	2.59	-73.43	-48.82
2041-2070	36.93	0.48	-77.20	-52.22
2071-2100	38.90	4.18	-78.66	-47.73
RCP4.5: 2011-2040	36.85	1.42	-77.54	-48.56
2041-2070	44.12	3.61	-79.85	-52.80
2071-2100	47.29	2.95	-79.39	-53.61
RCP8.5: 2011-2040	35.95	-4.90	-73.43	-45.50
2041-2070	49.61	3.86	-80.92	-56.30
2071-2100	64.77	3.43	-94.50	-70.95

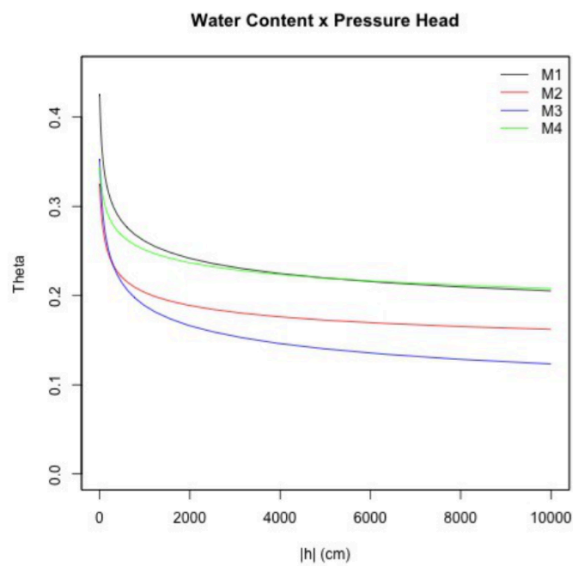
a)



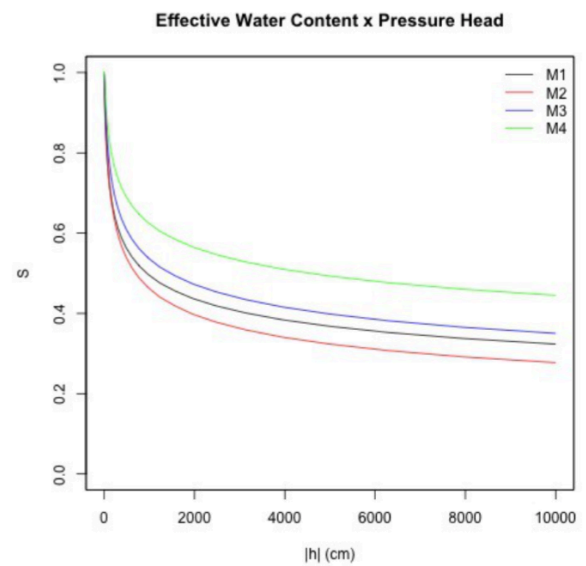
b)



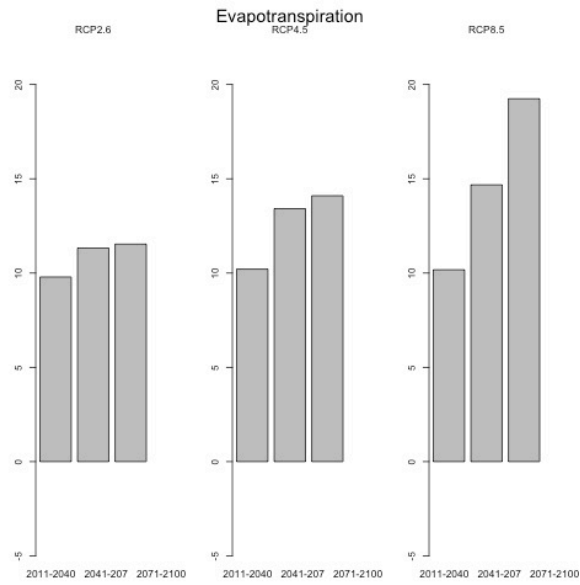
c)



d)



**Appendix B 1.** Hydraulic properties of a soil in Illinois (USA), between April to September (2015), considering the four layers of soil (M1, M2, M3, M4). Shows the relation between pressure head and a) hydraulic conductivity (log), b) hydraulic capacity, c) water content and d) effective water content.



**Appendix C 1.** Changes on evapotranspiration, considering the percentile of difference between climate projections (divided into periods: 2011-2040, 2041-2070, 2071-2100) and the reference period of 1976 to 2005. These changes were calculated for the scenarios RCP2.6, RCP4.5 and RCP8.5.

**Appendix D 1.** Percentile of changes in surface flux and cumulative surface flux, considering ANW and ASW field. The percentile was calculated for the climate projections RCP2.6, RCP4.5 and RCP8.5, considering the periods of 2011-4040; 2041-2070 and 2071-2100, compared to the reference period (1976-2005).

	Changes in Surface Flux (%)		Changes in Cumulative Surface Flux (%)	
	ANW	ASW	ANW	ASW
RCP2.6: 2011-2040	-5.34	-7.99	5.18	5.28
2041-2070	8.35	2.98	-15.12	-17.42
2071-2100	8.42	9.60	-9.48	-7.14
RCP4.5: 2011-2040	-14.84	-16.54	-12.14	-6.73
2041-2070	-5.94	-4.43	0.43	0.66
2071-2100	11.64	6.58	-5.56	-4.56
RCP8.5: 2011-2040	0.25	2.16	2.42	1.31
2041-2070	12.51	12.14	-12.13	-10.28
2071-2100	-2.02	5.20	-22.92	-15.80

**Appendix D 2.** Percentile of changes in surface runoff and cumulative surface runoff, considering ANW and ASW field. The percentile was calculated for the climate projections RCP2.6, RCP4.5 and RCP8.5, considering the periods of 2011-4040; 2041-2070 and 2071-2100, compared to the reference period (1976-2005).

	Changes in Surface Runoff (%)		Changes in Cumulative Surface Runoff (%)	
	ANW	ASW	ANW	ASW
RCP2.6: 2011-2040	17.25	13.22	28.27	27.98
2041-2070	39.32	32.23	34.90	34.12
2071-2100	16.73	19.98	38.43	38.30
RCP4.5: 2011-2040	24.40	18.47	41.41	40.07
2041-2070	21.03	16.45	25.51	24.55
2071-2100	10.97	7.35	22.60	22.97
RCP8.5: 2011-2040	12.09	5.61	9.90	9.54
2041-2070	20.56	15.91	16.35	15.44
2071-2100	8.26	3.32	26.57	25.75

**Appendix D 3.** Percentile of changes in soil water storage and cumulative infiltration, considering ANW and ASW field. The percentile was calculated for the climate projections RCP2.6, RCP4.5 and RCP8.5, considering the periods of 2011-4040; 2041-2070 and 2071-2100, compared to the reference period (1976-2005).

	Changes in Soil Water Storage (%)		Changes in Cumulative Infiltration (%)	
	ANW	ASW	ANW	ASW
RCP2.6: 2011-2040	0.08	0.07	15.83	13.02
2041-2070	0.17	0.13	18.77	18.39
2071-2100	0.08	0.05	14.79	11.88
RCP4.5: 2011-2040	0.15	0.15	18.72	18.22
2041-2070	-0.12	-0.05	10.09	8.84
2071-2100	0.31	0.23	10.92	11.99
RCP8.5: 2011-2040	-0.19	-0.14	1.89	3.30
2041-2070	-0.24	-0.16	3.59	3.22
2071-2100	-0.79	-0.62	-3.24	-2.91

**Appendix D 4.** Percentile of changes in soil water storage and cumulative infiltration, considering ANW and ASW field. The percentile was calculated for the climate projections RCP2.6, RCP4.5 and RCP8.5, considering the periods of 2011-4040; 2041-2070 and 2071-2100, compared to the reference period (1976-2005).

INDICE	RCP26			RCP45			RCP85		
	2011-2040	2041-2070	2071-2100	2011-2040	2041-2070	2071-2100	2011-2040	2041-2070	2071-2100
PREC	**	***	.	***	*	**			
TMED	***	***	***	***	***	***	***	***	***
TMAX	***	***	***	***	***	***	***	***	***
TMIN	***	***	***	***	***	***	***	***	***
RX1DAY	*	*	.	*	*	.	**	**	**
RX5DAY	*	.	.	*	**	*	*	**	*
CDD									*
CWD	***	***	***	***	***	***	**	***	**
TXX	***	***	***	**	***	***	***	***	***
TXN	***	***	***	***	***	***	***	***	***
TNX	***	***	***	**	***	***	***	***	***
TNN	***	***	***	***	***	***	***	***	***
SU	***	***	***	***	***	***	***	***	***
ID	***	***	***	***	***	***	***	***	***
DTR	*		**		**	**	***	**	***
FD	***	***	***	***	***	***	***	***	***
ANW	RCP26			RCP45			RCP85		
	2011-2040	2041-2070	2071-2100	2011-2040	2041-2070	2071-2100	2011-2040	2041-2070	2071-2100
Surface flux									
Cumulative surface flux	***	***	***	***	*	***	***	***	***
Surface runoff	.	***		*	.				
Cumulative surface runoff	***	***	***	***	***	***	***	***	***
Soil water storage	*	***	*	***	**	***	***	***	***
Cumulative infiltration	***	***	***	***	***	***	*	***	***
ASW	RCP26			RCP45			RCP85		
	2011-2040	2041-2070	2071-2100	2011-2040	2041-2070	2071-2100	2011-2040	2041-2070	2071-2100
Surface flux									
Cumulative surface flux	***	***	***	***	***	***	***	***	***
Surface runoff		**	.	.					
Cumulative surface runoff	***	***	***	***	***	***	***	***	***
Soil water storage	*	***		***	.	***	***	***	***
Cumulative infiltration	***	***	***	***	***	***	***	***	***

Level of significance: '\*\*\*' 0.001, '\*\*' 0.01, '\*' 0.05, '.' 0.1.